Université de Neuchâtel

Institut de Chimie

Coordination et activation d'alcynes par des clusters tri- et tétranucléaires

Version réduite de la thèse présentée à la faculté des sciences de l'Université de Neuchâtel pour l'obtention du titre de docteur ès science

par

Vincent Ferrand

Neuchâtel

1999

IMPRIMATUR POUR LA THÈSE

Coordination et activation d'alcynes par des clusters tri- et tétranucléaires

de M. Vincent Ferrand

UNIVERSITÉ DE NEUCHÂTEL

FACULTÉ DES SCIENCES

La Faculté des sciences de l'Université de Neuchâtel sur le rapport des membres du jury,

Mme H. Stoeckli-Evans,
MM. G. Süss-Fink (directeur de thèse),
et P. Dixneuf (Uni. de Rennes F)

autorise l'impression de la présente thèse.

Neuchâtel, le 6 septembre 1999

Le doyen:

F. Stoeckli

Liste des publications

"Triruthenium Clusters Containing Vinyl Ligands: Synthesis and Structure of $Ru_3(\mu_2\text{-}CO)_2(CO)_6[\mu_3\text{-}NS(O)MePh](\mu_2\text{-}\eta^1,\eta^2\text{-}PhCH_2C{=}CH_2)$, $Ru_3(\mu_2\text{-}CO)(CO)_7[\mu_3\text{-}NS(O)MePh](\mu_3\text{-}\eta^1,\eta^2\text{-}Pr^nC{=}CHPr^n)$, $Ru_3(\mu_2\text{-}CO)(CO)_7[\mu_3\text{-}NS(O)MePh](\mu_3\text{-}\eta^1,\eta^2\text{-}PhC{=}CHBu^n)$, and $(\mu_2\text{-}H)Ru_3(CO)_6(\mu_2\text{-}\eta^1,\eta^2\text{-}PhC{=}CHPh)(\mu_3\text{-}\eta^1,\eta^2\text{-}PhC{\equiv}CPh)[\mu_3\text{-}\eta^1,\eta^2\text{-}NS(O)Me(C_6H_4)]$"; **Vincent Ferrand**, Kurt Merzweiler, Gerd Rheinwald, Helen Stoeckli-Evans et Georg Süss-Fink, *J. Organomet. Chem.*, **1997**, (549), 263.

"Carbon-carbon coupling reactions on triruthenium clusters: synthesis and structure of $Ru_3(CO)_9[\mu_3\text{-}\eta^3\text{-}PhCCCC(H)Ph][\mu_2\text{-}NS(O)MePh]$ and $Ru_3(\mu_2\text{-}CO)(CO)_7[\mu_3\text{-}\eta^3\text{-}PhCCCC(H)\text{-}Ph][\mu_3\text{-}NS(O)MePh]$"; **Vincent Ferrand**, Céline Gambs, Nadine Derrien, Carsten Bolm, Helen Stoeckli-Evans et Georg Süss-Fink, *J. Organomet. Chem.*, **1997**, (549), 275.

"Triruthenium-iridium clusters containing alkyne ligands: synthesis, structure, and catalytic implications of $[(\mu_2\text{-}H)Ru_3Ir(CO)_{11}(\mu_3\text{-}\eta^2\text{-}PhC{\equiv}CPh)]$ and $[Ru_3Ir(CO)_{10}(\mu_4\text{-}\eta^2\text{-}PhC{\equiv}CPh)(\mu_2\text{-}\eta^2\text{-}PhC{=}CHPh)]$; **Vincent Ferrand**, Georg Süss-Fink, Antonia Neels et Helen Stoeckli-Evans, *J. Chem. Soc., Dalton Trans.*, **1998**, 3828.

"Tri- and Tetranuclear Mixed-Metal Clusters Containing Alkyne Ligands: Synthesis and Structure of $[Ru_3Ir(CO)_{11}(RCCR')]^-$, $[Ru_2Ir(CO)_9(RCCR')]^-$ and $[HRu_2Ir(CO)_9(RCCR')]$"; **Vincent Ferrand**, Georg. Süss-Fink, Antonia Neels et Helen Stoeckli-Evans, *Europ. J. Inorg. Chem.*, **1999**, 853.

"Carbon-carbon coupling reactions of but-2-yne on a triruthenium framework: Synthesis and molecular structure of $Ru_3(CO)_7[NS(O)MePh](HCMeCMeCMeCMeCO)$ and $Ru_3(CO)_8\text{-}(CMeCMeCMeCMe)$"; Vincent Ferrand, Antonia Neels, Helen Stoeckli-Evans et Georg Süss-Fink, *Inorg. Chem. Commun.*, **1999**, submitted.

Reprinted from

Journal of Organometallic Chemistry

Journal of Organometallic Chemistry 549 (1997) 263–274

Triruthenium clusters containing vinyl ligands: synthesis and structure of $Ru_3(\mu_2\text{-}CO)_2(CO)_6[\mu_3\text{-}NS(O)MePh](\mu_2\text{-}\eta^1,\eta^2\text{-}PhCH_2C{=}CH_2)$, $Ru_3(\mu_2\text{-}CO)(CO)_7[\mu_3\text{-}NS(O)MePh](\mu_3\text{-}\eta^1,\eta^2\text{-}Pr^nC{=}CHPr^n)$, $Ru_3(\mu_2\text{-}CO)(CO)_7[\mu_3\text{-}NS(O)MePh](\mu_3\text{-}\eta^1,\eta^2\text{-}PhC{=}CHBu^n)$, and $(\mu_2\text{-}H)Ru_3(CO)_6(\mu_2\text{-}\eta^1,\eta^2\text{-}PhC{=}CHPh)(\mu_3\text{-}\eta^1,\eta^2\text{-}PhC{\equiv}CPh)[\mu_3\text{-}\eta^1,\eta^2\text{-}NS(O)Me(C_6H_4)]$

Vincent Ferrand [a], Kurt Merzweiler [b], Gerd Rheinwald [a], Helen Stoeckli-Evans [a], Georg Süss-Fink [a,*]

[a] *Institut de Chimie, Université de Neuchâtel, Neuchâtel CH-2000, Switzerland*

[b] *Institut für Anorganische Chemie der Martin-Luther-Universität Halle-Wittenberg, Fachbereich Chemie, Halle D-06099, Germany*

Received 30 June 1997

ELSEVIER

ELSEVIER

Journal of Organometallic Chemistry 549 (1997) 263–274

Journal of Organometallic Chemistry

Triruthenium clusters containing vinyl ligands: synthesis and structure of $Ru_3(\mu_2\text{-}CO)_2(CO)_6[\mu_3\text{-}NS(O)MePh](\mu_2\text{-}\eta^1,\eta^2\text{-}PhCH_2C{=}CH_2)$, $Ru_3(\mu_2\text{-}CO)(CO)_7[\mu_3\text{-}NS(O)MePh](\mu_3\text{-}\eta^1,\eta^2\text{-}Pr^nC{=}CHPr^n)$, $Ru_3(\mu_2\text{-}CO)(CO)_7[\mu_3\text{-}NS(O)MePh](\mu_3\text{-}\eta^1,\eta^2\text{-}PhC{=}CHBu^n)$, and $(\mu_2\text{-}H)Ru_3(CO)_6(\mu_2\text{-}\eta^1,\eta^2\text{-}PhC{=}CHPh)(\mu_3\text{-}\eta^1,\eta^2\text{-}PhC{\equiv}CPh)[\mu_3\text{-}\eta^1,\eta^2\text{-}NS(O)Me(C_6H_4)]$

Vincent Ferrand [a], Kurt Merzweiler [b], Gerd Rheinwald [a], Helen Stoeckli-Evans [a], Georg Süss-Fink [a,*]

[a] *Institut de Chimie, Université de Neuchâtel, Neuchâtel CH-2000, Switzerland*

[b] *Institut für Anorganische Chemie der Martin-Luther-Universität Halle-Wittenberg, Fachbereich Chemie, Halle D-06099, Germany*

Received 30 June 1997

Abstract

The electron-deficient cluster $(\mu_2\text{-}H)Ru_3(CO)_9[\mu_3\text{-}NS(O)MePh]$ (**1**) reacts with the terminal alkyne $PhCH_2C{\equiv}CH$ to give the vinyl complex $Ru_3(\mu_2\text{-}CO)_2(CO)_6[\mu_3\text{-}NS(O)MePh](\mu_2\text{-}\eta^1,\eta^2\text{-}PhCH_2C{=}CH_2)$ (**2**). The analogous reaction with internal alkynes ($RC{\equiv}CR'$) affords the clusters $Ru_3(\mu_2\text{-}CO)(CO)_7[\mu_3\text{-}NS(O)MePh](\mu_3\text{-}\eta^1,\eta^2\text{-}RC{=}CHR')$ (**3**: $R = R' = Pr^n$; **4**: $R = Ph$; $R' = Bu^n$) in which the vinyl ligand has opened a Ru–Ru bond upon coordination the Ru_3 framework. In the case of diphenylacetylene, reaction with two equivalents of the alkyne, yields the vinyl–alkyne cluster $(\mu_2\text{-}H)Ru_3(CO)_6(\mu_2\text{-}\eta^1,\eta^2\text{-}PhC{=}CHPh)(\mu_3\text{-}\eta^1,\eta^2\text{-}PhC{\equiv}CPh)[\mu_3\text{-}\eta^1,\eta^2\text{-}NS(O)Me(C_6H_4)]$ (**5**) with *ortho*-metallation of the phenyl substituent of the sulfoximido cap. © 1997 Elsevier Science S.A.

Keywords: Clusters; Ruthenium; Alkynes; Vinyl ligands; Crystal structures

1. Introduction

The vinyl ligand, $-CH{=}CH_2$, and its derivatives have received much attention in coordination chemistry because of the synthetic potential of this function for vinylation processes such as the Heck Reaction [1]. Cluster complexes containing vinyl ligands have been discussed [2] as intermediates in catalytic processes such as alkene isomerisation [3], alkene hydrogenation [4], alkyne hydrogenation [5–7], and alkyne–alkene codimerization [8].

There are several coordination modes of the vinyl ligand in cluster chemistry, and for trinuclear clusters, three types of vinyl coordination have been found so far (Scheme 1). If the vinyl group is coordinated in a terminal fashion ('end-on') to the metal center, it is only σ-bound and acts as one-electron donor (type A). Only one example of this type is reported in the literature: the complex $Ru_3(CO)_9(\mu_3\text{-ampy})(\eta^1\text{-PhCCHPh})$ (ampyH=2-amino-6-methylpyridine) was fully characterized [5]. Unfortunately, no structural information is available for this complex, but the η^1-coordination is confirmed by the NMR data. This compound is only accessible from the corresponding $\mu_2\text{-}\eta^1,\eta^2$-vinyl complex $Ru_3(CO)_8(\mu_3\text{-ampy})(\mu_2\text{-}\eta^1,\eta^2\text{-PhCCHPh})$ by reaction with carbon monoxide, the latter complex being an example for type B (π-'side-on') [5]. If the vinyl ligand is coordinated in a $\mu_2\text{-}\eta^1,\eta^2$-fashion ($\sigma$-'end-on' to one metal center and π-'side-on' to another metal center) according to type B, it acts as a three-electron

* Corresponding author.

PII S0022-328X(97)00506-8

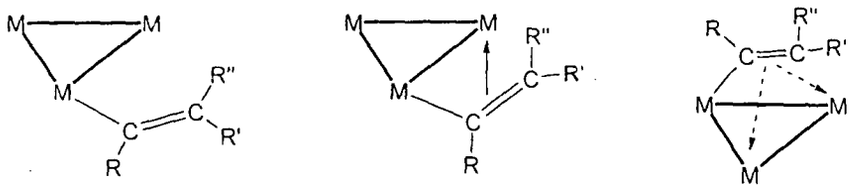

(A) (B) (C)

Scheme 1.

donor. Numerous examples of this type are known, the first compounds to be characterized being (μ_2-H)$Os_3(CO)_9$(μ_2-η^1,η^2-CHCHR) (R = Ph, Me, Et, *t*Bu) and (μ_2-H)$Os_3(CO)_9$(μ_2-η^1,η^2-CRCHR′) (R = Ph, R′ = Ph, Me, Et) [9]. Complexes of this type are accessible either by alkyne insertion into metal–hydrogen bonds or by C–H activation of an alkene on a metal cluster [10].

In type C, the vinyl ligand, while still being a three-electron donor, is coordinated in a μ_3-η^1,η^2-fashion (σ-'end-on' to one metal center and π-'side-one' to the other two metal centers). This coordination has been found in (μ_2-H)$Os_3(CO)_{10}$(μ_3-η^1,η^2-CF_3CCHCF_3) [11,12] and in (η^5-C_5Me_5)$WRu_2(CO)_7$(μ_2-NPh)(μ_3-η^1,η^2-CF_3CCHCF_3) [13]. The complex $Ru_3(CO)_8$(μ_3-η^1,η^2-$HNNMe_2$)(μ_3-η^1,η^2-$PhCCH_2$) [14] can be classified as type C, in as much as the vinyl group also acts as a three-electron donor coordinated to the three metal centres in a μ_3-η^1,η^2-fashion, but differs in as much as the vinyl cap bridges an open Ru_3 framework and not a closed trinuclear metal core.

In this paper, we report the synthesis and structural characterization of some new trinuclear vinyl complexes by the reaction of the electron-deficient cluster (μ_2-H)$Ru_3(CO)_9$[μ_3-NS(O)MePh] [15] with terminal and internal alkynes.

2. Results and discussion

2.1. Reaction of (μ_2-H)$Ru_3(CO)_9$[μ_3-NS(O)MePh] (1) with $PhCH_2C{\equiv}CH$

The thermal reaction between the electron-deficient cluster (μ_2-H)$Ru_3(CO)_9$[μ_3-NS(O)MePh] (**1**) [15] and

$$HRu_3(CO)_9[NS(O)MePh] + PhCH_2{-}C{\equiv}CH \longrightarrow$$

(1)

$$Ru_3(CO)_8[PhCH_2C{=}CH_2][NS(O)MePh] + CO$$

(2)

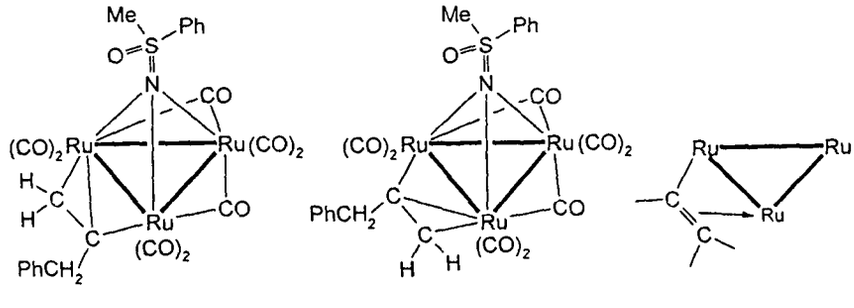

(2a) (2b)

Scheme 2.

Table 1
IR[a] and NMR[b] data of the complexes **2–5**

Complexes		δ
2a	2065(w), 2052(w), 2036(s), 2010(s), 1998(m), 1984(m), 1941(m), 1823(m)	3.25 (CH_3) s; 3.50 (C=CH*H*) s; 4.42 (C=C*H*H) s; 7–8 (Ph) m; 4.486 (PhCH*H*) d; $^2J_{H-H}$ = 13.2 Hz; 3.28 (PhC*H*H) d, $^2J_{H-H}$ = 13.2 Hz
2b	2066(w), 2053(w), 2038(s), 2012(s), 2000(m), 1985(m), 1946(m), 1826(m)	3.06 (CH_3) s; 3.99 (C=CH*H*) s; 4.20 (C=C*H*H) s; 7–8 (*Ph*) m; 4.51 (PhCH*H*) d; $^2J_{H-H}$ = 13.2 Hz; 3.49 (PhC*H*H) d, $^2J_{H-H}$ = 13.2 Hz
3[c]	2060(w), 2031(s), 2009(s), 1994(m), 1979(m), 1965(w), 1945(m), 1823(w)	2.59, 3.09, 3.26 (CH_3) s; 5.165, 4.95 (C=C*H*Pr^n) t, $^3J_{H-H}$ = 6 Hz; 5.05 (C=C*H*Pr^n) t; $^3J_{H-H}$ = 4 Hz; 0.7–3.1(*Pr*^{n}C=H*Pr*^{n}) m; 7.70 (Ph) m
4[c]	2061(w), 2049(vw),2030(s), 2012(s), 1995(m), 1968(w), 1947(m), 1875(vw), 1851(vw), 1826(w)	2.68, 3.10, 3.33 (CH_3) s; 5.55, 5.28 (C=C*H*Bu^n) t, $^3J_{H-H}$ = 6.3 Hz; 0.89, 0.91, 1.03 (–C=CH(CH_2)$_3$CH_3) t; $^3J_{H-H}$ = 7.3 Hz; 1.3–2.4 (C=CH(CH_2)$_3$$CH_3$) m; 7.50 (*Ph*) m
5[d]	2049(w), 2032(s), 2016(s), 1983(m), 1958(w)	–8.37 (Ru–*H*–Ru) s; 3.18 (CH_3) s; 6.62 (PhC=C*H*Ph) s; 6.7–7.8 (*Ph*) m

[a] In cyclohexane (**2–4**) or dichloromethane (**5**) solution.
[b] In a $CDCl_3$ solution.
[c] Three isomers in solution.

the terminal alkyne $PhCH_2C{\equiv}CH$ in refluxing tetrahydrofuran affords within four hours the vinyl complex $Ru_3(\mu_2\text{-}CO)_2(CO)_6[\mu_3\text{-}NS(O)MePh](\mu_2\text{-}\eta^1,\eta^2\text{-}PhCH_2C{=}CH_2)$ (**2**). Two isomers of **2** were separated from the reaction mixture by chromatographic methods (Scheme 2).

Both isomers were characterized by their analytical and spectroscopic data. While **2a** gave suitable crystals for the X-ray structure determination, **2b** did not crystallize, but there is spectroscopic evidence for **2b** being an isomer of **2a**. On the basis of the NMR and IR data, we believe that the $\mu_2\text{-}\eta^1,\eta^2$-vinyl ligand in **2b** is coordi-

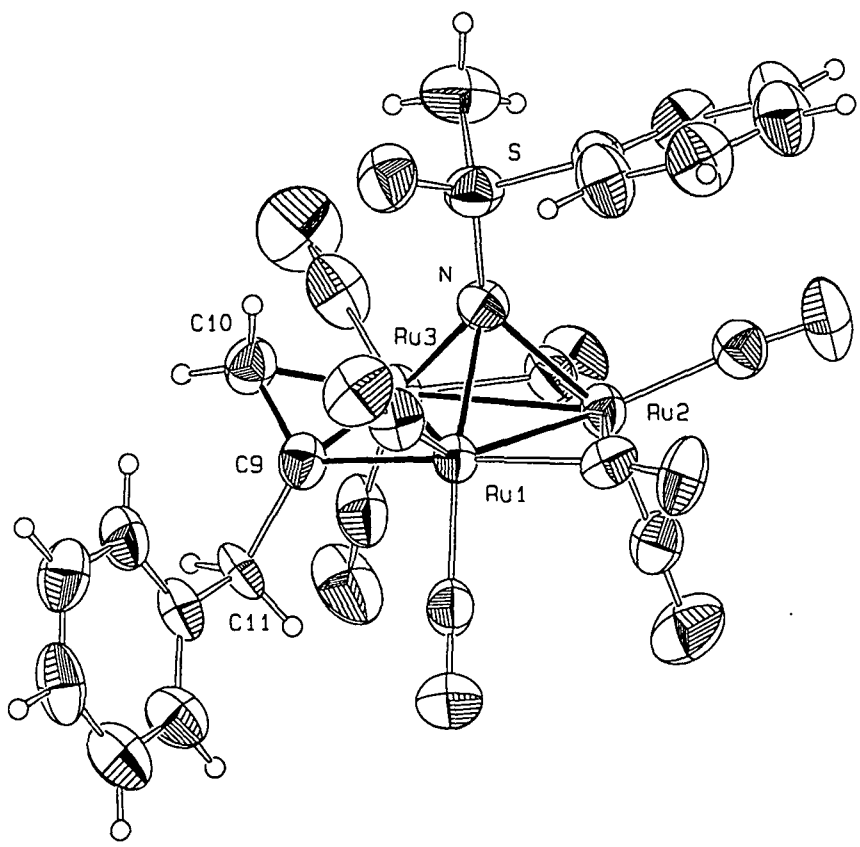

Fig. 1. ORTEP plot of **2a**. Thermal ellipsoids are drawn at 40% of probability.

nated in an inverted fashion with respect to **2a**. The IR spectra of the two isomers **2a** and **2b** in cyclohexane are very similar in the carbonyl region, both presenting six bands in the region of terminal CO vibrations and one absorption at 1823 cm^{-1} for **2a** and 1826 cm^{-1} for **2b**, which is attributed to bridging carbonyl ligands (Table 1). The ^1H NMR spectra of **2a** and **2b** also show a very similar pattern of signals, but differ in the chemical shifts (Table 1). In both cases, the hydride signal of the starting compound **1** at δ −15.84 ppm has disappeared, indicating the insertion of the carbon–carbon triple bond into the M–H bond. A multiplet between δ 7.0 and 8.0 ppm can be assigned to the phenyl protons. The two hydrogen atoms of the benzyl group are non-equivalent and resonate as two doublets (**2a**: δ 4.42 and 3.50 ppm; **2b**: δ 4.51 and 3.49 ppm, $^2J_{HH}$ 13.2 Hz]. The vinyl protons appear as two singlets (**2a**: δ 4.49 ppm and δ 4.28 ppm; **2b**: δ 4.20 and δ 3.99 ppm). The methyl group of the nitrogen cap is observed at higher field (**2a**: δ 3.25 ppm, **2b**: δ 3.06 ppm) than in **1** (δ 3.36 ppm).

The $^{13}C\{^1H\}$ spectrum of **2a** at low temperature (−80°C) in CD_2Cl_2 shows the two bridging carbonyls ligands at δ 238 and 227 ppm, and the six terminal carbonyl signals at δ 190, 192, 196, 199, 199.6, 205 ppm. The two carbon atoms of the vinyl group are found at δ 60.7 and 59 ppm, indicating these two carbon atoms are more sp^3 than sp^2 hybridized, due to the back-bonding from the ruthenium d orbitals.

Table 2
Selected bond lengths [Å] and bond angles [°] for **2a**

C(9)–C(10)	1.39(2)
C(9)–C(11)	1.57(2)
C(9)–Ru(1)	2.120(12)
C(9)–Ru(3)	2.231(12)
C(10)–Ru(3)	2.272(13)
N–S	1.559(10)
N–Ru(2)	2.158(10)
N–Ru(3)	2.170(9)
N–Ru(1)	2.166(10)
S–O(9)	1.481(10)
Ru(1)–Ru(2)	2.698(1)
Ru(2)–Ru(3)	2.703(1)
Ru(1)–Ru(3)	2.797(1)
C(10)–C(9)–C(11)	117.5(11)

Estimated standard deviations in parentheses.

2.2. *Molecular structure of* $Ru_3(\mu_2\text{-}CO)_2(CO)_6[\mu_3\text{-}NS(O)MePh](\mu_2\text{-}\eta^1,\eta^2\text{-}PhCH_2C{=}CH_2)$ (2a)

The molecular structure of **2a** was confirmed by single-crystal X-ray analysis. Suitable crystals of **2a** were obtained by crystallization at 20°C from a mixture of cyclohexane and pentane. Fig. 1 shows the molecular

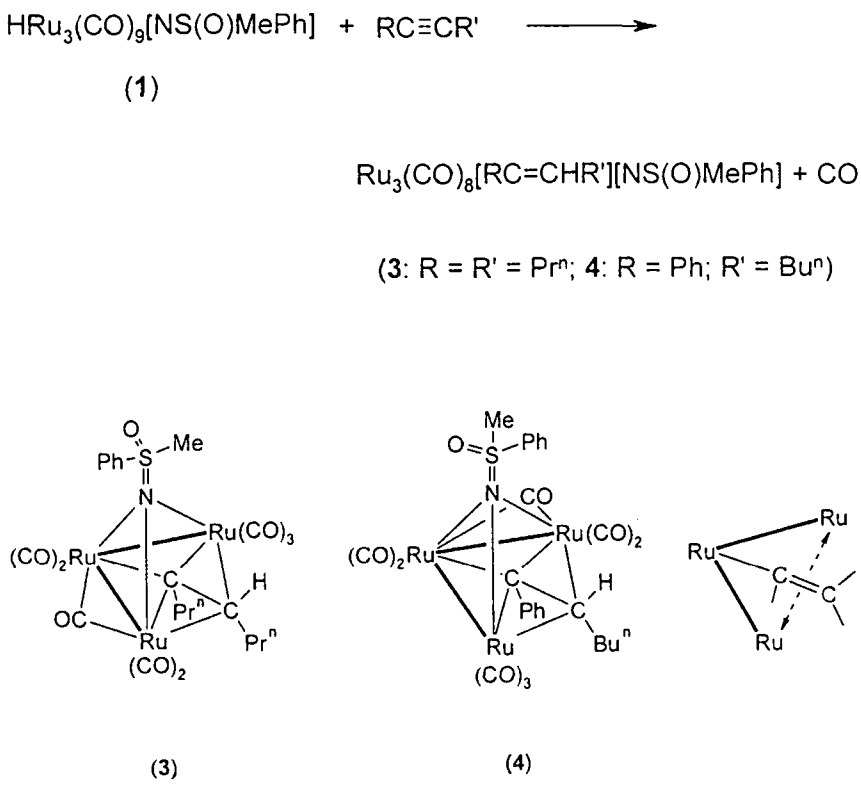

Scheme 3.

structure of **2a**; selected bond lengths and angles are presented in Table 2.

The three ruthenium atoms form a closed isoceles triangle [Ru(1)–Ru(2) 2.698(1); Ru(1)–Ru(3) 2.797(1); Ru(2)–Ru(3) 2.703(1) Å]. Each ruthenium atom is bonded to two terminal CO groups and to the nitrogen cap, as in **1** [15]. Two of the three ruthenium–ruthenium bonds, Ru(1)–Ru(2) and Ru(2)–Ru(3), are bridged by CO groups which are in the same plane as the metal framework, while the Ru(1)–Ru(3) edge is bonded by the vinyl ligand. The vinyl group is almost perpendicular to the metal plane [C(9)–C(10) ⊥ Ru(1)–Ru(3): 98.5°]. The carbon atom C(9) occupies an equatorial site and is σ-bonded to Ru(1). Due to the coordination to the Ru(1)–Ru(3) bond, the C(9)–C(10) double bond is longer (1.39(2) Å) than a free carbon–carbon double bond (average 1.316Å) [16]. The nitrogen cap is further away from the metal plane in **2a** than in complex **1**, the average Ru–N distances in **2a** being 2.16 Å, whereas in **1** they are 2.11 Å. At present we have no other explanation for this elongation.

The structure of **2a** compares well with previously reported vinyl complexes, for example $Ru_3(CO)_8[\mu_3\text{-}\eta^2\text{-}N(Me)_2NH](\mu\text{-}\eta^2\text{-}PhC{=}CH_2)$ [14]. However, while all these clusters present the expected electron count of 48 e, the complexes **2a** and **2b** contain only 46 e and are electron-deficient.

2.3. Reaction of $(\mu_2\text{-}H)Ru_3(CO)_9[\mu_3\text{-}NS(O)MePh]$ (1) with $RC{\equiv}CR'$ (3: $R = R' = Pr^n$; 4: $R = Ph$; $R' = Bu^n$)

With internal alkynes, $(\mu_2\text{-}H)Ru_3(CO)_9[\mu_3\text{-}NS(O)MePh]$ (**1**) reacts differently in refluxing THF: with an excess of $Pr^nC{\equiv}CPr^n$ or $PhC{\equiv}CBu^n$, the vinyl complexes $Ru_3(\mu_2\text{-}CO)(CO)_7[\mu_3\text{-}NS(O)MePh](\mu_3\text{-}\eta^1,\eta^2\text{-}Pr^nC{=}CHPr^n)$ (**3**) and $Ru_3(\mu_2\text{-}CO)(CO)_7[\mu_3\text{-}NS(O)MePh](\mu_3\text{-}\eta^1,\eta^2\text{-}PhC{=}CHBu^n)$ (**4**) are obtained in good yields (Scheme 3).

The IR spectra of **3** and **4** (Table 1) show the same carbonyl pattern with seven bands in the region of terminal carbonyl groups and one absorption at 1823 cm^{-1} (**3**) and 1826 cm^{-1} (**4**) which is assigned to a bridging carbonyl ligand. The ^1H NMR spectra of **3** and **4** in $CDCl_3$ are very complicated, indicating the presence of several isomers in solution (Table 1): while the crystals of **3** and **4** contain only one isomer (see Section 2.4 below), the solution in $CDCl_3$ contains, in both cases, three isomers which can be recognized by the different singlets for the methyl substituents at the sulfur atom and by three triplets for the vinyl proton. Two of these three triplets are well resolved and with a 1:1 ratio, having a coupling constant of 6.0 Hz (**3**), or 6.3 Hz (**4**), whereas the third triplet is not well resolved. A multiplet centered around δ 7.70 ppm (**3**) or δ 7.50 ppm (**4**) is caused by the various phenyl protons. In the case of **4**, the three isomers give rise to three triplets at δ 1.03, 0.95, 0.89 ppm which are assigned to the methyl groups of the butyl chains.

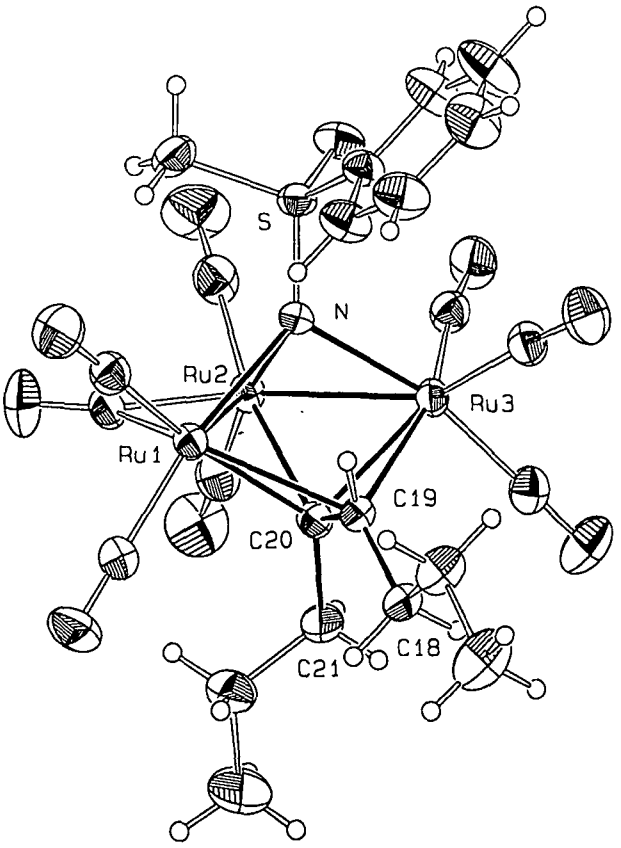

Fig. 2. ORTEP plot of **3**. Thermal ellipsoids are drawn at 40% of probability.

2.4. Molecular structure of $Ru_3(\mu_2\text{-}CO)(CO)_7[\mu_3\text{-}NS(O)MePh](\mu_3\text{-}\eta^1,\eta^2\text{-}RC{=}CHR')$ (3: $R = R' = Pr^n$; 4: $R = Ph$; $R' = Bu^n$)

Suitable crystals of **3** and **4** were obtained at −18°C from hexane or a mixture of CH_2Cl_2 and hexane, respectively. The molecular structure of **3** is depicted in Fig. 2, and that of **4** in Fig. 3. Selected bond lengths and angles of both compounds are presented in Tables 3 and 4. Both **3** and **4** have the same overall structure, showing the same carbonyl and vinyl coordination. The three ruthenium atoms form an open triangle with three different ruthenium–ruthenium distances [**3**: Ru(1)–Ru(2) 2.690(1), Ru(1) · · · Ru(3) 3.542(2), Ru(2)–Ru(3) 2.776(1) Å; **4**: Ru(1)–Ru(2) 2.6786(13), Ru(1) · · · Ru(3) 3.5394(7), Ru(2)–Ru(3) 2.7649(13) Å]. Two of the three ruthenium atoms, Ru(1) and Ru(2), are bonded to two terminal CO groups, whereas Ru(3) is bonded to three terminal CO groups. A carbonyl group bridges the Ru(1)–Ru(2) edge and lies in the same plane as the metal framework; probably due to this linkage, this bond is shorter than the other ruthenium–ruthenium bonds.

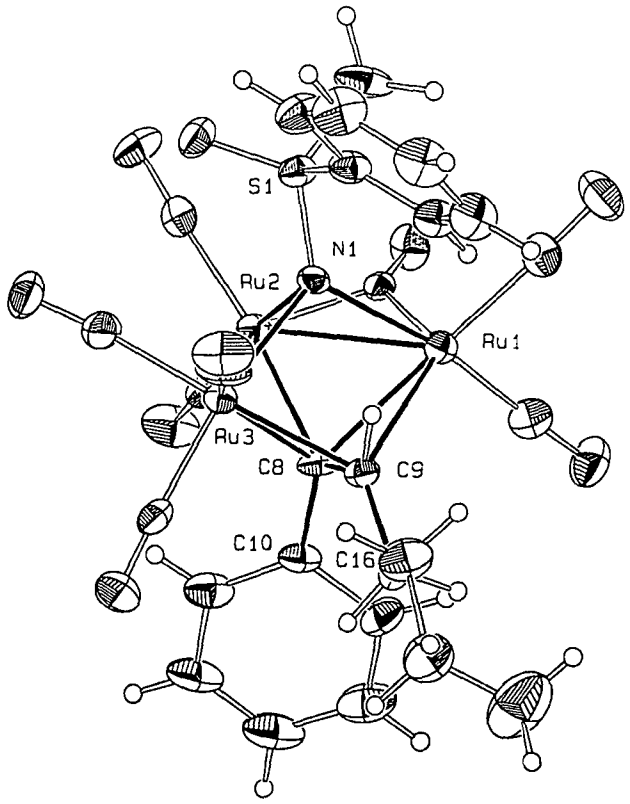

Fig. 3. ORTEP plot of 4. Thermal ellipsoids are drawn at 40% of probability.

We also observe that in 3 and 4 the nitrogen cap is further away from the Ru_3 triangle than in 1, all the Ru–N bond lengths being different [3: Ru(1)–N 2.23(3), Ru(2)–N 2.14(3), Ru(3)–N 2.19(3) Å; 4: Ru(1)–N 2.224(9), Ru(2)–N 2.128(9), Ru(3)–N 2.156(8) Å], in contrast to 2. The vinyl ligand, being a three-electron donor, is coordinated in a similar fashion as a μ_3-η^1,η^2-alkynyl group which is a five-electron donor.

Table 3
Selected bond lengths [Å] and bond angles [°] for 3

C(19)–C(20)	1.425(6)
C(18)–C(19)	1.510(5)
C(20)–C(21)	1.529(5)
C(20)–Ru(3)	2.235(4)
C(20)–Ru(2)	2.241(4)
C(20)–Ru(1)	2.329(4)
C(19)–Ru(3)	2.243(4)
C(19)–Ru(1)	2.427(4)
C(19)–H(19)	0.96(5)
N–S	1.554(3)
N–Ru(2)	2.144(3)
N–Ru(3)	2.193(3)
N–Ru(1)	2.233(3)
S–O(9)	1.448(3)
Ru(1)–Ru(2)	2.690(1)
Ru(2)–Ru(3)	2.776(1)
Ru(1) · · · Ru(3)	3.542(2)
C(18)–C(19)–C(20)	125.7(3)
C(19)–C(20)–C(21)	116.7(3)

Estimated standard deviations in parentheses.

Table 4
Selected bond lengths [Å] and bond angles [°] for 4

C(8)–C(9)	1.42(2)
C(8)–C(10)	1.51(2)
C(9)–C(16)	1.54(2)
C(8)–Ru(3)	2.235(12)
C(8)–Ru(2)	2.274(10)
C(8)–Ru(1)	2.292(12)
C(9)–C(16)	1.54(2)
C(9)–Ru(3)	2.195(11)
C(9)–Ru(1)	2.499(11)
C(9)–H(9)	0.93(1)
N(1)–S(1)	1.560(9)
N(1)–Ru(2)	2.130(9)
N(1)–Ru(3)	2.156(8)
N(1)–Ru(1)	2.224(9)
S(1)–O(1)	1.450(9)
Ru(1)–Ru(2)	2.6786(13)
Ru(2)–Ru(3)	2.7649(13)
Ru(1) · · · Ru(3)	3.5394(7)
C(9)–C(8)–C(10)	117.7(9)
C(8)–C(9)–C(16)	126.1(10)

Estimated standard deviations in parentheses.

This type of vinyl coordination has only been observed so far in $Ru_3(CO)_8(\mu_3\text{-}\eta^1,\eta^2\text{-}PhC{=}CH_2)[\mu_3\text{-}\eta^1,\eta^2\text{-}N(Me)_2NH]$ [14]. The C=C double bond [3: C(19)–C(20); 4: C(8)–C(9)] adopts a perpendicular coordination with respect to the open edge [Ru(1) · · · Ru(3) ⊥ C(8)–C(9): 84°; Ru(1) · · · Ru(3) ⊥ C(19)–C(20): 89°] and is situated above the metal plane. The nitrogen atom, the three ruthenium atoms, and the carbon atoms C(20) in 3 and C(8) in 4, form a trigonal-bipyramidal CRu_3N core (Figs. 2 and 3). The carbon–carbon double bond of the vinyl is longer in clusters 3 and 4 [3: C(19)–C(20) 1.425(6) Å; 4: C(8)–C(9) 1.425(2) Å] than in 2 [C(9)–C(10) 1.39(2) Å], probably due to the coordination to the three metal centers.

The σ–π coordination of the vinyl ligand in 3 and 4 is not easy to describe in terms of localized bonds. Whereas the distances Ru(2)–C(20) 3 and Ru(2)–C(8) 4 of 2.241(4) and 2.274(10) Å, respectively, correspond to a σ-single bond, the π-bonding of the C(20)–C(19) backbone in 3 and the C(8)–C(9) backbone in 4 is divided between the two ruthenium atoms Ru(3) and Ru(1). In both cases the C=C unit is, however, closer to Ru(3) than to Ru(1) [3: Ru(1)–C(19) 2.427(4), Ru(3)–C(19) 2.243(4) Å; 4: Ru(1)–C(9) 2.499(11), Ru(3)–C(9) 2.195(11) Å]. Unlike in $Ru_3(CO)_8(\mu_3\text{-}\eta^1,\eta^2\text{-}PhC{=}CH_2)[\mu_3\text{-}\eta^1,\eta^2\text{-}N(Me)_2NH]$ [14] which represents a 48e cluster, clusters 3 and 4 present an electron count of only 46 e. For an open M_3 triangle, the noble gas rule would require 50 e, hence, 3 and 4 are even more electron-deficient than the closed clusters 1 and 2.

2.5. Reaction of $(\mu_2\text{-}H)Ru_3(CO)_9[\mu_3\text{-}NS(O)MePh]$ (1) with $PhC{\equiv}CPh$

With diphenylacetylene, the electron-deficient cluster $(\mu_2\text{-}H)Ru_3(CO)_9[\mu_3\text{-}NS(O)\text{–}MePh]$ (1) reacts at 100°C

$HRu_3(CO)_9[NS(O)MePh] + 2\ PhC{\equiv}CPh \longrightarrow$

(1)

$HRu_3(CO)_6[PhC{=}CHPh][PhC{\equiv}CPh][NS(O)Me(C_6H_4)] + 3\ CO$

(5)

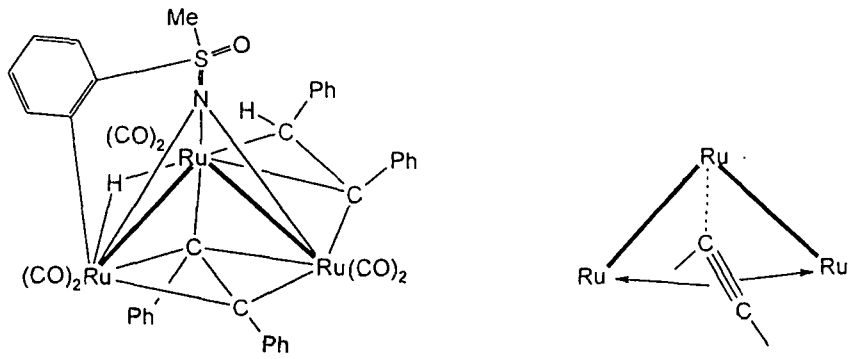

(5)

Scheme 4.

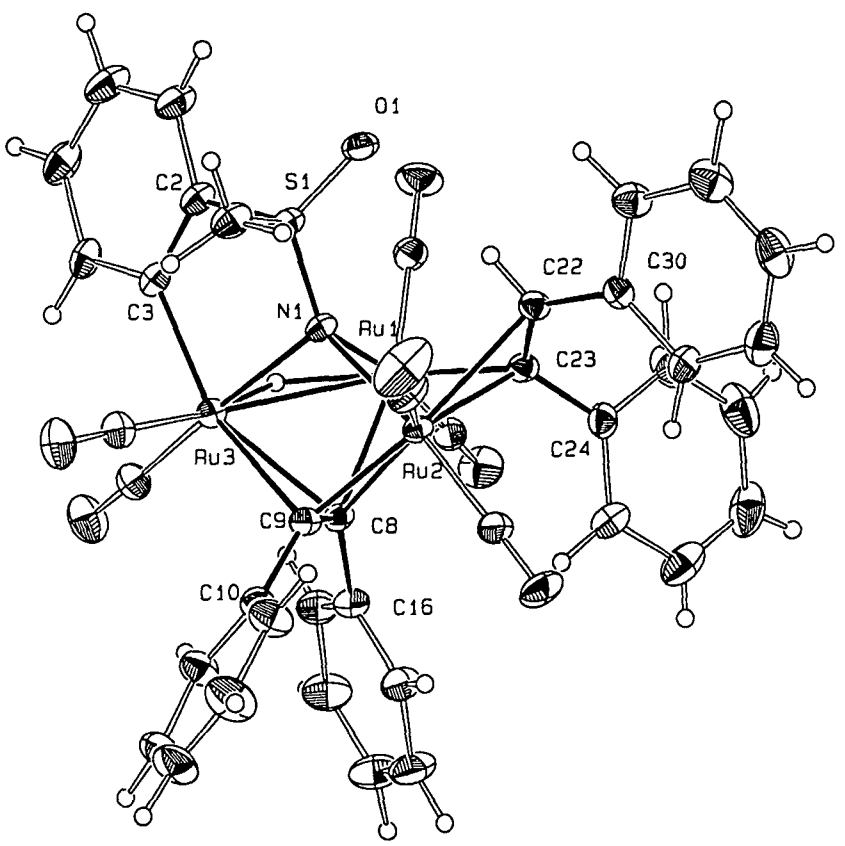

Fig. 4. ORTEP plot of **5**. Thermal ellipsoids are drawn at 40% of probability.

in THF to afford the vinyl–alkyne complex (μ_2-H)$Ru_3(CO)_6$(μ_2-η^1,η^2-PhC=CHPh)(μ_3-η^1,η^2-PhC≡CPh)[μ_3,η^1,η^2-NS(O)Me(C_6H_4)] (**5**). In this case, two equivalents of the alkyne are consumed to replace three carbonyl ligands: one alkyne inserts into the ruthenium–hydrogen bridge, whereas the other one opens up a ruthenium–ruthenium bond and coordinates as an almost perpendicular 4 e donor across the open site. In addition, the phenyl substituent at the sulfur atom undergoes, an *ortho*-metallation and transfers a hydrogen atom to the ruthenium framework (Scheme 4).

The IR spectrum of **5** (Table 1) shows only absorptions of terminal carbonyl ligands in the ν_{CO} region. The ^{1}H NMR spectrum exhibits a single hydride resonance at δ −8.37 ppm. The methyl group of the nitrogen cap is observed at δ 3.18 ppm, and the vinyl proton appears as a singlet at δ 6.60 ppm. A multiplet centered around δ 7.5 ppm is assigned to the different phenyl groups. The structure of **5** was confirmed by a single crystal X-ray structure analysis.

2.6. Molecular structure of (μ_2-H)$Ru_3(CO)_6$(μ_2-η^1,η^2-PhC=CHPh)(μ_3-η^1,η^2-PhC≡CPh)[μ_3,η^1,η^2-NS(O)Me(C_6H_4)] (5)

Suitable crystals of **5** were grown at room temperature crystallization from a mixture of CH_2Cl_2 and hexane. The molecular structure of **5** is depicted in Fig. 4. Selected bond lengths and angles are presented in Table 5. The molecular structure of **5** is quite complex, because it contains not only a μ_2-η^1,η^2-vinyl ligand, but also an alkyne ligand coordinated in a rare fashion over an open ruthenium–ruthenium site; furthermore the phenyl group of the sulfoximido cap has undergone an *ortho*-metallation. The three ruthenium atoms form an open triangle [Ru(1)–Ru(2) 2.7336(9), Ru(1)–Ru(3) 2.7376(8), Ru(2)···Ru(3) 3.3957(10) Å], each ruthenium atom being bonded to two terminal CO groups. The hydride ligand is coordinated quasi-symmetrically between Ru(1) and Ru(3) [Ru(1)–H(1Ru1) 1.79(5), Ru(3)–H(1Ru1) 1.77(5) Å] forming a dihedral angle of 4.198° with the Ru_3 core. The other metal–metal bond Ru(1)–Ru(2) is bridged by the vinyl ligand in the classical μ_2-η^1,η^2-fashion. The ligand is coordinated almost perpendicularly with respect to the Ru(1)–Ru(2) edge [Ru(1)–Ru(2) ⊥ C(22)–C(23): 100°] and adopts a *cis* configuration in order to avoid steric hindrance, in line with other vinyl complexes [5–8,17–30], e.g. $Ru_3(CO)_8$[μ-η^2-N(C_6H_5)(C_5H_4N)](μ_2-η^2-PhC=CHPh) [8]. The diphenylacetylene ligand adopts the μ_3-η^1,η^2-coordination, almost perpendicular with regard to the Ru(2)···Ru(3) edge [C(8)–C(9) ⊥ Ru(2)–Ru(3) 80°]. The perpendicular coordination of an alkyne to a metal cluster [31–33] was first observed for the unsaturated complex $Fe_3(CO)_9$(μ_3-η^2-RC≡CR) [34]. In trinuclear ruthenium cluster chemistry, there is only one alkyne complex known to have a perpendicular alkyne coordination: Ru_3(μ_3-η^2-PhC≡CPh)$(CO)_7$ (dppm) [35,36]. In the vinyl–alkyne complex CpW$Ru_2(CO)_5$(μ_2-NPh)[μ_3-η^2-$C_2(CF_3)_2$][μ_2-η^2-C(CF_3)CH(CF_3)], the bis(trifluoromethyl) acetylene ligand is coordinated in a parallel fashion with respect to the metal–metal bond, and the Ru_2W core forms a closed metal triangle [37]. In the case of **5**, the alkyne axis is not exactly perpendicular with respect to the Ru(2)···Ru(3) vector (80°), unlike the known complex [35,36], and there is no metal–metal bond between the two ruthenium atoms Ru(2) and Ru(3). The carbon atom C(8) is closer to Ru(1) and Ru(3) than to Ru(2) [Ru(1)–C(8) 2.309(4), Ru(2)–C(8) 2.385(4), Ru(3)–C(8) 2.296(4) Å], whereas the carbon atom C(9) is closer to Ru(2) than to Ru(3) [Ru(2)–C(9) 2.084(4), Ru(3)–C(9) 2.401(4) Å]. The C(8)–C(9) bond length is shorter (C(8)–C(9) 1.3515(4) Å) than in Ru_3(μ_3-η^2-PhC$_2$Ph)$(CO)_7$ (dppm) [35,36] (C≡C 1.409(6) Å), probably due to reduced back bonding from the Ru_3 core in **5**.

Table 5
Selected bond lengths [Å] and bond angles [°] for 5

C(8)–C(9)	1.352(5)
C(8)–C(16)	1.493(5)
C(9)–C(10)	1.482(5)
C(8)–Ru(1)	2.309(4)
C(8)–Ru(2)	2.385(4)
C(8)–Ru(3)	2.296(4)
C(9)–Ru(2)	2.084(4)
C(9)–Ru(3)	2.401(4)
C(22)–C(23)	1.395(5)
C(22)–Ru(2)	2.419(4)
C(23)–Ru(1)	2.111(4)
C(23)–Ru(2)	2.308(4)
C(22)–H(22)	0.94(4)
C(22)–C(30)	1.479(5)
C(23)–C(24)	1.489(5)
Ru(1)–H(1Ru)	1.79(5)
Ru(3)–H(1Ru)	1.77(5)
N(1)–S(1)	1.558(3)
S(1)–C(2)	1.756(4)
C(2)–C(3)	1.396(6)
C(3)–Ru(3)	2.084(4)
N(1)–Ru(1)	2.122(3)
N(1)–Ru(2)	2.132(3)
N(1)–Ru(3)	2.135(3)
S(1)–O(1)	1.450(3)
Ru(1)–Ru(2)	2.7336(9)
Ru(2)···Ru(3)	3.396(1)
Ru(1)–Ru(3)	2.7376(8)
C(8)–C(9)–C(10)	129.7(4)
C(9)–C(8)–C(16)	124.2(3)
C(23)–C(22)–C(30)	127.7(4)
C(22)–C(23)–C(24)	122.9(3)
Ru(3)–Ru(1)–Ru(2)–H(1Ru)	4.198

Estimated standard deviations in parentheses.

The other important point of this structure is the *ortho*-metallation of the phenyl group. The complex $H_2Ru_3(CO)_7(PPh_3)_2[\mu_2\text{-}NC(Ph)C_6H_4]$ [38], which contains an *ortho*-metalated 1-azavinylidene ligand, also shows a five membered ring. The main difference between this complex and **5** resides in the fact that to our knowledge, **5** is the first example of a cluster presenting an *ortho*-metallation involving four different atoms in a five-membered ring: 1Ru, 1N, 1S, 2C, whereas the known *ortho*-metallation clusters normally contain four-membered rings [39]. The five-membered ring is not planar, and two of the five bonds, [Ru(3)–C(3) 2.084(4) and Ru(3)–N 2.135(3) Å] are longer than the others (Table 5). Complex **5** is also unique in as much as it presents both, a $\mu_2\text{-}\eta^1,\eta^2$-vinyl and a $\mu_3\text{-}\eta^1,\eta^2$-alkyne coordination at the same Ru_3 framework. With an electron-count of 48e, **5** is electron-deficient like **1** and **2**.

3. Experimental

All manipulations were carried out in a nitrogen atmosphere, using standard Schlenk techniques. The organic solvents were refluxed over appropriate desiccants [40], distilled and saturated with nitrogen prior to use. The NMR spectra were recorded using a Varian Gemini 200 BB instrument or a Bruker AMX 400. The IR spectra were recorded using a Perkin–Elmer FTIR 1720X spectrophotometer (4000–400 cm^{-1}). Microanalytical data were obtained from the Mikroelementaranalytisches Laboratorium der ETH Zürich. The mass spectrum was recorded by Professor T.A. Jenny, University of Fribourg (Switzerland). The starting compound $(\mu_2\text{-}H)Ru_3(CO)_9[\mu_3\text{-}NS(O)MePh]$ (**1**) was synthesized according to the published method [15]. Methyl phenyl sulfoximine (racemate) was obtained from Professor Carsten Bolm, RWTH Aachen. $PhCH_2C{\equiv}CH$, $Pr^nC{\equiv}CPr^n$, $PhC{\equiv}CBu^n$ were purchased from Aldrich, and diphenylacetylene from Fluka, and were used without further purification.

3.1. Synthesis of $Ru_3(\mu_2\text{-}CO)_2(CO)_6(\mu_2\text{-}\eta^1,\eta^2\text{-}PhCH_2C{=}CH_2)[\mu_3\text{-}NS(O)MePh]$ (2)

A solution of $(\mu_2\text{-}H)Ru_3(CO)_9[\mu_3\text{-}NS(O)MePh]$ (**1**) (150 mg, 0.21 mmol) and $PhCH_2C{\equiv}CH$ (79 μl, 0.63 mmol) in THF (25 ml) was heated in a pressure Schlenk tube to 55°C for 4 h. After evaporation of the solvent the residue was dissolved in CH_2Cl_2 and submitted to thin-layer chromatography (silica gel, CH_2Cl_2/cyclohexane 1:1). The two isomers of **2** separated into two main orange bands. The first one contained **2b**, the second one **2a**. Both isomers were extracted with CH_2Cl_2 and crystallized from pentane, **2a** was recrystallized from cyclohexane/pentane. The orange crystals were dried in vacuo (**2a**: 30 mg, 17%; **2b**: 30 mg, 17%). Anal. Found **2a**: C, 35.91; H, 2.25; N, 1.73. $C_{24}H_{17}NO_9SRu_3$. Calc. C, 36.09; H, 2.14; N, 1.75%. Found **2b**: C, 38.53; H, 2.49; N, 1.65. $C_{24}H_{17}NO_9SRu_3 \cdot 0.5\ C_6H_{14}$, Calc. C, 38.52; H, 2.85; N, 1.66%. Mass Spectrum (FAB) *m/z*: **2b**: 801(M^+) (^{102}Ru).

3.2. Synthesis of $Ru_3(\mu_2\text{-}CO)(CO)_7(\mu_3\text{-}\eta^1,\eta^2\text{-}Pr^nC{=}CHPr^n)[\mu_3\text{-}NS(O)MePh]$ (3)

A solution of $(\mu_2\text{-}H)Ru_3(CO)_9[\mu_3\text{-}NS(O)MePh]$ (**1**) (150 mg, 0.21 mmol) and $Pr^nC{\equiv}CPr^n$ (93 μl, 0.63 mmol) in THF (25 ml) was heated in a pressure Schlenk tube to 55°C for 5 h. After evaporation of the solvent, the residue was dissolved in CH_2Cl_2 and separated by thin-layer chromatography (silica gel, CH_2Cl_2/cyclohexane 1:1). The main orange band was extracted by CH_2Cl_2 and further purified by thin-layer chromatography (silica gel, CH_2Cl_2/hexane/acetone 20:70:5). The main orange band was extracted with CH_2Cl_2, and **3** was recrystallized from hexane at −18°C. The orange–yellow crystals were dried in vaccuo (**3**: 30 mg, 17%). Anal. Found: C, 35.08; H, 2.94; N, 1.82. $C_{23}H_{23}NO_9SRu_3$, Calc. C, 34.85; H, 2.92; N, 1.77%.

3.3. Synthesis of $Ru_3(\mu_2\text{-}CO)(CO)_7(\mu_3\text{-}\eta^1,\eta^2\text{-}PhC{=}CHBu^n)[\mu_3\text{-}NS(O)MePh]$ (4)

A solution of $(\mu_2\text{-}H)Ru_3(CO)_9[\mu_3\text{-}NS(O)MePh]$ (**1**) (150 mg, 0.21 mmol) and $PhC{\equiv}CBu^n$ (111 μl, 0.63 mmol) in THF (25 ml) was heated in a pressure Schlenk tube to 55°C for 5 h. After evaporation of the solvent, the residue was dissolved in CH_2Cl_2 and separated by a thin-layer chromatography (silica gel, CH_2Cl_2/cyclohexane 1:1). The main red–orange band was extracted by CH_2Cl_2 and further purified by thin-layer chromatography (silica gel, CH_2Cl_2/hexane/acetone 20:70:5). The main red–orange band was extracted with CH_2Cl_2, and **4** was recrystallized from CH_2Cl_2/hexane at −18°C. The orange crystals were dried in vaccuo (**4**: 30 mg, 17%). Anal. Found: C, 38.51; H, 2.80, N, 1.70. $C_{27}H_{23}NO_9SRu_3$, Calc. C, 38.57; H, 2.76; N, 1.67%.

3.4. Synthesis of $Ru_3(\mu_2\text{-}H)(CO)_6(\mu_2\text{-}\eta^1,\eta^2\text{-}PhC{=}CHPh)(\mu_3\text{-}\eta^1,\eta^2\text{-}PhC{\equiv}CPh)[\mu_3\text{-}NS(O)MePh]$ (5)

A solution of $(\mu_2\text{-}H)Ru_3(CO)_9[\mu_3\text{-}NS(O)MePh]$(**1**) (150 mg, 0.21 mmol) and $PhC{\equiv}CPh$ (75 mg, 0.28 mmol) in THF (30 ml) was heated in a pressure Schlenk tube to 100°C for 7 h. After evaporation of the solvent, the residue was dissolved in CH_2Cl_2 and separated by a thin-layer chromatography (silica gel,

Table 6
Crystallographic and refinement data for **2a, 3, 4, 5**

Compound	**2a**	**3**	**4**	**5**
Empirical formula	$C_{24}H_{17}NO_9Ru_3S$	$C_{23}H_{23}NO_9Ru_3S \cdot 0.5\ C_6H_{14}$	$C_{27}H_{23}NO_9Ru_3S \cdot 0.5\ CH_2Cl_2$	$C_{41}H_{29}NO_7Ru_3S$
Formula weight (g mol^{-1})	798.66	835.78	883.19	982.92
Temperature (K)	293(2)	293(2)	223(2)	193(2)
Crystal system	orthorhombic	triclinic	monoclinic	triclinic
Space group	*P*bca	$P\bar{1}$	$P2_1/c$	$P\bar{1}$
a, *b*, *c* (Å)	30.573(5), 14.865(2), 12.2252(12)	8.812(3), 9.225(3), 20.904(7)	10.0523(13), 10.9279(14), 28.915(6)	8.998(3), 12.239(3), 17.214(4)
α, β, γ (°)	90, 90, 90	93.39(3), 98.83(3), 110.36(3)	90, 96.43(1), 90	83.92(2), 87.70(2), 81.68(2)
Volume (Å^3)	5556.0(12)	1562.6(9)	3156.4(9)	1864.6(9)
Z	8	2	4	2
D_{calc} (g cm^{-3})	1.910	1.776	1.856	1.751
Absorption coefficient (Mo K α, mm^{-1})	1.735	1.546	1.619	1.307
F(000)	3104	826	1728	972
Crystal size	0.1 × 0.2 × 0.05	0.1 × 0.2 × 0.2	0.64 × 0.34 × 0.95	0.95 × 0.84 × 0.57
θ scan range (°)	2.54 to 24.00	2.46 to 28.01	2.04 to 24.96	1.69 to 27.51
h, *k*, *l* ranges	−40 to 40, −19 to 19, −15 to 15	−10 to 10, −12 to 12, 0 to 27	−11 to 11, 0 to 12, 0 to 14	−11 to 11, −15 to 15, 0 to 22
Reflections collected	30467	6944	5526	8676
Independent reflections	4342	6944	5526	8491[*R*(int) = 0.0316]
Reflections observed [$I > 2\sigma(I)$]	2850	5320	4269	8043
Data/restraints/parameters	4342/0/343	6944/0/349	5526/0/387	8406/0/594
Goodness of fit on F^2	1.049	1.011	1.095	1.075
Final *R* indices [$I > 2\sigma(I)$]	*R*1 = 0.0658, *wR*2 = 0.1466	*R*1 = 0.0331, *wR*2 = 0.0893	*R*1 = 0.0588, *wR*2 = 0.1486	*R*1 = 0.0469, *wR*2 = 0.1264
R indices (all data)	*R*1 = 0.1067, *wR*2 = 0.1697	*R*1 = 0.0502, *wR*2 = 0.0943	*R*1 = 0.1009, *wR*2 = 0.2019	*R*1 = 0.0489, *wR*2 = 0.1291
Largest differential; peak and hole (e Å^3)	1.997 and −1.147	0.732 and −0.511	1.764 and −1.463	2.120 and −1.970
Empirical absorption correction	–	–	DIFABS	Semi empirical from Ψ scans
Transmission factors: min max	–	–	0.702/1.561	0.1768/0.6497

CH_2Cl_2/cyclohexane 1:1). From the major yellow band, **5** was extracted by CH_2Cl_2 and **5** was recrystallized from CH_2Cl_2/hexane (1:1) at room temperature. The yellow crystals were dried in vaccuo (**5**: 60 mg, 44%). Anal. Found: C, 49.87; H, 2.79; N, 1.49. $C_{41}H_{29}NO_7SRu_3$, Calc. C, 50.10; H, 2.97; N, 1.42%.

3.5. X-ray structure analysis of 2a, 3, 4 and 5

Suitable crystals of **2**, **3**, **4** and **5** were obtained as indicated Sections 3.1, 3.2, 3.3 and 3.4. Intensity data were collected on a STOE IPDS at room temperature for **2a** and **3**, and, on a Stoe–Siemens AED2 4-circle diffractometer at −50°C for **4** and −80°C for **5** (Mo Kα graphite monochromated radiation, $\lambda = 0.71073$ Å; $\omega/2\theta$ scans). Table 6 summarizes the crystallographic and selected experimental data for **2a**, **3**, **4** and **5**. The structures were solved by direct methods using the program SHELXS-86 [41]. The refinement, using weighted full-matrix least-square on F^2, was carried out using the program SHELXL-93 [42]. For **4**, an empirical absorption correction was applied using DIFABS [43] and for **5** based on Ψ scans. The vinyl hydrogen atoms of **3**, **4** and **5** were located from difference maps and refined isotropically. In the case of **3** the temperature factor was fixed at 0.08 Å^2. The methyl, methylene and phenyl hydrogens of **2a**, **3** and **4** were included in calculated positions and refined as riding atoms using the SHELXL 93 default parameters. For **5**, the remainder of the hydrogens were located from difference maps and refined isotropically. The figures were drawn with ZORTEP [44] (thermal ellipsoides, 40% probability level). Full tables of atomic parameters and bond lengths and angles may be obtained from the Cambridge Crystallographic Data Centre, 12 Union Road, Cambridge CB2 1EZ (UK) on quoting the full journal citation.

Acknowledgements

Financial support of this work by the Swiss National Science Foundation and a generous loan of ruthenium(III) chloride hydrate from The Johnson Matthey Research Centre are gratefully acknowledged. We thank Professor Michael I. Bruce, University of Adelaide, for valuable discussions.

References

[1] M.F. Semmelhack, Organic synthesis using transition-metal complexes containing π-bonded ligands, in: R.B. King (Ed.), Encyclopedia of Inorganic Chemistry, Vol. 5, Wiley, Chichester, 1994, p. 2784.
[2] B. Walther, Z. Chem. 28 (1989) 117.
[3] A.J. Deeming, S. Hasso, J. Organomet. Chem. 114 (1976) 313.
[4] J.B. Keister, J.R. Shapley, J. Am. Chem. Soc. 98 (1976) 1056.
[5] J.A. Cabeza, J.M. Fernández-Colinas, A. Llamazares, V. Riera, S. García-Granda, J.F. Van der Maelen, Organometallics 13 (1994) 4352.
[6] S. Alvarez, P. Briard, J.A. Cabeza, I. del Río, J.M. Fernández-Colinas, F. Mulla, L. Ouahab, V. Riera, Organometallics 13 (1994) 4360.
[7] G. Lavigne, N. Lugan, S. Rivomanana, F. Mulla, J.M. Soulié, P. Kalck, J. Cluster Sci. 4 (1993) 49.
[8] N. Lugan, F. Laurent, G. Lavigne, T.P. Newcomb, E.W. Limatta, J.-J. Bonnet, J. Am. Chem. Soc. 112 (1990) 8607.
[9] W.G. Jackson, B.F.G. Johnson, J.W. Kelland, J. Lewis, K.T. Schorpp, J. Organomet. Chem. 87 (1975) C27.
[10] J. Lewis, B.F.G. Johnson, Gazz. Chim. Ital. 109 (1979) 271.
[11] M. Liang, P. Sommerville, Z. Dawoodi, M.J. Mays, P.J. Wheatley, J. Chem. Soc., Chem. Commun. (1978) 1035.
[12] Z. Dawoodi, M.J. Mays, J. Chem. Soc., Dalton Trans. (1984) 1931.
[13] R.-C. Lin, Y. Chi, S.-M. Peng, G.-H. Lee, J. Chem. Soc., Dalton Trans. (1993) 227.
[14] B. Hansert, H. Vahrenkamp, Chem. Ber. 126 (1993) 2017.
[15] G. Süss-Fink, G. Rheinwald, H. Stoeckli-Evans, C. Bolm, D. Kaufmann, Inorg. Chem. 35 (1996) 3081.
[16] F.H. Allen, O. Kennard, D.G. Watson, L. Brammer, A. Orpen, R. Taylor, J. Chem. Soc., Perkin Trans. II (1987) S1.
[17] D. Heineke, H. Vahrenkamp, Chem. Ber. 126 (1993) 365.
[18] D. Heineke, H. Vahrenkamp, J. Organomet. Chem. 451 (1993) 147.
[19] N. Lugan, F. Laurent, G. Lavigne, T.P. Newcomb, E.W. Limatta, J.-J. Bonnet, Oganometallics 11 (1992) 1351.
[20] P. Nombel, N. Lugan, F. Mulla, G. Lavigne, Organometallics 13 (1994) 4673.
[21] J.A. Cabeza, S. García-Granda, A. Llamazares, V. Riera, J.F. Van der Maelen, Organometallics 12 (1993) 2973.
[22] J.A. Cabeza, S. García-Granda, A. Llamazares, V. Riera, J.F. Van der Maelen, Organometallics 12 (1993) 157.
[23] P. Briard, J.A. Cabeza, A. Llamazares, L. Ouahab, V. Riera, Organometallics 12 (1993) 1006.
[24] J.A. Cabeza, J.M. Fernández-Colinas, A. Llamazares, V. Riera, J. Mol. Catal. 71 (1992) L7.
[25] J.A. Cabeza, J.M. Fernández-Colinas, A. Llamazares, Synlett. (1995) 579.
[26] J.A. Cabeza, A. Llamazares, V. Riera, P. Briard, L. Ouahab, J. Organomet. Chem. 480 (1994) 205.
[27] J.A. Cabeza, I. Del Río, A. Llamazares, V. Riera, J. Organomet. Chem. 511 (1-2) (1996) 103.
[28] Y. Chi, H.-F. Hsu, L.-K. Liu, S.-M. Peng, G.-H. Lee, Organometallics 11 (1992) 1763.
[29] D.L. Davies, M.J. Parrott, P. Sherwood, F.G.A. Stone, J. Chem. Soc., Dalton Trans. (1987) 1201.
[30] D.M. Dalton, J.B. Keister, J. Organomet. Chem. 290 (1985) C37.
[31] J.A. Clucas, P.A. Dolby, M.M. Harding, A.K. Smith, J. Chem. Soc., Chem. Commun. (1987) 1829.
[32] A.K. Smith et al., J. Chem. Soc., Dalton Trans. (1993) 827.
[33] R.A. Harding, A.K. Smith, J. Chem. Soc., Dalton Trans. (1996) 117.
[34] J.F. Blount, L.F. Dahl, C. Hoogzand, W. Hübel, J. Am. Chem. Soc. 88 (1966) 292.
[35] S. Rivomanana, G. Lavigne, N. Lugan, J.-J. Bonnet, Inorg. Chem. 30 (1991) 4110.
[36] S. Rivomanana, C. Mongin, G. Lavigne, Organometallics 15 (1996) 1195.
[37] Y. Chi, R.-C. Lin, S.-M. Peng, G.-H. Lee, J. Cluster Sci. 3 (1992) 333.

[38] P.L. Andreu, J.A. Cabeza, I. del Río, V. Riera, Organometallics 15 (1996) 3004.
[39] M.I. Bruce, Angew. Chem., Int. Ed. Engl. 16 (1977) 73.
[40] D.D. Perrin, W.L.F. Armarego, Purification of laboratory Chemicals, 3rd edn., Pergamon, Oxford, 1988.
[41] G.M. Sheldrick, Acta Crystallogr. A 46 (1990) 467.
[42] G.M. Sheldrick, SHELXL-93, University of Göttingen, Germany, 1993.
[43] N. Walker, D. Stuart, Acta Crystallogr. A 46 (1990) 158.
[44] C.K. Johnson, ORTEP, Oak Ridge National Laboratory, Oak Ridge, TN, modified for PC by L. Zsolnai, H. Pritzkow, University of Heidelberg, Germany (1994).

Reprinted from

Journal of Organometallic Chemistry

Journal of Organometallic Chemistry 549 (1997) 275–282

Carbon–carbon coupling reactions on triruthenium clusters: synthesis and structure of $Ru_3(CO)_9[\mu_3-\eta^3$-PhCCCC(H)Ph][μ_2-NS(O)MePh] and $Ru_3(\mu_2$-CO)$(CO)_7[\mu_3-\eta^3$-PhCCCC(H)Ph][μ_3-NS(O)MePh]

Vincent Ferrand [a], Céline Gambs [a], Nadine Derrien [b], Carsten Bolm [b], Helen Stoeckli-Evans [a], Georg Süss-Fink [a,*]

[a] *Institut de Chimie, Université de Neuchâtel, Neuchâtel, CH-2000, Switzerland*
[b] *Institut für Organische Chemie, RWTH Aachen, Aachen, D-52058, Germany*

Received 30 June 1997

ELSEVIER

ELSEVIER

Journal of Organometallic Chemistry 549 (1997) 275–282

Journal of Organometallic Chemistry

Carbon–carbon coupling reactions on triruthenium clusters: synthesis and structure of $Ru_3(CO)_9[\mu_3-\eta^3$-PhCCCC(H)Ph][μ_2-NS(O)MePh] and $Ru_3(\mu_2$-CO)(CO)$_7[\mu_3-\eta^3$-PhCCCC(H)Ph][μ_3-NS(O)MePh]

Vincent Ferrand [a], Céline Gambs [a], Nadine Derrien [b], Carsten Bolm [b], Helen Stoeckli-Evans [a], Georg Süss-Fink [a,*]

[a] *Institut de Chimie, Université de Neuchâtel, Neuchâtel, CH-2000, Switzerland*
[b] *Institut für Organische Chemie, RWTH Aachen, Aachen, D-52058, Germany*

Received 30 June 1997

Abstract

The reaction of the electron-deficient cluster (μ_2-H)$Ru_3(CO)_9[\mu_3$-NS(O)MePh] (**1**) with *para*-nitrotolane gives, with coupling of two alkyne units and elimination of the *para*-nitrophenyl fragment, the trinuclear complexes $Ru_3(CO)_9[\mu_3-\eta^3$-PhCCCC(H)Ph][μ_2-NS(O)MePh] (**2**) and $Ru_3(\mu_2$-CO)(CO)$_7[\mu_3-\eta^3$-PhCCCC(H)Ph][μ_3-NS(O)MePh] (**3**). The resulting organic moiety, coordinated as $\mu_3-\eta^3$-5e-donor, is best considered as a butenynyl (PhC≡C–C=C(H)Ph) ligand in **2** and as a butatrienyl (PhC=C=C=C(H)Ph) ligand in **3**. From the reaction mixture, the two isomeric vinyl complexes $Ru_3(\mu_2$-CO)$_2$(CO)$_6[\mu_2-\eta^2$-PhC=C(H)(C$_6$H$_4$-*p*-NO$_2$)][μ_3-NS(O)MePh] (**4a**) and $Ru_3(\mu_2$-CO)$_2$(CO)$_6[\mu_2-\eta^2$-(C$_6$H$_4$-*p*-NO$_2$)–C=C(H)Ph]-[μ_3-NS(O)MePh] (**4b**) complexes can also be isolated. © 1997 Elsevier Science S.A.

Keywords: Clusters; Ruthenium; Alkynes; Carbon–carbon coupling; Crystal structures

1. Introduction

Reactions involving carbon–carbon bond formation in transition metal clusters are of considerable interest because of their potential for generating new and unusual types of hydrocarbon fragments [1,2]. Reactions of this type are also considered as models for related processes occurring on metal surfaces [3–5]. In particular, alkynes can be coupled in the coordination sphere of transition metal clusters to give C_4, C_6, C_8, and C_{12} hydrocarbyls [6–37]. Thus, the cluster $Cp'_2Mo_2Co_2(CO)_4S_3$ reacts with phenylacetylene, in a first step to give the $\mu_3-\eta^2$-alkyne cluster $Cp'_2Mo_2Co_2(CO)_2S_3$(PhCCH) which, in a second step, adds another equivalent of phenylacetylene to give Cp'_2Mo_2-$Co_2(CO)_2S_3$(CPhCHCHCPh) in which the two alkynes are coupled to give a cyclopentadiene unit [38]. On a Ru_4 metal core, diphenylacetylene can be coupled to give a C_8 hydrocarbyl: The cluster $Ru_4(CO)_8(\mu_4$-PPh)[$\eta^1,\eta^1,\eta^2,\eta^2$-(Ph)CC(Ph)C(Ph)C-$\eta^4$-CC(Ph)C(Ph)-C(Ph)] is formed from the reaction of $Ru_4(CO)_{13}(\mu_3$-PPh)with C_2Ph_2 [39].

In the preceding publication [40], we reported the reaction of the electron-deficient cluster (μ_2-H)$Ru_3(CO)_9[\mu_3$-NS(O)MePh] (**1**) with non-functional alkynes to give various types of vinyl complexes. In an effort to generalize this concept, we extended this reaction also to functional alkynes. In this paper, we report the reaction of **1** with PhC≡C(C$_6$H$_4$-*p*-NO$_2$) to give Ru_3 clusters containing C_4 hydrocarbyl ligands resulting from the carbon–carbon coupling of two alkyne units.

2. Results

2.1. Reaction of (μ_2-H)$Ru_3(CO)_9[\mu_3$-NS(O)MePh] (1) with PhC≡C(C$_6$H$_4$-*p*-NO$_2$)

The thermal reaction of the electron-deficient cluster (μ_2-H)$Ru_3(CO)_9[\mu_3$-NS(O)-MePh] (**1**) and the alkyne

* Corresponding author.

PII S0022-328X(97)00507-X

Table 1
IR and NMR data of the complexes 2–4

Complexes	ν_{CO} [cm^{-1}]	$\delta(^1H)$ [ppm]
2[a]	2070(vs), 2048(s), 2008(s)	2.94 (CH_3) s; 7.09–8.54 (C=C(Ph)H and C_6H_5)
3[a]	2080(m), 2040(vs), 2011(vs), 1974(m), 1805(w)	2.98 (CH_3 s; 7.08–8.54 (C=C(Ph)H and C_6H_5)
4a + 4b[b]	2065(vw), 2057(w), 2039(s), 2015(s), 2005(sh), 1988(m), 1950(m), 1828(w)	3.192, 3.348 (CH_3)s; 6.015, 6.237 (C=CHPh or C=CH(C_6H_4-p-NO_2) s, 6.60–8.00 (C_6H_5 and C_6H_4-p-NO_2) m

[a] In CH_2Cl_2.
[b] In cyclohexane solution.
[c] In a $CDCl_3$ solution.

PhC=C(C_6H_4-p-NO_2), containing an electron-withdrawing group in one of the two aromatic substituents, affords in refluxing THF the two C_4-hydrocarbyl clusters $Ru_3(CO)_9[\mu_3$-η^3-PhCCCC(H)Ph][μ_2-NS(O)MePh] (**2**) and $Ru_3(\mu_2$-CO)$(CO)_7[\mu_3$-η^3-PhCCCC(H)Ph][μ_3-NS(O)MePh] (**3**). The reaction solution also contains the two isomeric vinyl complexes $Ru_3(\mu_2$-CO)$_2(CO)_6[\mu_2$-η^2-PhCC(H)($C_6H_4NO_2$)][μ_3-NS(O)MePh] (**4**), which are presumably intermediates in the formation of **2** and **3**. The products **2**, **3** and **4** can

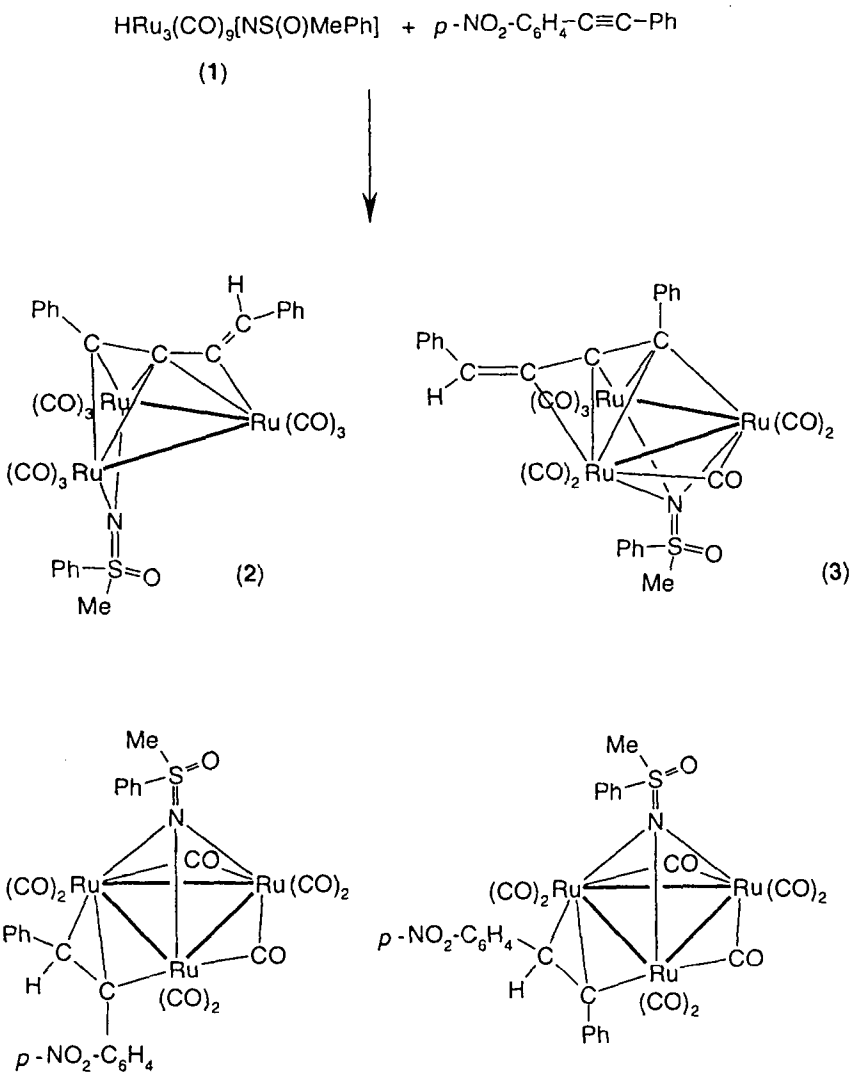

Scheme 1.

be separated from the reaction mixture by thin-layer chromatography—however, **4** does not resolve into the two isomers **4a** and **4b** clearly distinguishable in the NMR spectrum of **4**.

Compounds **2**, **3** and **4** were characterized by their analytical and spectroscopic data, **2** and **3** also gave suitable crystals for X-ray structure analysis. The IR spectrum of **2** exhibits three υ_{CO} absorptions corresponding to only terminal CO ligands, whereas the IR spectrum of **3** presents four bands assigned to the terminal CO ligands and one absorption at 1805 cm^{-1} which can be attributed to the bridging CO group (Table 1). The ^1H NMR spectra of both **2** and **3** are very similar, showing the same pattern of signals but differing in the chemical shifts, in accordance with the molecular structures of **2** and **3** (Table 1).

The constitution of **4** is proposed on the basis of the spectroscopic and analytical data: In the FAB mass spectrum, the molecular peak is found at m/z 908 (^{102}Ru); in addition a complete fragmentation series corresponding to the subsequent loss of eight CO ligands is observed, all ions presenting the characteristic Ru_3 isotope pattern. The infrared spectrum of **4** (Table 1) displays a υ_{CO} pattern almost identical to that of the vinyl cluster $Ru_3(\mu_2\text{-}CO)_2(CO)_6[\mu_3\text{-}NS(O)MePh](\mu_2\text{-}\eta^1,\eta^2\text{-}PhCH_2C{=}CH_2)$ characterized by X-ray crystallography (Ref. [40], see preceding paper); we therefore assign the absorption at 1828 cm^{-1} to two bridging carbonyl ligands, being located over the two ruthenium–ruthenium bonds which are not bridged by the vinyl ligand. The ^1H NMR spectrum of **4** (Table 1) clearly reveals the presence of two isomers by two signals for the vinyl hydrogen (δ 6.015 and 6.237 ppm) and two signals for the methyl substituent on the sulfur atom (δ 3.192 and 3.348 ppm). This is also reflected in the ^{13}C NMR spectrum of **4** which shows the signals for the methyl substituent on the sulfur atom (δ 45.6 and 48.4 ppm) and two singlets at δ 67.8 and 72.0 ppm for the alkenyl carbon atoms (C=*C*H).

We interpret these findings by the presence of two isomers which differ only in the orientation of the $\mu_2\text{-}\eta^2$-vinyl ligand: $Ru_3(\mu_2\text{-}CO)_2(CO)_6[\mu_2\text{-}\eta^2\text{-}PhCC(H)\text{-}(C_6H_4NO_2)][\mu_3\text{-}NS(O)MePh]$ (**4a**) and $Ru_3(\mu_2\text{-}CO)_2(CO)_6[\mu_2\text{-}\eta^2\text{-}(C_6H_4NO_2)CC(H)Ph][\mu_3\text{-}NS(O)\text{-}MePh]$ (**4b**) (Scheme 1), but it is not possible to assign the NMR signals unambiguously to **4a** or **4b**.

2.2. *Molecular structure of $Ru_3(CO)_9[\mu_3\text{-}\eta^3\text{-}PhCCCC(H)Ph][\mu_2\text{-}NS(O)MePh]$ (2)*

The molecular structure of **2** was confirmed by a single crystal X-ray structure analysis. Suitable crystals of **2** were grown at 4°C from a mixture of CH_2Cl_2 and hexane. The unit cell contains two independent

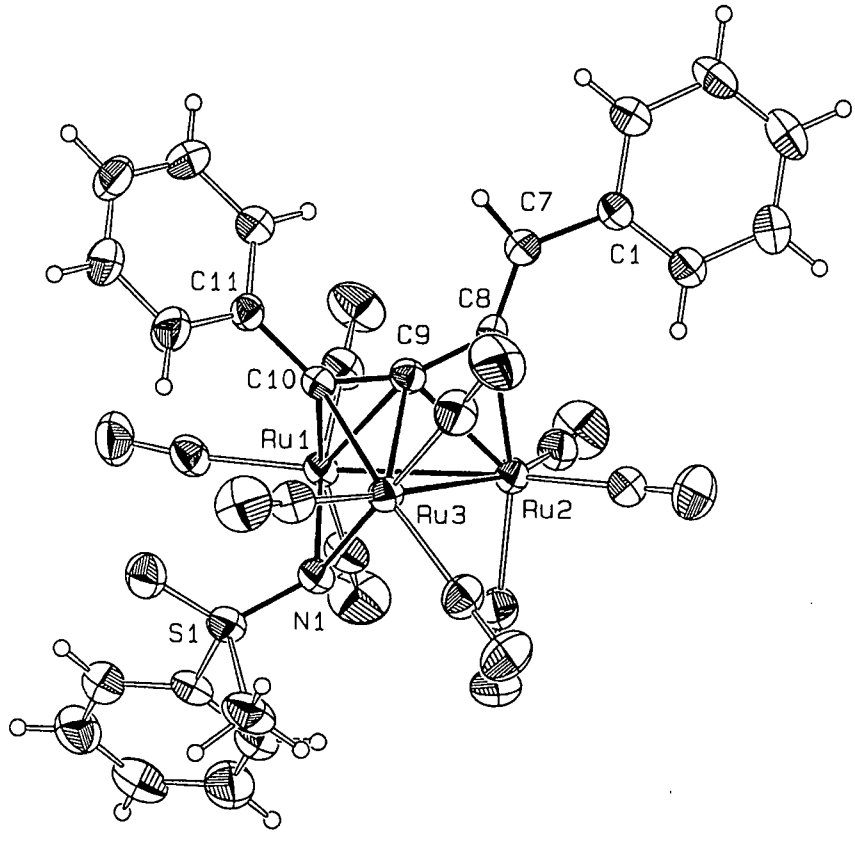

Fig. 1. ORTEP plot of **2** (Molecule A). Thermal ellipsoids are drawn at 40% of probability.

molecules of **2** which have the same constitution but differ in bond angles and bond lengths. The structure of the two molecules of **2** is presented in Figs. 1 and 2. Selected bond lengths and angles of the two molecules are listed in Table 2.

The organic fragment arising from the C–C coupling of two alkyne units is best described as a butenynyl ligand PhC≡C–C=C(H)Ph. Each of the three ruthenium atoms are bonded to three terminal CO groups. The nitrogen cap is bridging only the two ruthenium atoms Ru(1) and Ru(3) in a μ_2-fashion [Ru(1)–N 2.166(5); Ru(3)–N 2.161(5) Å], in contrast to **1** where the nitrogen links the three metal centers in a μ_3-mode. We also observe that in **2** the nitrogen–sulfur double bond is shorter [N(1)–S(1) 1.514(5) Å] than in **1** [N–S 1.566(7)], probably due to the coordination to only two metal atoms, the NS(O)MePh ligand still being a three-electron donor ligand. The C_4 ligand is coordinated to the Ru_3 framework by only three carbon atoms and acts as a five-electron ligand (Figs. 1 and 2). The carbon–carbon double bond of the vinyl part of the C_4 ligand is not involved in the coordination. The carbon atom C(8) is σ-bonded to Ru(2) [Ru(2)–C(8) 2.095(6) Å] and donates one electron, whereas the C(9)–C(10) triple bond is π-bonding to both, Ru(1) and Ru(3) [Ru(1)–C(9) 2.339(5); Ru(1)–C(10) 2.234(6); Ru(3)–C(9) 2.326(6); Ru(3)–C(10) 2.202(5)] and acts as a four-electron donor. Compound **2** can be compared to $HOs_3(CO)_9(\mu_3-\eta^3-H_2CC{\equiv}C\text{-}Me)$, which is the only complex presenting the same CCC coordination mode, according to the interpretation of the spectroscopic data, since no crystal

Table 2
Selected bond lengths [Å] and bond angles [deg] for **2**

Molecule A		Molecule B	
C(7)–C(8)	1.328(8)	C(46)–C(47)	1.339(8)
C(7)–H(7)	0.98(6)	C(46)–H(46A)	0.99(5)
C(8)–C(9)	1.394(8)	C(47)–C(48)	1.383(8)
C(8)–Ru(2)	2.095(6)	C(47)–Ru(6)	2.082(6)
C(9)–C(10)	1.350(8)	C(48)–C(49)	1.341(8)
C(9)–Ru(2)	2.197(6)	C(48)–Ru(6)	2.207(6)
C(9)–Ru(3)	2.326(6)	C(48)–Ru(4)	2.342(6)
C(9)–Ru(1)	2.339(5)	C(48)–Ru(5)	2.358(6)
C(10)–C(11)	1.468(7)	C(49)–C(50)	1.483(8)
C(10)–Ru(3)	2.202(5)	C(49)–Ru(5)	2.187(6)
C(10)–Ru(1)	2.234(6)	C(49)–Ru(4)	2.212(6)
Ru(1)–Ru(2)	2.8644(7)	Ru(4)–Ru(6)	2.8570(7)
Ru(2)–Ru(3)	2.9030(7)	Ru(5)–Ru(6)	2.8908(8)
Ru(1)–Ru(3)	3.1703(2)	Ru(4)–Ru(5)	3.1654(2)
O(1)–S(1)	1.462(5)	O(2)–S(2)	1.461(5)
N(1)–S(1)	1.514(5)	N(2)–S(2)	1.516(5)
N(1)–Ru(3)	2.161(5)	N(2)–Ru(5)	2.163(5)
N(1)–Ru(1)	2.166(5)	N(2)–Ru(4)	2.170(5)
C(8)–C(7)–C(1)	129.2(6)	C(46)–C(47)–C(48)	134.4(6)
C(7)–C(8)–C(9)	133.5(5)	C(49)–C(48)–C(47)	162.0(6)
C(10)–C(9)–C(8)	158.4(6)	C(48)–C(49)–C(50)	130.5(5)
C(9)–C(10)–C(11)	131.7(5)	C(51)–C(50)–C(49)	122.0(6)

Estimated standard deviations in parentheses.

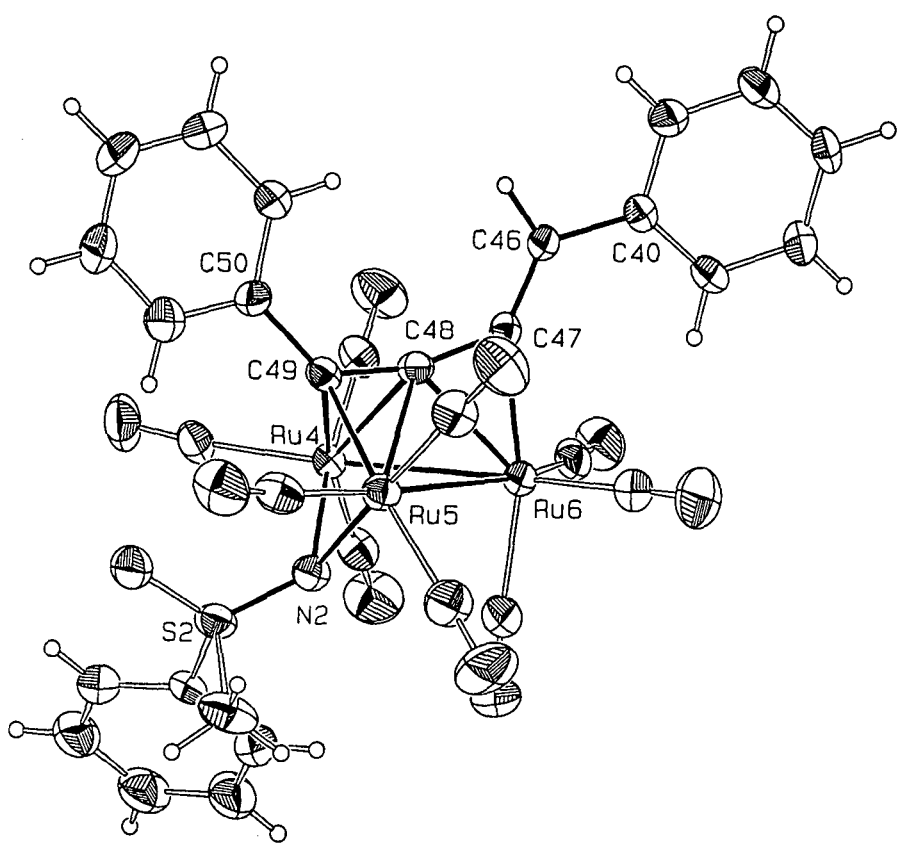

Fig. 2. ORTEP plot of **2** (Molecule B). Thermal ellipsoids are drawn at 40% of probability.

structure analysis is available [41]. The short distance between Ru(2) and C(9) [Ru(2)–C(9) 2.1972(1) Å] is presumably due to a geometric arrangement of the C_4 chain with respect to the Ru_3 core. This description of the C_4 ligand as a σ,π,π-donor is however, an over-simplification because of the mixing of the σ and π contributions of each metal-ligand interaction [42,43].

The electron count of **2** being 50e is in accordance with an open M_3 triangle. We therefore consider the Ru(1) · · · Ru(3) vector as an open edge, even if the distance is shorter [Ru(1) · · · Ru(3) 3.1703(2) Å] than in open Ru_3 clusters (average Ru · · · Ru 3.430 Å). The C(8)C(9)C(10) angle is 158.4°(6), confirming the description of a butenynyl fragment; for a allenyl (butatrienyl) moiety, the average CCC angle is normally between 138°(2) and 152°(1) [42].

2.3. Molecular structure of $Ru_3(\mu_2\text{-}CO)(CO)_7[\mu_3\text{-}\eta^3\text{-}PhCCCC(H)Ph][\mu_3\text{-}NS(O)MePh]$ (3)

The molecular structure of **3** was confirmed by a X-ray structure analysis of a suitable crystal obtained by room temperature crystallization from a mixture of CH_2Cl_2 and hexane. The molecular structure of **3** is depicted in Fig. 3, selected bond lengths and angles are presented in Table 3.

The three ruthenium atoms in **3** form an open triangle [Ru(1)–Ru(2) 2.7164(5); Ru(1)–Ru(3) 2.8290(5); Ru(2) · · · Ru(3) 3.4324(3) Å], all ruthenium–ruthenium distances being different. Two of the three ruthenium atoms, Ru(1) and Ru(2), are bonded to two terminal CO groups, whereas Ru(3) is bonded to three terminal CO ligands. A carbonyl group bridges the Ru(1)–Ru(2) edge and lies in the same plane as the metal framework (dihedral angle 175.7°). The position of the carbonyl ligand is not symmetrical between both ruthenium atoms, and C(29) is closer to Ru(1) than to Ru(2) [Ru(1)–C(29)

Table 3
Selected bond lengths [Å] and bond angles [deg] for **3**

C(8)–C(9)	1.407(5)	N(1)–Ru(1)	2.129(3)
C(8)–C(11)	1.497(5)	N(1)–Ru(3)	2.165(3)
C(8)–Ru(3)	2.227(4)	N(1)–Ru(2)	2.228(3)
C(8)–Ru(1)	2.314(4)	O(1)–S	1.445(3)
C(8)–Ru(2)	2.319(4)	Ru(1)–Ru(2)	2.7164(5)
C(9)–C(10)	1.336(6)	Ru(1)–Ru(3)	2.8290(5)
C(9)–Ru(3)	2.099(4)	Ru(2)–Ru(3)	3.4324(3)
C(9)–Ru(2)	2.250(4)		
C(10)–C(17)	1.326(6)	C(9)–C(8)–C(11)	121.1(3)
C(10)–Ru(2)	2.286(4)	C(10)–C(9)–C(8)	139.7(4)
C(17)–H(17)	0.99(4)	C(17)–C(10)–C(9)	150.5(4)
N(1)–S	1.554(3)	C(10)–C(17)–C(18)	122.4(4)

Estimated standard deviations in parentheses.

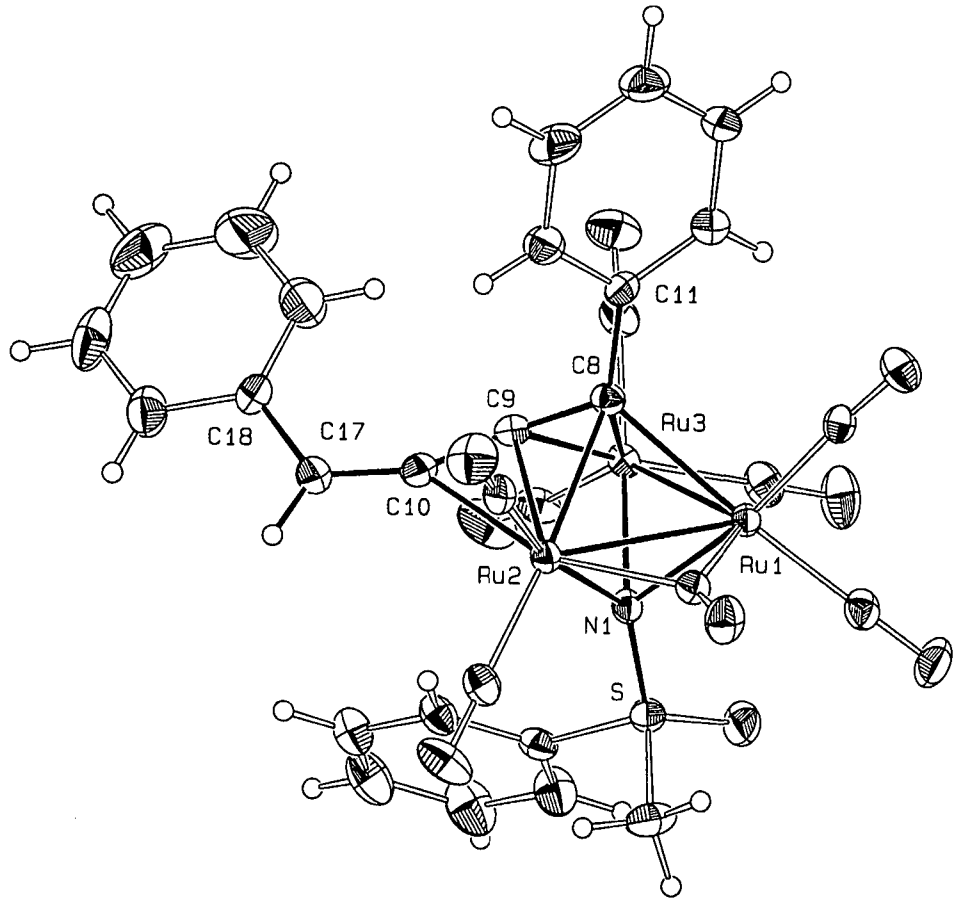

Fig. 3. ORTEP plot of **3**. Thermal ellipsoids are drawn at 40% of probability.

2.0208(2); Ru(2)–C(29) 2.1199(2) Å]. We also observed that the nitrogen cap is asymmetrically coordinated to the Ru_3 core, all the Ru–N bond lengths being different [Ru(1)–N 2.129(3); Ru(2)–N 2.228(3); Ru(3)–N 2.165(3) Å].

The coordination of the C_4 fragment in **3** is different from that in **2**, inasmuch as it is best described as butatrienyl ligand PhC=C=C=C(H)Ph, although it also acts as a 5e-donor and it is also coordinated by three carbon atoms. The double bond C(10)=C(17) does not interact with any ruthenium as in **2** [Ru(1)–C(17) 5.5385(5); Ru(2)–C(17) 3.3886(4); Ru(3)–C(17) 4.2806(5) Å]. In a first approximation, we can consider the C_4 ligand to be σ-bonded by C(8) to Ru(1) and Ru(2) ('shared σ-bond') [Ru(1)–C(8) 2.3136(2); Ru(2)–C(8) 2.3186(2) Å] and π-bonded by C(8)=C(9) to Ru(3) [Ru(3)–C(8) 2.2275(2); Ru(3)–C(9) 2.0989(3)], and π-bonded by C(9)=C(10) to Ru(2) [Ru(2)–C(9) 2.2501(2); Ru(2)–C(10) 2.2857(3)]. A comparison of the butatrienyl ligand in **3** with allenyl complexes such as $Ru_3(CO)_9[\mu_3\text{-}\eta^3\text{-}EtCCC(H)CH_3]$ [44] or $Ru_3(CO)_8[\mu_3\text{-}\eta^3\text{-}CH_2CC(^iPr)](\mu_2\text{-}PPh_2)$ [45] reveals the C(8)C(9)C(10) angle of 139.7°(4) to be similar to the corresponding allenyl angles of 143.7°(3) [45] or 142.3°(6) [44].

3. Discussion

Despite the different coordination of the C_4 ligand in **2** and **3**, the nature of the C_4 hydrocarbyl fragment is the same. The two ligands can in fact be considered as two mesomeric representations of the same hydrocarbyl radical.

$$Ph\text{–}C\equiv C\text{–}C{=}C(H)Ph \leftrightarrow Ph - C{=}C{=}C{=}C(H)Ph$$

In both, **2** and **3**, the C_4 hydrocarbyl ligand is coordinated to the Ru_3 framework by only three carbon atoms, the C=C(H)Ph double bond of the ligand is not interacting with a metal atom. The main difference between clusters **2** and **3** is the electron-deficient character of **3** (48e), while **2** is electron-precise comprising 50e.

It is interesting to note that the C_4 hydrocarbyl ligands in **2** and **3**, formed by a carbon–carbon coupling of two C_2 units, can obviously not be generated from the corresponding C_4 hydrocarbon. The reaction of $Ru_3(CO)_{12}$ with the enyne PhC≡C–CH=C(H)Ph leads to the formation of three isomeric binuclear complexes $Ru_2(CO)_6[C_4Ph_2(CH{=}CHPh)_2]$ as well as to two trinuclear clusters $Ru_3(CO)_6(\mu\text{-}CO)_2[C_4Ph_2(CH{=}CHPh)_2]$ and $Ru_3(CO)_8[\mu_3\text{-}\eta^1,\eta^1,\eta^4,\eta^2\text{-}C_4Ph_2(CH{=}CHPh)_2]$, none of which contains a C_4 hydrocarbyl ligand [46].

The isolation and characterisation of the vinyl complex **4** (two isomers **4a** and **4b**) from the reaction mixture would suggest that the C–C coupling of the two alkyne units on the Ru_3 core implies insertion of the alkyne into the ruthenium-hydrido bond in **1** to give a vinyl complex followed by the coordination of a second alkyne to give an alkyne-vinyl complex in which the C–C coupling takes place. However, the reaction of **4** (isomer mixture) with *para*-nitrotolane under the same reaction conditions did not yield **2** or **3**. We therefore rule out the intermediacy of **4a** or **4b** in the formation of **2** and **3**.

4. Experimental

All manipulations were carried out in a nitrogen atmosphere, using standard Schlenk techniques. The organic solvents were destilled over appropriate drying agents [47], saturated with nitrogen prior to use. The NMR spectra were recorded using a Varian Gemini 200 BB instrument or a Bruker AMX 400 at 297 K. The IR spectra were recorded using a Perkin-Elmer FTIR 1720X spectrophotometer (4000–400 cm^{-1}). Microanalytical data were obtained from the Mikroelementaranalytisches Laboratorium der ETH Zürich. The mass spectrum was recorded by Professor T.A. Jenny, University of Fribourg (Switzerland). The starting compounds $(\mu_2\text{-}H)Ru_3(CO)_9[\mu_3\text{-}NS(O)MePh]$ (**1**) [48] and $PhC{=}C(C_6H_4\text{-}p\text{-}NO_2)$ were synthesized according to published methods [49]. Methyl phenyl sulfoximine (racemate) was obtained from Professor Carsten Bolm, RWTH Aachen (Germany).

4.1. Reaction of $(\mu_2\text{-}H)Ru_3(CO)_9[\mu_3\text{-}NS(O)MePh]$ (1) with $PhC{=}C(C_6H_4\text{-}p\text{-}NO_2)$

A solution of $(\mu_2\text{-}H)Ru_3(CO)_9[\mu_3\text{-}NS(O)MePh]$ (**1**) (200 mg, 0.28 mmol) and $PhC{\equiv}C(C_6H_4\text{-}p\text{-}NO_2)$ (188 mg, 0.84 mmol) in THF (40 ml) was heated in a pressure Schlenk tube to 50°C for 6 h. After evaporation of the solvent the residue was dissolved in CH_2Cl_2 and separated by thin-layer chromatography (first: aluminum oxide, CH_2Cl_2/hexane 1:1; second: silica gel CH_2Cl_2/cyclohexane 1:1). From the first main band (red) **2** was extracted with CH_2Cl_2 and recrystallized from CH_2Cl_2/hexane at 4°C. **3** was extracted from the second main band (red–orange) with CH_2Cl_2 and recrystallized from CH_2Cl_2/hexane at room temperature. The third main band (orange) contained **4** as the isomer mixture **4a** and **4b**, which was extracted with CH_2Cl_2 and obtained as a brownish powder. All compound were dried in vacuo. **2**: yield 36 mg, 14%. Anal. Found **2**: C, 43.94; H, 2.22; N, 1.78. $C_{32}H_{19}NO_{10}SRu_3(0.5\ C_6H_{14})$, Calc. C, 43.98; H, 2.74; N, 1.47%. **3**: yield 27 mg, 11%. Anal. Found **3**: C, 45.34; H, 2.95; N, 1.53. $C_{31}H_{19}NO_9SRu_3(0.75\ C_6H_{14})$. Calc. C, 45.33; H, 2.95; N,1.47%. **4**: yield 17 mg, 7%. Anal. Found **4**: C, 44.34;

Table 4
Crystallographic and refinement data for 2, 3

Compound	2	3
Empirical formula	$C_{32}H_{19}NO_{10}Ru_3S$	$C_{31}H_{19}NO_9Ru_3S \cdot CH_2Cl_2$
Formula weight (g mol^{-1})	912.79	969.71
Temperature (K)	293(2)	293(2)
Crystal system	monoclinic	monoclinic
Space group	$P2_1/a$	$P2_1/n$
a, b, c (Å)	19.649(2), 29.004(2), 11.7751(8)	10.0921(11), 16.326(2),21.525(3)
α, β, γ (°)	90, 90.026(7), 90	90, 99.763(12), 90
Volume (Å^3)	6710.5(10)	3495.1(7)
Z	8	4
D_{calc}/g cm^{-3}	1.807	1.843
Absorption coefficient (Mo Kα, mm^{-1})	1.306	1.397
F(000)	3568	1896
Crystal size	0.57 × 0.53 × 0.30	0.53 × 0.30 × 0.30
θ Scan range (°)	2.07 to 25.50	2.11 to 25.52
h, k, l ranges	−23 to 23, 0 to 35, 0 to 14	−12 to 12, 0 to 19, 0 to 26
Reflections collected	12476	6517
Independent reflections	12476	6517
Reflections observed [$I > 2\sigma(I)$]	10047	5833
Data/restraints/parameters	12473/0/936	6510/0/455
Goodness of fit on F^2	1.155	1.144
Final R indices [$I > 2\sigma(I)$]	$R1 = 0.0492$, $wR2 = 0.0856$	$R1 = 0.0322$, $wR2 = 0.0742$
R indices (all data)	$R1 = 0.0691$, $wR2 = 0.0930$	$R1 = 0.0386$, $wR2 = 0.0804$
Largest diff. peak and hole (e Å^3)	1.054 and −0.473	0.885 and −0.444
Empirical absorption correction	DIFABS	–
Transmission factors: min/max	0.758/1.156	–

H, 3.27; N, 2.91. $C_{29}H_{18}N_2O_{11}SRu_3(1.5\ C_6H_{14})$, Calc. C, 44.92; H, 3.57; N, 2.75%. Mass spectrum (FAB) m/z: **4** 908 (M^+) (^{102}Ru).

4.2. X-ray structure analysis of 2 and 3

Suitable crystals of **2**, **3**, were obtained as indicated in Section 4. Intensity data were collected on a Stoe-Siemens AED2 4-circle diffractometer at room temperature (Mo–K_α graphite monochromated radiation, λ = 0.71073 Å; $\omega/2\theta$ scans). Table 4 summarizes the crystallographic and selected experimental data for **2** and **3**. The structures were solved by direct methods using the program SHELXS-86 [50]. The refinement, using weighted full matrix least-square on F^2, was carried out using the program SHELXL-93 [51]. For **2**, an empirical absorption correction was applied using [DIFABS] [52]. Complex **3** crystallizes with a molecule of CH_2Cl_2 per unit cell. The hydrogen atoms of the C_4 hydrocarbyl chains of **2** and **3** were located from difference maps and refined isotropically. The methyl, and phenyl hydrogens of **2** and **3** were included in calculated positions and refined as riding atoms using the SHELXL 93 default parameters. The figures were drawn with ZORTEP [53] (thermal ellipsoides, 40% probability level). Full tables of atomic parameters and bond lengths and angles may be obtained from the Cambridge Crystallographic Data Centre, 12 Union Road, Cambridge CB2 1EZ (UK) on quoting the full journal citation.

Acknowledgements

Financial support of this work by the Swiss National Science Foundation and a generous loan of ruthenium(III) chloride hydrate from the Johnson Matthey Research Centre are gratefully acknowledged. We thank Professor Michael I. Bruce, University of Adelaide, for valuable discussions.

References

[1] S.A.R. Knox, J. Cluster Sci. 3 (1992) 385.
[2] E. Sappa, J. Cluster Sci. 5 (1994) 211.
[3] E.L. Muetterties, T.N. Rhodin, E. Band, C.F. Brucker, W.R. Pretzer, Chem. Rev. 79 (1979) 91.
[4] E.L. Muetterties, Angew. Chem., Int. Ed. Engl. 17 (1978) 545.
[5] J. Evans, J. Chem. Soc. Rev. (1981) 159.
[6] K.J. Adams, J.J. Barker, S.A.R. Knox, A.G. Orpen. J. Chem. Soc., Dalton Trans. (1996) 975.
[7] J.F. Corrigan, N.J. Taylor, A.J. Carty, Organometallics 13 (1994) 3778.
[8] J.F. Corrigan, S. Doherty, N.J. Taylor, A.J. Carty, Organometallics 12 (1993) 1365.
[9] H. Matsuzaka, Y. Hirayama, M. Nishio, Y. Mizobe, M. Hidia, Organometallics 12 (1993) 36.

[10] S. Aime, G. Gervasio, L. Milone, E. Sappa, Inorg. Chim. Acta 27 (1978) 145.
[11] R. Yanez, N. Lugan, R. Mathieu, Organometallics 9 (1990) 2998.
[12] R.D. Adams, J.E. Babin, M. Tasi, J.-G. Wang, Organometallics 7 (1988) 755.
[13] Yun Chi, Der-Kweng Hwang, Shen-Feng Chen, Ling-Kang Liu, J. Chem. Soc., Chem. Commun. (1989) 1540.
[14] E. Sappa, A.M. Manotti-Lanfredi, G. Predieri, A. Tiripicchio, Inorg. Chim. Acta 61 (1982) 217.
[15] E. Sappa, A.M. Manotti-Lanfredi, G. Predieri, A. Tiripicchio, Inorg. Chim. Acta 42 (1980) 255.
[16] O. Gambino, E. Sappa, A.M. Manotti-Lanfredi, A. Tiripicchio, Inorg. Chim. Acta 36 (1979) 189.
[17] F. Muller, I.M. Han, G. Van Koten, K. Vrieze, Inorg. Chim. Acta 158 (1989) 81.
[18] S.A.R. Knox, R.F.D. Stansfield, F.G.A. Stone, M.J. Winter, P. Woodward, J. Chem. Soc., Dalton Trans. (1982) 173.
[19] R.B. King, G.W. Eavenson, J. Organomet. Chem. 42 (1972) C95.
[20] F. Muller, G. van Koten, L.H. Polm, K. Vrieze, M.C. Zoutberg, D. Heijdenrijk, E. Kragten, C.H. Stam, Organometallics 8 (1989) 1340.
[21] S. Rivomanana, C. Mongin, G. Lavigne, Organometallics 15 (1996) 1195.
[22] G. Gervasio, E. Sappa, A.M. Manotti-Lanfredi, A. Tiripicchio, Inorg. Chim. Acta 68 (1983) 171.
[23] R.B. King, A. Efraty, J. Am. Chem. Soc. 94 (1972) 3021.
[24] R.B. King, I. Haiduc, C.W. Eavenson, J. Am. Chem. Soc. 95 (1973) 2508.
[25] T. Rukachaisirikul, S. Arabi, F. Hartstock, N.J. Taylor, A.J. Carty, Organometallics 3 (1984) 1587.
[26] A.A. Koridze, A.I. Yanovsky, Y.T. Struchkov, J. Organomet. Chem. 441 (1992) 277.
[27] M.V. Capparelli, Y. De Sanctis, A.J. Arce, Acta Crystallogr. C 51 (1995) 1819.
[28] M.I. Bruce, P.A. Humphrey, E. Horn, E.R.T. Tiekink, J. Organomet. Chem. 429 (1992) 207.
[29] S. Jeannin, Y. Jeannin, F. Robert, C. Rosenberg, Inorg. Chem. 33 (1994) 243.
[30] A.J. Edwards, N.E. Leadbeater, J. Lewis, P. Raithby, J. Chem. Soc., Dalton Trans. (1995) 3785.
[31] A.A. Koridze, N.M. Astakhova, F.M. Dolgushin, A.I. Yanovsky, Yu.T. Struchkov, P.V. Petrovskii, Organometallics 14 (1995) 2167.
[32] F. Muller, D.I.P. Dijkhuis, G. van Koten, K. Vrieze, D. Heijdrenrijk, M.A. Rotteveel, C.H. Stam, M.C. Zoutberg, Organometallics 8 (1989) 992.
[33] M. Green, P.A. Kale, R.J. Mercer, J. Chem. Soc., Chem. Commun. (1987) 375.
[34] A.A. Koridze, O.A. Kizas, N.E. Kolobova, V.N. Vinogradova, N.A. Ustynyuk, P.U. Petrovskii, A.I. Yanovsky, Y.T. Struchkov, J. Chem. Soc., Chem. Commun. (1984) 1158.
[35] M.I. Bruce, P.A. Humphrey, H. Miyamae, B.W. Skleton, A.H. White, J. Organomet. Chem. 429 (1992) 187.
[36] J.A. Beck, S.A.R. Knox, R.F.D. Stansfield, F.G.A. Stone, M.J. Winter, P. Woodward, J. Chem. Soc., Dalton Trans. (1982) 195.
[37] A.M. Boileau, A.G. Orpen, R.F.D. Stansfield, P. Woodward, J. Chem. Soc., Dalton Trans. (1982) 187.
[38] U. Riaz, M.D. Curtis, A. Rheingold, B.S. Haggerty, Organometallics 9 (1990) 2647.
[39] J.F. Corrigan, S. Doherty, N.J. Taylor, A.J. Carty, Organometallics 11 (1992) 3160.
[40] V. Ferrand, Kurt Merzweiler, Gerd Rheinwald, Helen Stoeckli-Evans, Georg Süss-Fink, J. Organomet. Chem., preceeding paper.
[41] A.J. Deeming, S. Hasso, M. Underhill, J. Chem. Soc., Dalton Trans. (1975) 1614.
[42] A. Wojcicki, J. Cluster Sci. 4 (1993) 59.
[43] G. Granozzi, E. Tondello, R. Bertoncello, S. Aime, D. Osella, Inorg. Chem. 24 (1985) 570.
[44] G. Gervasio, D. Osella, M. Valle, Inorg. Chem. 15 (1976) 1221.
[45] D. Nucciarone, S.A. MacLaughlin, N.J. Taylor, A.J. Carty, Organometallics 7 (1988) 106.
[46] A.A. Koridze, V.I. Zdanovich, N.V. Andrievskaya, Yu. Siromakhova, P.V. Petrovskii, M.G. Ezernitskaya, F.M. Dolgushin, A.I. Yanovsky, Yu.T. Struchkov, Russ. Chem. Bull. 45 (1996) 1200.
[47] D.D. Perrin, W.L.F. Armarego, Purification of laboratory chemicals, 3rd edn., Pergamon, Oxford, Elmsford, NY, 1988.
[48] G. Süss-Fink, G. Rheinwald, H. Stoeckli-Evans, C. Bolm, D. Kaufmann, Inorg. Chem. 35 (1996) 3081.
[49] R. Stephens, C. Castro, J. Org. Chem. 28 (1963) 3313.
[50] G.M. Sheldrick, Acta Crystallogr. A 46 (1990) 467.
[51] G.M. Sheldrick, SHELXL-93, University of Göttingen, Germany, 1993.
[52] N. Walker, D. Stuart, Acta Crystallogr. A 46 (1990) 158.
[53] C.K. Johnson, ORTEP, Oak Ridge National Laboratory, Oak Ridge, TN, modified for PC by L. Zsolnai and H. Pritzkow, University of Heidelberg, Germany (1994).

DALTON
FULL PAPER

Triruthenium–iridium clusters containing alkyne ligands: synthesis, structure, and catalytic implications of $[(\mu\text{-H})IrRu_3(CO)_{11}(\mu_3\text{-}\eta^2\text{-}PhC{\equiv}CPh)]$ and $[IrRu_3(CO)_{10}(\mu_4\text{-}\eta^2\text{-}PhC{\equiv}CPh)(\mu\text{-}\eta^2\text{-}PhC{=}CHPh)]$

Vincent Ferrand, Georg Süss-Fink,* Antonia Neels and Helen Stoeckli-Evans

Institut de Chimie, Université de Neuchâtel, CH-2000 Neuchâtel, Switzerland

Received 27th July 1998, Accepted 9th October 1998

The mixed-metal cluster $[HIrRu_3(CO)_{13}]$ **1** reacts with one equivalent of disubstituted alkynes RC≡CR to give $[HIrRu_3(CO)_{11}(\mu_3\text{-}\eta^2\text{-}RC{\equiv}CR)]$ (R = Ph **2**; R = Me **3**), with a second equivalent of the alkyne the clusters $[IrRu_3(CO)_{10}(\mu_4\text{-}\eta^2\text{-}RC{\equiv}CR)(\mu\text{-}\eta^2\text{-}RC{=}CHR)]$ (R = Ph **4**; R = Me **5**) are obtained. The single-crystal X-ray structure analyses of **2** and **3** show these clusters to have a tetrahedral Ru_3Ir framework containing the alkyne ligand coordinated in a parallel fashion over the Ru_3 face of the metal skeleton. In contrast, the clusters **4** and **5** consist of a butterfly arrangement of the Ru_3Ir framework with the alkyne ligand coordinated to all four metal atoms, giving an overall octahedral Ru_3IrC_2 skeleton, as demonstrated by the single-crystal structure analysis of **4**. Cluster **1** is an excellent catalyst for the hydrogenation of diphenylacetylene to give stilbene (catalytic turnover number 990 within 15 min), clusters **2** and **4** are also catalytically active but seem to represent side-channels of the catalytic cycle.

The synthesis of mixed-metal alkyne clusters has received much attention due to their potential as models for the carbon–carbon triple bond activation on metal surfaces[1,2] and for their catalytic potential in hydrogenation reactions.[3] Different metals in a cluster may also have synergistic effects for catalytic transformations. On the other hand, the increase of the catalytic activity of a transition metal catalyst by addition of another metal complex gives rise to speculations about the formation of mixed-metal clusters to account for the synergistic effect observed.[4]

The reaction of tetranuclear clusters with internal and terminal alkynes often affords the corresponding butterfly complexes where the C_2 unit bonds to the M_4 framework in a $\mu_4\text{-}\eta^2$-fashion to form a quasi-octahedral M_4C_2 skeleton.[5] The co-ordination in a $\mu_3\text{-}\eta^2$-mode of the alkynes on a face of a tetrahedral metal framework is not common and only a few examples have been reported in the literature.[6]

In a recent publication, we have described the synthesis and the reactivity of the mixed-metal cluster $[HIrRu_3(CO)_{13}]$ **1** towards H_2.[7] We now report on the reactivity of **1** towards internal alkynes such as diphenylacetylene and 2-butyne, and on the catalytic activity of **1** in the hydrogenation of diphenylacetylene.

Results and discussion

Synthesis and characterisation of $[HIrRu_3(CO)_{11}(RC{\equiv}CR)]$ (2 R = Ph; 3 R = Me)

The thermal reaction of $[HIrRu_3(CO)_{13}]$ **1** with one equivalent of alkyne in hexane leads to the formation of the new tetrahedral mixed-metal alkyne clusters $[HIrRu_3(CO)_{11}(PhC{\equiv}CPh)]$ **2** and $[HIrRu_3(CO)_{11}(MeC{\equiv}CMe)]$ **3** (Scheme 1). The two complexes **2** and **3**, isolated by chromatographic methods, are stable towards air and moisture. The infrared spectra of clusters **2** and **3** are very similar in the carbonyl region, both presenting six bands in the region of terminal CO vibrations and one absorption at 1842 cm^{-1} (**2**) and 1844 cm^{-1} (**3**) which is attributed to the bridging carbonyl ligand (Table 1).

In the ^1H NMR spectra of **2** and **3**, the hydride signals are observed at higher field with respect to **1**. In the case of **2**, a

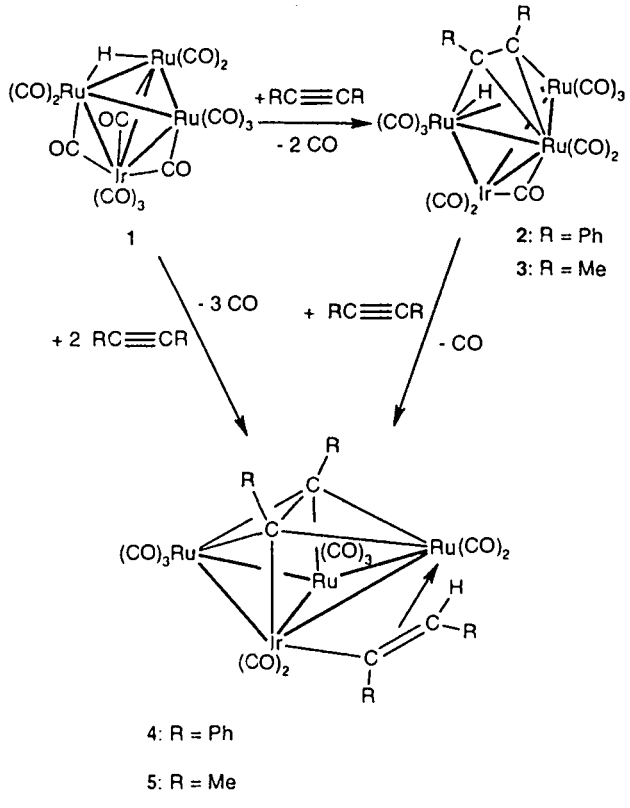

Scheme 1 *Synthetic routes to clusters* **2**–**5**.

multiplet centred around δ 7.15 can be assigned to the phenyl protons, whereas in the case of **3** the two methyl groups of the alkyne ligand are equivalent and give only one singlet at δ 2.72, indicating that the alkyne is co-ordinated symmetrically over the Ru_3Ir framework.

Solid state structures of $[HIrRu_3(CO)_{11}(\mu_3\text{-}\eta^2\text{-}RC{\equiv}CR)]$ (2 R = Ph; 3 R = Me)

The molecular structures of **2** and **3** have been solved by single-crystal X-ray structure analysis. Suitable crystals of **2** and **3**

Table 1 IR and ^1H NMR data

Complex	ν(CO)[a]/cm^{-1}	δ[b]
[$HRu_3Ir(CO)_{11}(PhC{\equiv}CPh)$] 2	2095w, 2071s, 2053s, 2037vs, 2012m, 1994m, 1842w	7.30–7.00 (C_6H_5, m), −18.88 (H, s)
[$HRu_3Ir(CO)_{11}(MeC{\equiv}CMe)$] 3	2094w, 2068s, 2049s, 2033vs, 2009m, 1988m, 1844w	2.72 (CH_3, s), −18.98 (H, s)
[$Ru_3Ir(CO)_{10}(PhC{\equiv}CPh)(PhCH{=}CPh)$] 4	2078m, 2043vs, 2037s, 2027m, 2001w, 1990vw, 1964vw	7.70–6.20 (C_6H_5, m), 4.90 (H, s)
[$Ru_3Ir(CO)_{10}(MeC{\equiv}CMe)(MeCH{=}CMe)$][c] 5	2078m, 2066w, 2043vs, 2032vs, 2014s, 1997m, 1983w, 1959w	4.80 (CH_3CHCCH_3, dq $^3J_{HH}$ 6.1 $^4J_{HH}$ 0.7) 3.09 (CH_3CHCCH_3, d $^4J_{HH}$ 0.7 Hz), 2.90 (CH_3CCCH_3, s) 2.74 (CH_3CCCH_3, s) 1.82 (CH_3CHCCH_3, d $^3J_{HH}$ 6.1 Hz) 4.86 (CH_3CHCCH_3, dq $^3J_{HH}$ 5.95 Hz $^4J_{HH}$ 0.8 Hz) 3.07 (CH_3CHCCH_3), 2.88 (CH_3CCCH_3, s) 2.71 (CH_3CCCH_3, s), 1.77 (CH_3CHCCH_3, d $^3J_{HH}$ 5.95 Hz)

[a] Recorded in dichloromethane 2 and 3, in hexane 4 and 5. [b] Measured in $CDCl_3$ solution at 294 K, J in Hz. [c] Two isomers in solution (ratio 7:1).

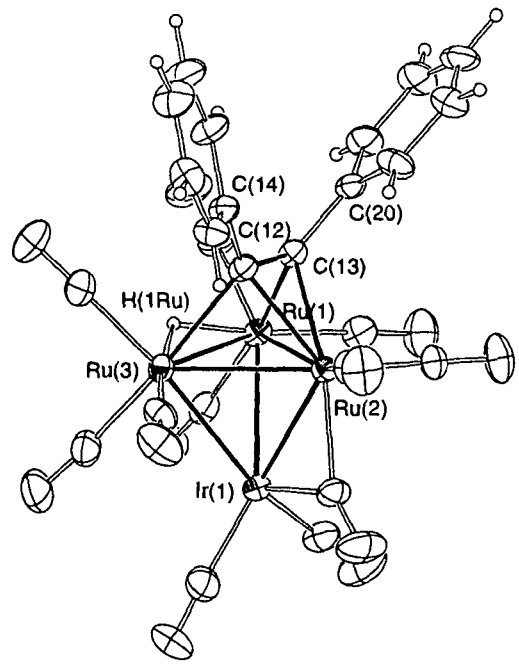

Fig. 1 ORTEP plot of [$HIrRu_3(CO)_{11}(\mu_3$-η^2-$C_2Ph_2)$] 2. Thermal ellipsoids are drawn at 30% of probability.

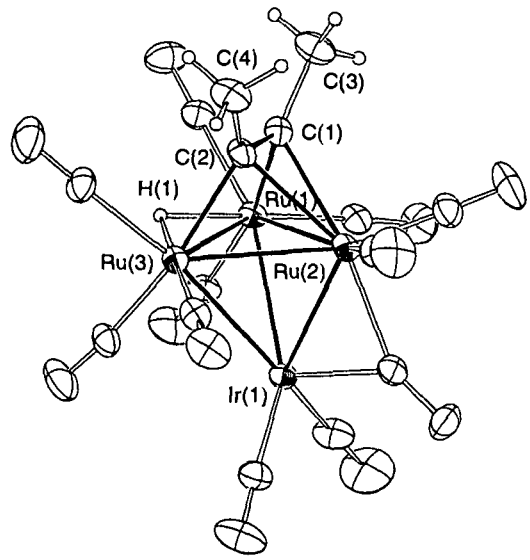

Fig. 2 ORTEP plot of [$HIrRu_3(CO)_{11}(\mu_3$-η^2-$C_2Me_2)$] 3. Thermal ellipsoids are drawn at 30% of probability.

were grown at −18 °C in hexane. The molecular structure of 2 is depicted in Fig. 1 and that of 3 in Fig. 2. Selected bond lengths and angles of both compounds 2 and 3 are listed in Tables 2 and 3. Both, 2 and 3 have the same overall structure showing the same carbonyl, alkyne and hydride co-ordination. The four metal atoms form a tetrahedron where the Ru–Ir distances vary from 2.6985(7) to 2.8092(7) Å for 2 and from 2.4972(7) to 3.0591(8) Å for 3. The clusters 2 and 3 present, as expected for a tetrahedral arrangement, an electron count of 60. The short distances Ru(2)–Ir(1) [2 2.6985(7); 3 2.4972(7) Å] are due to the bridging carbonyl ligand over this edge. The base of the tetrahedron is composed of three ruthenium atoms, each of the Ru–Ru distances being different. In both complexes the longer Ru(1)–Ru(3) distance [2 2.8513(9); 3 2.8847(10) Å] suggests the presence of the hydrido bridge across this edge. The hydride ligand in 2 is not symmetrically co-ordinated to the Ru(1)–Ru(3) edge [2 Ru(1)–HRu(1) 1.51(8), Ru(3)–HRu(1) 1.91(8) Å], whereas in complex 3 the hydride is quasi symmetrically co-ordinated to the Ru(1)–Ru(3) vector [Ru(1)–H(1) 1.76(6)

Table 2 Selected bond lengths (Å) and angles (°) for molecule 2

Ir(1)–Ru(2)	2.6985(7)	Ru(2)–C(13)	2.208(7)
Ir(1)–Ru(1)	2.7736(8)	Ru(2)–Ru(3)	2.7654(9)
Ir(1)–Ru(3)	2.8092(7)	Ru(3)–C(12)	2.191(8)
Ru(1)–C(13)	2.134(8)	Ru(3)–HRu(1)	1.91(8)
Ru(1)–Ru(2)	2.8476(9)	C(12)–C(13)	1.399(10)
Ru(1)–Ru(3)	2.8513(9)	C(12)–C(14)	1.495(11)
Ru(1)–HRu(1)	1.51(8)	C(13)–C(20)	1.481(11)
Ru(2)–C(12)	2.170(8)		
Ru(2)–Ir(1)–Ru(1)	62.70(2)	Ir(1)–Ru(2)–Ru(1)	59.94(2)
Ru(2)–Ir(1)–Ru(3)	60.24(2)	Ru(3)–Ru(2)–Ru(1)	61.04(2)
Ru(1)–Ir(1)–Ru(3)	61.42(2)	Ru(2)–Ru(3)–Ir(1)	57.90(2)
Ir(1)–Ru(1)–Ru(2)	57.361(19)	Ru(2)–Ru(3)–Ru(1)	60.90(2)
Ir(1)–Ru(1)–Ru(3)	59.91(2)	Ir(1)–Ru(3)–Ru(1)	58.67(2)
Ru(2)–Ru(1)–Ru(3)	58.06(2)	C(13)–C(12)–C(14)	125.8(7)
Ir(1)–Ru(2)–Ru(3)	61.86(2)	C(12)–C(13)–C(20)	124.6(7)

Estimated standard deviations in parentheses.

Table 3 Selected bond lengths (Å) and angles (°) for molecule 3

Ir(1)–Ru(2)	2.4972(7)	Ru(2)–C(1)	2.446(10)
Ir(1)–Ru(3)	2.7839(7)	Ru(2)–Ru(3)	2.8156(10)
Ir(1)–Ru(1)	3.0591(8)	Ru(3)–C(2)	2.049(8)
Ru(1)–C(1)	1.901(7)	Ru(3)–H(1)	1.75(6)
Ru(1)–Ru(2)	2.8665(10)	C(1)–C(2)	1.385(12)
Ru(1)–Ru(3)	2.8847(10)	C(1)–C(3)	1.534(13)
Ru(1)–H(1)	1.76(6)	C(2)–C(4)	1.388(10)
Ru(2)–C(2)	2.299(9)		
Ru(2)–Ir(1)–Ru(3)	64.17(2)	Ir(1)–Ru(2)–Ru(1)	69.15(2)
Ru(2)–Ir(1)–Ru(1)	61.13(2)	Ru(3)–Ru(2)–Ru(1)	61.01(2)
Ru(3)–Ir(1)–Ru(1)	58.94(2)	Ir(1)–Ru(3)–Ru(2)	52.966(19)
Ru(2)–Ru(1)–Ru(3)	58.62(2)	Ir(1)–Ru(3)–Ru(1)	65.29(2)
Ru(2)–Ru(1)–Ir(1)	49.717(18)	Ru(2)–Ru(3)–Ru(1)	60.37(2)
Ru(3)–Ru(1)–Ir(1)	55.76(2)	C(2)–C(1)–C(3)	129.3(7)
Ir(1)–Ru(2)–Ru(3)	62.87(2)	C(4)–C(2)–C(1)	121.6(8)

Estimated standard deviations in parentheses.

Ru(3)–H(1) 1.75(6) Å]. Two of the three ruthenium atoms are bonded to three terminal CO groups, whereas Ru(2) and Ir(1) are bonded to two terminal CO groups and share the bridging CO ligand. The alkynes are co-ordinated in a μ_3-η^2-bonding mode, which is commonly observed in trinuclear alkyne complexes:[8] compounds **2** and **3** compare well with the mixed-metal clusters $[HCpWOs_3(CO)_{10}(\mu_3\text{-}\eta^2\text{-}C_2Tol_2)]$ (Tol = tolyl)[6a] and with $[H_2Os_4(CO)_9(\mu_3\text{-}\eta^2\text{-}C_2Ph_2)(\eta^2\text{-}C_2Ph_2)]$.[6c] The μ_3-η^2-RCCR ligand (**2** R = Ph; **3** R = Me) lies on the Ru_3 face of the $IrRu_3$ framework and is formally π-bonded to Ru(2) [**2** Ru(2)–C(12) 2.170(8), Ru(2)–C(13) 2.208(7) Å; **3** Ru(2)–C(1) 2.446(10), Ru(2)–C(2) 2.299(9) Å] and is σ-bonded to Ru(1) and Ru(3) [**2** Ru(1)–C(13) 2.134(8), Ru(3)–C(12) 2.191(8) Å; **3** Ru(1)–C(1) 1.901(7), Ru(3)–C(2) 2.049(8) Å]. The formal electron counts at the individual metal atoms are 18.5 for Ru(1) and Ru(3), 18 for Ru(2) and 17 for Ir(1).

The electron deficiency of the Ir atom is apparently compensated for by direct donation from the ruthenium atoms. This is confirmed by the very short Ir(1)–Ru(2) distance [**2** Ir(1)–Ru(2) 2.6985(7); **3** Ir(1)–Ru(2) 2.4972(7) Å] and by the presence of the bridging carbonyl ligand over Ru(2)–Ir(1).

Owing to the co-ordination of the alkyne group to the metal core, the carbon–carbon triple bond is lengthened [**2** C(12)–C(13) 1.399(10); **3** C(1)–C(2) 1.385(12) Å], being in the same range as observed for other clusters such as $[HCpWOs_3(CO)_{10}(\mu_3\text{-}\eta^2\text{-}C_2Tol_2)]$ [isomer 1 1.38(6), isomer 2 1.45(6) Å][6a] and $[H_2Os_4(CO)_9(\mu_3\text{-}\eta^2\text{-}C_2Ph_2)(\eta^2\text{-}C_2Ph_2)]$ [1.44(1) Å].[6c] The alkyne ligands PhC≡CPh and MeC≡CMe are bent, the angles being 125.8(7)° [C(14)–C(12)–C(13)] and 124.6(7)° [C(12)–C(13)–C(20)] for **2**, 129.3(7)° [C(2)–C(1)–C(3)] and 121.6(8)° [C(1)–C(2)–C(4)] for **3**.

A comparison of both structures shows that in **3** the distances Ru(1)–C(1) [1.901(7) Å] and Ru(3)–C(2) [2.049(8) Å] are shorter than the analogous distances in **2** [Ru(1)–C(13) 2.134(8) Å; Ru(3)–C(12) 2.191(8) Å]. These differences in the formal ruthenium–carbon σ-bonds may be explained by steric effects, the methyl substituents being less demanding than the phenyl substituents. For the distances corresponding to the formal ruthenium–carbon π-bonds, the inverse effect is observed. In **3** the distances Ru(2)–C(1) [2.446(10) Å] and Ru(2)–C(2) [2.299(9) Å] are longer than the corresponding distances in **2** [Ru(2)–C(13) 2.208(7) Å; Ru(2)–C(12) 2.170(8) Å], probably due to the higher electron density of 2-butyne with respect to diphenylacetylene.

Synthesis and characterisation of $[IrRu_3(CO)_{10}(RC{\equiv}CR)(RCH{=}CR)]$ (4 R = Ph; 5 R = Me)

Reaction of the tetrahedral alkyne clusters **2** and **3** with a further equivalent of the corresponding alkyne gives the butterfly clusters $[IrRu_3(CO)_{10}(RCCR)(RCH{=}CR)]$ (**4** R = Ph; **5** R = Me), also accessible directly from **1** with at least two equivalents of PhCCPh or MeCCMe (Scheme 1). The infrared spectra of **4** and **5** exhibit almost the same ν(CO) pattern in the area of terminal carbonyls (Table 1). The ^1H NMR spectra of **4** and **5** reveal the presence of a vinyl in addition to the alkyne ligand; **4** shows a multiplet centred around δ 6.95 which is assigned to the various phenyl protons. The vinyl proton appears as a singlet at δ 4.90, being characteristic for vinyl complexes.[9] In the case of **5**, the ^1H NMR spectrum is more complicated, indicating the presence of two isomers in $CDCl_3$ solution (ratio 7:1). We believe the major isomer to be analogous to **4**, whereas in the minor isomer the μ-η^2-$CH_3CH{=}CCH_3$ vinyl ligand is co-ordinated in an inverse fashion with respect to the Ru and Ir atoms. The structure of **4** was confirmed by a single-crystal X-ray structure analysis.

Solid state structure of $[IrRu_3(CO)_{10}(\mu_4\text{-}\eta^2\text{-}PhC{\equiv}CPh)(\mu\text{-}\eta^2\text{-}PhCH{=}CPh)]$ 4

Suitable crystals of **4** were obtained by slow diffusion of methanol into a concentrated dichloromethane solution at room temperature. The molecular structure of **4** is depicted in Fig. 3. Selected bond lengths and angles are presented in Table 4. The cluster **4** is the second compound known with μ_4-η^2-alkyne and a μ-η^2-vinyl ligand co-ordinated to a tetranuclear butterfly skeleton; it compares well with $[FeCo_3(CO)_9(\mu_4\text{-}\eta^2\text{-}PhC{\equiv}CPh)(\mu\text{-}\eta^2\text{-}PhCH{=}CPh)]$.[10] The butterfly backbone consists of a ruthenium and an iridium atom which are bound to two wingtip ruthenium atoms. The Ir(1)–Ru(1) bond distance is longer [2.8311(7) Å] than the other metal–metal distances in **4**, but it is nevertheless in the usual range of the hinge lengths in Ru_4C_2 butterfly complexes.[5,11] The non-bonding Ru(2)···Ru(3) edge [3.9380(5) Å] can be compared to the values of 3.485(4) and 4.123(1) Å reported for the related butterfly clusters $[FeCo_3(CO)_9(\mu_4\text{-}\eta^2\text{-}PhC{\equiv}CPh)(\mu\text{-}\eta^2\text{-}PhCH{=}CPh)]$[10] and $[Co_2Mo_2(\mu_4\text{-}C_2Me_2)(\mu\text{-}CO)_4(CO)_4(\eta^5\text{-}C_5H_5)_2]$.[12] respectively. The dihedral angle between the intersection of the two planes of $IrRu_2$ is 117.27(3)° usual for butterfly clusters.[5b,10] All carbonyl ligands in **4** are terminal (the angles Ir–C–O and Ru–C–O being in the range of 174–179°). Two of the three ruthenium atoms, Ru(1) and Ru(3) are bonded to two CO ligands, whereas Ru(2) and Ir(1) are bonded to three carbonyls.

The PhCCPh ligand interacts with all four metal atoms in a μ_4-η^2-fashion. The carbon–carbon backbone [C(25)–C(26)] is nearly parallel to the Ru(1)–Ir(1) hinge of the cluster, and the torsion angle of the diphenylacetylene unit C(25)–Ir(1)–Ru(1)–C(26) measures 1.9(2)°. The two carbon atoms C(25) and C(26) can be considered as σ-bound to Ir(1) and Ru(1) respectively [Ir(1)–C(25) 2.176(7); Ru(1)–C(26) 2.194(7) Å] and as π-bound

Table 4 Selected bond lengths (Å) and angles (°) for molecule **4**

Ir(1)–C(11)	2.115(6)	Ru(2)–C(25)	2.250(6)
Ir(1)–C(25)	2.176(7)	Ru(2)–C(26)	2.283(6)
Ir(1)–Ru(3)	2.6518(6)	Ru(3)–C(11)	2.185(6)
Ru(2)···Ru(3)	3.9380(5)	Ru(3)–C(26)	2.250(6)
Ir(1)–Ru(2)	2.7373(7)	Ru(3)–C(12)	2.262(7)
Ir(1)–Ru(1)	2.8311(7)	Ru(3)–C(25)	2.290(7)
Ru(1)–C(26)	2.194(7)	C(11)–C(12)	1.419(10)
Ru(1)–Ru(3)	2.7101(8)	C(12)–H(12)	1.03(8)
Ru(1)–Ru(2)	2.7233(9)	C(25)–C(26)	1.431(10)
C(12)–C(11)–C(13)	122.6(5)	C(26)–C(25)–C(27)	127.9(6)
C(11)–C(12)–C(19)	127.5(6)	C(25)–C(26)–C(33)	125.5(7)
Ru(3)–Ir(1)–Ru(1)–Ru(2)	117.27(3)		

Estimated standard deviations in parentheses.

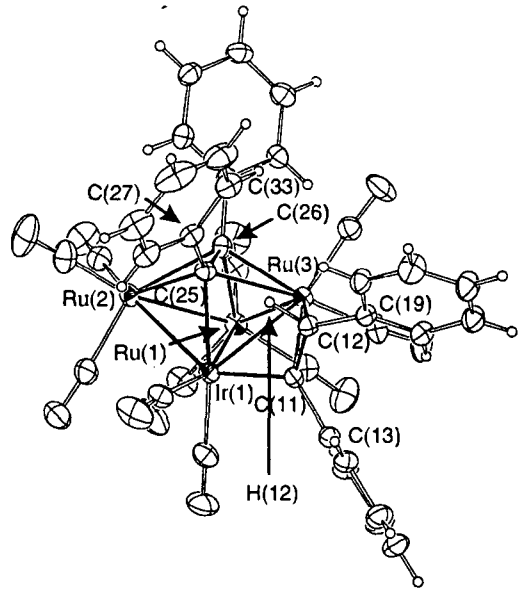

Fig. 3 ORTEP plot of $[IrRu_3(CO)_{10}(\mu_4\text{-}\eta^2\text{-}C_2Ph_2)(\mu\text{-}\eta^2\text{-}PhCH{=}CPh)]$ **4**. Thermal ellipsoids are drawn at 30% of probability.

Table 5 Catalytic hydrogenation of diphenylacetylene

Catalyst	Product (%)				TON	TOF/min^{-1}
	PhCCPh	*trans*-PhCHCHPh	*cis*-PhCHCHPh	$PhCH_2CH_2Ph$		
$[HIrRu_3(CO)_{13}]$	0	98.8	0.2	1	990	66
$[H_3IrRu_3(CO)_{12}]$	17	48.5	33	1.5	815	54
$[HIrRu_3(CO)_{11}(PhCCPh)]$	6	73	18	3	910	60
$[HIrRu_3(CO)_{10}(PhCCPh)(PhCH{=}CPh)]$	30	30	37	3	670	45

Conditions: $P(H_2) = 10$ bar, $T = 120$ °C, hexane = 30 ml, $t = 15$ min. Catalyst: 1.174×10^{-5} mol. Catalyst–substrate ratio 1:1000. TOF: catalytic turnover frequency. TON: catalytic turnover number.

Table 6 Catalytic hydrogenation of diphenylacetylene in presence of CO

Catalyst	Product (%)				TOF/min^{-1}	t/min
	PhCCPh	*trans*-PhCHCHPh	*cis*-PhCHCHPh	$PhCH_2CH_2Ph$		
$[HIrRu_3(CO)_{13}]$	0.1	4.4	95.3	0.09	16	30
$[H_3IrRu_3(CO)_{12}]$	2	3	95	0	11	45
$[HIrRu_3(CO)_{11}(PhCCPh)]$	0.5	4.4	95	0.08	13	40
$[HIrRu_3(CO)_{10}(PhCCPh)(PhCH{=}CPh)]$	0	16	80	0	11	45

Conditions: $P(H_2) = 9$ bar, $P(CO) = 1$ bar, $T = 120$ °C, hexane = 30 ml. Catalyst: 1.174×10^{-5} mol. Catalyst–substrate ratio 1:500. TOF: catalytic turnover frequency.

to the two wingtip ruthenium atoms [Ru(2)–C(25) 2.250(6); Ru(2)–C(26) 2.283(6); Ru(3)–C(26) 2.250(6); Ru(3)–C(25) 2.290(7) Å].

Owing to the co-ordination to the four metal atoms, the C–C bond is longer [C(25)–C(26) 1.431(10) Å] than in clusters **2** and **3**. The vinyl ligand is co-ordinated to Ir(1) and Ru(3) in a classical μ-η^2-mode; the C(11)–C(12) group is σ-bound to Ir(1) [Ir(1)–C(11) 2.115(6) Å] and is π-bound to Ru(3) [Ru(3)–C(11) 2.185(6); Ru(3)–C(12) 2.262(7) Å]. Also due to the co-ordination to the metal framework the C–C bond is lengthened [C(25)–C(26) 1.431(10) Å] with respect to a free carbon–carbon double bond.

With an electron count of 60, cluster **4** is electron-deficient, since a M_4 butterfly cluster consistent with the noble gas rule would require 62 electrons. However, considering **4** as an octahedral Ru_3IrC_2 cluster, it is consistent with Wade's rules predicting a *closo*-structure.[13]

Catalytic hydrogenation of diphenylacetylene

The mixed-metal cluster $[HIrRu_3(CO)_{13}]$ **1** turned out to be an excellent catalyst for the hydrogenation of diphenylacetylene in hexane solution (Table 5). Within 15 min, the substrate is completely converted, the catalyst–substrate ratio being 1:1000, the catalytic turnover frequency (TOF) being 66 min^{-1} (120 °C, 10 bar). The selectivity is very high, giving 98.8% *trans*-stilbene, 0.2% *cis*-stilbene and 1% 1,2-diphenylethane. The main product, *trans*-stilbene precipitates directly from the reaction mixture.

At the end of the catalytic reaction, the yellow solution contains the intact $IrRu_3$ cluster system however, it is not the $[HIrRu_3(CO)_{13}]$ complex employed but $[H_3IrRu_3(CO)_{12}]$ which forms quantitatively from $[HIrRu_3(CO)_{13}]$ under hydrogen pressure.[7] $[H_3IrRu_3(CO)_{12}]$ as well as the alkyne derivatives isolated, $[IrRu_3(CO)_{10}(\mu_3\text{-}\eta^2\text{-}PhC{\equiv}CPh)]$ **2** and $[IrRu_3(CO)_{10}(\mu_4\text{-}\eta^2\text{-}PhC{\equiv}CPh)(\mu\text{-}\eta^2\text{-}PhCH{=}CPh)]$ **4**, also catalyse the hydrogenation of diphenylacetylene. However, the selectivities and activities are not as good as in the case of $[HIrRu_3(CO)_{13}]$ **1** (Table 5). If the hydrogenation is carried out in the presence of carbon monoxide (H_2–CO 9:1), both selectivity and activity decrease (Table 6). In particular, it is interesting to note that under these conditions the main product is *cis*-stilbene.

On the basis of these findings, the recovery of the intact $IrRu_3$ cluster, and the isolation and characterisation of the two acetylene derivatives $[IrRu_3(CO)_{11}(\mu_3\text{-}\eta^2\text{-}PhC{\equiv}CPh)]$ **2** and $[IrRu_3(CO)_{10}(\mu_4\text{-}\eta^2\text{-}PhC{\equiv}CPh)(\mu\text{-}\eta^2\text{-}PhCH{=}CPh)]$ **4**, we propose a tentative mechanism involving intact $IrRu_3$ intermediates for the catalytic hydrogenation of diphenylacetylene (Scheme 2). The cluster $[HIrRu_3(CO)_{13}]$ **1** can react with the alkyne under CO substitution to give an intermediate $[HIrRu_3(CO)_{12}(PhC{\equiv}CPh)]$. After hydrogen transfer from the metal framework onto the co-ordinated alkyne, the vinyl species $[IrRu_3(CO)_{12}(PhCH{=}CPh)]$ is formed. Uptake of molecular hydrogen should give $[H_2IrRu_3(CO)_{12}(PhCH{=}CPh)]$ which, after reaction with CO gives stilbene and the catalyst $[HIrRu_3(CO)_{13}]$ **1** (cycle A). Under the reaction conditions (H_2 pressure) the catalyst is converted into $[H_3IrRu_3(CO)_{12}]$, the only organometallic species detected (by IR spectroscopy) at the end of the reaction and which can be isolated. This cycle parallels the hydrogenation mechanism proposed by Cabeza *et al.* using the trinuclear cluster $[HRu_3(CO)_9(ampy)]$ (Hampy = 2-amino-6-methylpyridine) as the catalyst.[14] We consider the two alkyne clusters **2** and **4** which we isolated from the reaction of **1** with diphenylacetylene to be members of a side channel which operates only in the absence of hydrogen. The hydrogenated species $[H_3IrRu_3(CO)_{12}]$ also reacts with the alkyne to give, with formation of the corresponding olefin, the intermediate $[HIrRu_3(CO)_{12}(PhC{\equiv}CPh)]$ (cycle B). This is in accordance with the observation that **1** reacts more rapidly with H_2 than with diphenylacetylene. The infrared spectrum shows that under a pressure of 2 bar of H_2 at 120 °C (after 2 min), **1** is quantitatively converted into $[H_3IrRu_3(CO)_{12}]$, in the presence or absence of diphenylacetylene.

Experimental

All reactions were carried out in an atmosphere of pure nitrogen using standard Schlenk techniques. Solvents were distilled over appropriate drying agents and deoxygenated and nitrogen-saturated prior to use.[15] Preparative thin-layer chromatography was performed using 20 × 20 cm plates coated with Fluka silica gel G. The starting complex $[HIrRu_3(CO)_{13}]$ was prepared according to the published method.[7] Diphenylacetylene and octadecane were purchased from Fluka, *cis*- and *trans*-stilbene as well as 1,2-diphenylethane were purchased from Aldrich and used as received. NMR spectra were recorded using a Varian Gemini 200 BB or a Bruker AMX 400 spectrometer, using the resonance of the residual protons of the deuteriated solvents as reference. Infrared spectra were recorded with a Perkin-Elmer 1720X FT-IR spectrometer. Mass spectra were measured by

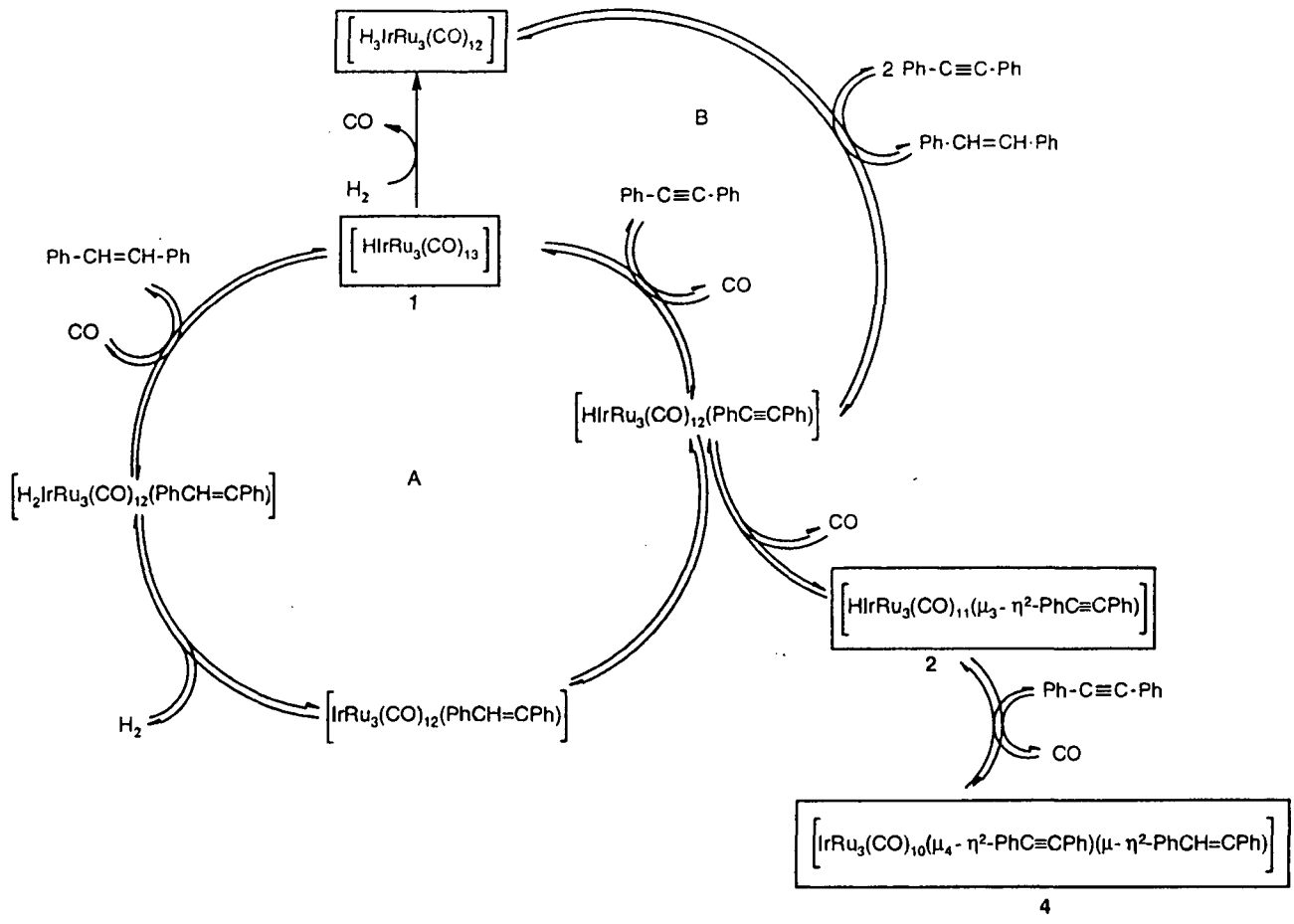

Scheme 2 Proposed mechanism for the catalytic hydrogenation of diphenylacetylene catalysed by $[HIrRu_3(CO)_{13}]$. Isolated and fully characterised species are indicated by a frame.

Professor T. A. Jenny at the University of Fribourg, Switzerland. Microanalyses were carried out by the Mikroelementaranalytisches Laboratorium of the ETH Zürich, Switzerland. GC spectra were recorded with a DANI 86.10 gas chromatograph using a Chrompack (WCOT fused silica 25 M X 0.32 mm) capillary column and octadecane as internal standard.

Preparations

$[HIrRu_3(CO)_{11}(PhC{\equiv}CPh)]$ 2. A solution of $[HIrRu_3(CO)_{13}]$ **1** (73 mg, 0.085 mmol) and PhC≡CPh (15 mg, 0.085 mmol) in hexane (30 ml) was stirred at 80 °C in a pressure Schlenk tube. During the reaction the pressure was released once. After 1 h the solution changed from red to orange. After removal of the solvent, the dark orange residue was dissolved in 5 ml of CH_2Cl_2 and submitted to thin-layer chromatography (silica gel, CH_2Cl_2–hexane 1 : 3). Two main bands were obtained. The first one contained $[IrRu_3(CO)_{10}(PhC{\equiv}CPh)(PhCH{=}CPh)]$ **4** (9.1 mg, 11%). The second one (orange) contained **2**, it was extracted with CH_2Cl_2 and recrystallised from hexane at −18 °C. The FAB mass spectrum of **2** shows the molecular peak at *m/z* 985 (^{102}Ru, ^{191}Ir), followed by a fragmentation series of $[HIrRu_3(CO)_n(PhC{\equiv}CPh)]$ (n = 1–10). The orange air-stable crystals were dried *in vacuo*. Yield 17.3 mg, 23% (Found: C, 30.64; H, 1.11. $C_{25}H_{11}O_{11}Ru_3Ir$ requires C, 30.55; H, 1.13%).

$[HIrRu_3(CO)_{11}(CH_3C{\equiv}CCH_3)]$ 3. A solution of $[HIrRu_3(CO)_{13}]$ **1** (100 mg, 11.6 mmol) and a slight excess of cold $CH_3C{\equiv}CCH_3$ (10 μl, 12.8 mmol) in hexane (30 ml) was stirred at 85 °C in a pressure Schlenk tube. During the reaction the pressure was released once. After 90 min the solution had changed from red to orange. After removal of the solvent, the dark orange residue was dissolved in 5 ml of CH_2Cl_2 and purified by thin layer chromatography (silica gel, CH_2Cl_2–hexane 1 : 3). Two bands were obtained, the first one contained $[IrRu_3(CO)_{10}(CH_3C{\equiv}CCH_3)(CH_3CH{=}CCH_3)]$ **5** (3 mg, 3%), the second one (orange) contained **3**. The product was extracted with CH_2Cl_2 and recrystallized from hexane at −18 °C. The orange air-stable crystals were dried *in vacuo*. Yield 40 mg, 40% (Found: C, 21.01; H, 0.78. $C_{15}H_7O_{11}Ru_3Ir$ requires C, 20.98; H, 0.82%).

$[IrRu_3(CO)_{10}(PhC{=}CPh)(PhCH{=}CPh)]$ 4. A solution of $[HIrRu_3(CO)_{13}]$ **1** (100 mg, 11.6 mmol) and PhC≡CPh (62 mg, 34.8 mmol) in hexane (30 ml) was stirred at 85 °C in a pressure Schlenk tube. During the reaction the pressure was released once. After 90 min the solution had changed from red to dark brown. After removal of the solvent, the dark brown residue was dissolved in 5 ml of CH_2Cl_2 and purified by thin layer chromatography (silica gel, CH_2Cl_2–hexane 1 : 3). Cluster **4** was extracted from the main brown band with CH_2Cl_2 and recrystallized at room temperature from a biphasic mixture of CH_2Cl_2–MeOH. The black air-stable crystals were dried *in vacuo*. Yield 53 mg, 40% (Found: C, 40.56; H, 1.74. $C_{38}H_{21}O_{10}Ru_3Ir$ requires C, 40.28; H, 1.87%). The product **4** is also accessible from **2** (17.3 mg, 0.0176 mmol) and PhC≡CPh (3.45 mg 0.0176 mmol) by heating in hexane (30 ml, 90 °C, 60 min, one pressure release) in 78% yield after thin-layer chromatography.

$[IrRu_3(CO)_{10}(CH_3C{\equiv}CCH_3)(CH_3CH{=}CCH_3)]$ 5. A solution of $[HIrRu_3(CO)_{13}]$ **1** (100 mg, 11. 62 mmol) and a large excess of $CH_3C{\equiv}CCH_3$ (91 μl, 116. 2 mmol) in hexane (30 ml) was stirred at 85 °C in a pressure Schlenk tube. During the reaction the pressure was released once. After 4 hours the solution had changed from red to dark yellow. After removal of the solvent,

Table 7 Crystallographic graphic data and refinement details for compounds 2, 3 and 4

	2	3	4
Formula	$C_{25}H_{11}IrO_{11}Ru_3$	$C_{15}H_2IrO_{11}Ru_3$	$C_{38}H_{21}IrO_{10}Ru_3$
M	982.75	858.62	1132.96
Crystal system	Monoclinic	Monoclinic	Triclinic
Space group	$P2_1/n$	$P2/c$	$P\bar{1}$
a/Å	9.3321(14)	14.0189(12)	9.7805(9)
b/Å	32.744(3)	9.6264(15)	10.9610(10)
c/Å	9.3486(15)	15.7007(6)	18.1569(16)
α/°	90	90	83.294(11)
β/°	98.413(12)	90.005(5)	85.845(11)
γ/°	90	90	69.536(10)
U/Å^3	2825.9(7)	2118.8(4)	1810.1(3)
Z	4	4	2
Crystal size/mm	0.38 × 0.38 × 0.27	0.34 × 0.34 × 0.23	0.30 × 0.23 × 0.15
Colour	Red	Orange	Black
D_c/g cm^{-3}	2.310	2.692	2.079
μ/mm^{-1}	6.323	8.411	4.949
Transmission factors: min/max	0.0595/0.1764	0.0404/0.1376	0.170/0.642
$F(000)$	1832	1576	1076
θ limits/°	2.29–25.49	2.12–28.79	2.22–25.88
hkl ranges	−11 to 11, 0 to 39, 0 to 11	−19 to 0, 0 to 11, −16 to 16	−11 to 11, −13 to 13, −22 to 21
Reflections measured	5254	3956	14184
Independent reflections	5254	3956	6501
Observed reflections	4596	3479	5168
$R1[I > 2\sigma(I)]/R1$ (all data)[a]	0.0366/0.0478	0.0359/0.0443	0.0349/0.0469
$wR2[I > 2\sigma(I)]/wR2$ (all data)[b]	0.0735/0.0820	0.0824/0.0876	0.0890/0.0922
Goodness of fit on F^2[c]	1.130	1.129	1.024
Maximum δ/σ	0.000	0.001	0.001
Largest difference peak and hole/e Å^3	0.932/−0.912	1.406/−1.162	1.187/−0.943

[a] $R1 = \Sigma||F_o| - |F_c||/\Sigma|F_o|$. [b] $wR2 = [\Sigma w(F_o^2 - F_c^2)^2/\Sigma w(F_o)^4]^{\frac{1}{2}}$. [c] $S = [\Sigma w(F_o^2 - F_c^2)^2/(n - p)]^{\frac{1}{2}}$ (n = number of reflections, p = number of parameters).

the dark brown residue was dissolved in 5 ml of CH_2Cl_2 and purified by thin layer chromatography (silica gel, CH_2Cl_2–hexane 1:4). Complex **5** (existing as a mixture of two isomers) was extracted from the main brown band with CH_2Cl_2 and was precipitated as a brown powder from methanol–pentane at 28 °C. The powder was dried *in vacuo*. Yield 13.2 mg, 13% (Found: C, 25.23; H, 2.38. $C_{18}H_{13}O_{10}Ru_3Ir{\cdot}2CH_3OH$ requires C, 25.32; H, 2.23%). The product **5** is also accessible from **3** (57 mg, 66.4 mmol) and an excess of $CH_3C{\equiv}CCH_3$ (50 μl, 10 equivalents) by heating in hexane (30 ml, 90 °C, 3 hours, one pressure release) in 41% yield after thin-layer chromatography.

Catalytic runs

In a typical experiment, 1.174×10^{-5} mol of the catalyst were dissolved in hexane (30 ml). To this solution, placed in a 100 ml stainless-steel autoclave, 1000 equivalents of the substrate were added. After purging three times with H_2, the autoclave was pressurised with hydrogen (10 bar) and heated to 120 °C under vigorous stirring of the reaction mixture. After the reaction time indicated in Tables 5 and 6, the autoclave was cooled to room temperature and the pressure released. The reaction mixture was then analysed by gas chromatography.

Crystallography

Single crystals of **2** and **3** were obtained in hexane at −18 °C, whereas **4** was recrystallized at room temperature by diffusion of methanol into CH_2Cl_2. Selected crystallographic data for the three complexes are summarised in Table 7 and significant bond lengths and bond angles are listed in Tables 2, 3 and 4.

Data collection, solution and structure refinement. Single-crystal X-ray diffraction data of **2** and **3** were collected at room temperature on a Stoe-Siemens AED2-four circle diffractometer using Mo-Kα graphite-monochromated radiation (λ = 0.71073 Å: ω–2θ scans) and for **4** on a Stoe Imaging Plate Diffractometer System (Stoe & Cie, 1995) equipped with a one-circle goniometer and a graphite-monochromator. 200 exposures (3 min per exposure) were obtained at an image plate distance of 70 mm with $0 < \varphi < 200°$ and with the crystal oscillating through 1° in φ. The resolution was $D_{min} - D_{max}$ 0.81–12.45 Å. The structures were solved by direct methods using the program SHELXS-97[16] and refined by full matrix least squares on F^2 with SHELXL-97.[17] The positions of the hydrides in **2** and **3** as well as the vinyl proton in **4** were located from Fourier-difference maps and refined isotropically, while the remaining hydrogen atoms were included in calculated positions and treated as riding atoms using SHELXL-97 default parameters. For **2** and **3** an empirical absorption was applied based on ψ scans[18] and for **4** using DIFABS.[19] Crystallographic details are given in Table 7 and significant bond lengths and bond angles are listed in Tables 2, 3 and 4. The Figures were drawn with ORTEP[20] (thermal ellipsoides, 30% probability level).

CCDC reference number 186/1194.

See http://www.rsc.org/suppdata/dt/1998/3825/ for crystallographic files in .cif format.

Acknowledgements

We thank the Fonds National Suisse de la Recherche Scientifique for financial support of this work. A generous loan of ruthenium(III) chloride hydrate from the Johnson Matthey Research Centre is gratefully acknowledged.

References

1 E. Sappa, A. Tiripicchio and P. Braunstein, *Chem. Rev.*, 1983, **83**, 203.

2 N. T. Allison, J. R. Fritch, K. P. C. Vollhardt and E. C. Walborsky, *J. Am. Chem. Soc.*, 1983, **105**, 1384; A. D. Clauss, J. R. Shapley, C. N. Wilkes and R. Hoffmann, *Organometallics*, 1984, **3**, 169; J. R. Fox, W. L. Gladfelter, G. L. Goeffroy, I. Tavanaiepour, S. Abdel-Mequid and V. W. Day, *Inorg. Chem.*, 1981, **20**, 3230; E. Roland and H. Vahrenkamp, *Organometallics*, 1983, **2**, 183.

3 G. Süss-Fink and M. Jahncke, *Synthesis of Organic Compounds Catalysed by Transition Metal Clusters*, in *Catalysis by Di- and Polynuclear Metal Cluster Complexes*, ed. R. D. Adams and F. A. Cotton, Wiley-VCH, Chichester, 1998, ch. 6, p. 167.

4 G. Süss-Fink and F. Neumann, *The Use of Transition Metal Clusters in Organic Synthesis*, in *The Chemistry of the Metal-Carbon Bond*, ed. F. R. Hartley, Wiley, Chichester, 1989, vol. 5, ch. 7, p. 231.
5 (*a*) R. K. Pomeroy, *Tetranuclear Clusters of Ruthenium and Osmium*, in *Comprehensive Organometallic Chemistry 2*, ed. E. W. Abel, F. G. A. Stone and G. Wilkinson, Elsevier, Oxford, 1995, vol. 7, ch. 15, p. 835; (*b*) E. Sappa, A. Tiripicchio, A. J. Carty and G. E. Toogood, *Prog. Inorg. Chem.*, 1987, **35**, 437.
6 (*a*) J. T. Park, J. R. Shapley, C. Bueno, J. W. Ziller and M. Rowen Churchill, *Organometallics*, 1988, **7**, 2307; (*b*) J. T. Park, J. R. Shapley, M. Rowen Churchill and C. Bueno, *J. Am. Chem. Soc.*, 1983, **105**, 6182; (*c*) H. Chen, B. F. G. Johnson, J. Lewis, D. Braga, F. Grepioni and P. Sabatino, *J. Organomet. Chem.*, 1991, **405**, C22; (*d*) U. Riaz, M. D. Curtis, A. Rheingold and B. S. Haggerty, *Organometallics*, 1990, **9**, 2647; (*e*) Ming-Tsun Kuo, Der-Kweng Hwang, Chao-Shiuan Liu, Yun Chi, Shie-Ming Peng and Gene-Hsiang Lee, *Organometallics*, 1994, **13**, 2142.
7 G. Süss-Fink, S. Haak, V. Ferrand and H. Stoeckli-Evans, *J. Chem. Soc., Dalton Trans.*, 1997, 3861.
8 S. Deabate, R. Giordano, E. Sappa, *J. Cluster Sci.*, 1997, **8**, 407.
9 V. Ferrand, K. Merzweiler, G. Rheinwald, G. Süss-Fink and H. Stoeckli-Evans, *J. Organomet. Chem.*, 1997, **549**, 263 and refs. therein.
10 S. Aime, D. Osella, L. Milone, A. M. Manotti Lanfredi and A. Tiripicchio, *Inorg. Chim. Acta*, 1983, **71**, 141.
11 P. Mathur, S. Ghosh, Md. Munkir Hossain, C. V. V. Satyanarayana, A. L. Rheingold and G. P. A. Yap, *J. Organomet. Chem.*, 1997, **538**, 57 and refs. therein; A. A. Koridze, A. M. Sheloumov, F. M. Dolgushin, A. I. Yanovsky, Y. T. Struchkov and P. V. Petrovskii, *J. Organomet. Chem.*, 1997, **536**, 381.
12 H. Adams, N. A. Barley, L. J. Gill, M. J. Morris and T. A. Wildgoose, *J. Chem. Soc., Dalton Trans.*, 1996, 1437.
13 K. Wade, *Adv. Inorg. Chem. Radiochem.*, 1976, **18**, 1.
14 J. A. Cabeza, J. M. Ferandez-Colinas and A. Llamazares, *Synlett*, 1995, 579.
15 D. D. Perrin and W. L. F. Armarego, *Purification of Laboratory Chemicals*, Pergamon Press, Oxford, 3rd edn., 1988.
16 G. M. Sheldrick, *Acta Crystallogr., Sect. A*, 1990, **46**, 467.
17 G. M. Sheldrick, SHELXL-97, Program for crystal structure refinement, University of Göttingen, 1997.
18 A. C. T. North, D. C. Phillips and F. C. Mathews, *Acta Crystallogr., Sect. A*, 1968, **24**, 351.
19 N. Walker and D. Stuart, *Acta Crystallogr., Sect. A*, 1990, **46**, 158.
20 C. K. Johnson, ORTEP, Oak Ridge National Laboratory, Oak Ridge, TN, modified for PC by L. Zsolnai and H. Pritzkow, University of Heidelberg, Germany, 1994.

Paper 8/05852K

Tri- and Tetranuclear Mixed-Metal Clusters Containing Alkyne Ligands: Synthesis and Structure of $[Ru_3Ir(CO)_{11}(RCCR')]^-$, $[Ru_2Ir(CO)_9(RCCR')]^-$, and $[HRu_2Ir(CO)_9(RCCR')]$

Vincent Ferrand,[a] Georg Süss-Fink,*[a] Antonia Neels,[a] and Helen Stoeckli-Evans[a]

Keywords: Cluster compounds / Ruthenium / Iridium / Alkynes / Butterfly structures

The tetrahedral cluster anion $[Ru_3Ir(CO)_{13}]^-$ (**1**) reacts with internal alkynes RC≡CR' to afford the alkyne derivatives $[Ru_3Ir(CO)_{11}(RCCR')]^-$ (**2**: R = R' = Ph; **3**: R = R' = Et; **4**: R = Ph; R' = Me; **5**: R = R' = Me) which have a butterfly arrangement of the Ru_3Ir skeleton in which the alkyne is coordinated in a μ_4-η^2 fashion. Under CO pressure they undergo fragmentation to give the trinuclear cluster anions $[Ru_2Ir(CO)_9(RCCR')]^-$ (**6**: R = R' = Ph; **7**: R = R' = Et; **8**: R = Ph; R' = Me; **9**: R = R' = Me), in which the alkyne ligand is coordinated in a μ_3-η^2 parallel fashion. Protonation of these trinuclear anions leads to the formation of the corresponding neutral hydrido clusters $[HRu_2Ir(CO)_9(RC{\equiv}CR')]$ (**10**: R = R' = Ph; **11**: R = R' = Et; **12**: R = Ph; R' = Me; **13**: R = R' = Me). The protonation of the butterfly anions **2** and **3**, however, gives rise to the formation of the neutral tetrahedral clusters $[HRu_3Ir(CO)_{11}(RCCR')]$ (**14**: R = R' = Ph and **15**: R = R' = Et), respectively. The analogous clusters $[HRu_3Ir(CO)_{11}(PhCCCH_3)]$ (**16**) and $[HRu_3Ir(CO)_{11}(CH_3CCCH_3)]$ (**17**) are only accessible from the reaction of the neutral cluster $[HRu_3Ir(CO)_{13}]$ with the corresponding alkynes. The complexes **2**, **4**, **5**, **6**, **10**, **12** and **15** are characterised by X-ray structure analysis.

Introduction

The chemistry of mixed-metal clusters of transition metals has been studied in great detail in recent years,[1][2] stimulated by their possible catalytic potential and the combination of different metals in the same complex.[3a,3b] The mixed-metal cluster $Pt_3Ru_6(CO)_{20}(\mu_3\text{-}PhC_2Ph)(\mu_3\text{-}H)(\mu\text{-}H)$ has been shown by R. D. Adams et al. to be an very active catalyst for the hydrogenation of alkynes[3c–3e]. Tetranuclear clusters with the butterfly structure[4][5] have received much attention, due to their intermediary position between tetrahedral and square-planar clusters. They have been also considered as a model for chemisorption of small molecules,[6] and they have been studied as intermediates in homogeneous catalytic processes.[4,7,8] Both, metal atoms and ligands can vary widely in butterfly-type clusters, which determines, on the one hand, the structural properties of the butterfly framework and, on the other hand, the chemistry of the coordinated ligands.[4]

In a recent publication,[8] we have described the reactivity of the neutral tetrahedral cluster $[HRu_3Ir(CO)_{13}]$[9] towards alkynes and its catalytic potential in hydrogenation reactions. We now report the reaction of its precursor, the cluster anion $[Ru_3Ir(CO)_{13}]^-$[9] with internal alkynes, which affords anionic alkyne clusters of the type $[Ru_3Ir(CO)_{11}(RCCR')]^-$, and we also report on the reactivity of the latter anions towards CO and H^+.

[a] Institut de Chimie, Université de Neuchâtel,
Avenue de Bellevaux 51, CH-2000 Neuchâtel, Switzerland
Fax: (internat.) + 41-32/718-2400
E-mail: Georg.Suess-Fink@ch.unine.ch

Results and Discussion

Synthesis of the Cluster Anions $[Ru_3Ir(CO)_{11}(RCCR')]^-$ (2–5)

The thermal reaction of the tetrahedral cluster anion $[Ru_3Ir(CO)_{13}]^-$ (**1**) with the internal alkynes diphenylacetylene, 3-hexyne, 1-phenyl-1-propyne, or 2-butyne yields, at 90 °C in CH_2Cl_2 solution (pressure Schlenk tube), the alkyne derivatives $[Ru_3Ir(CO)_{11}(RCCR')]^-$ (**2**: R = R' = Ph; **3**: R = R' = Et; **4**: R = Ph; R' = Me; **5**: R = R' = Me) (Scheme 1). These anions can be isolated as the bis(triphenylphosphoranylidene)ammonium salts from a mixture of diethyl ether and hexane (**2**, **4**, and **5**), or from a mixture of ethanol and pentane (**3**). Complexes **2**, **4**, and **5** gave suitable crystals for X-ray structure analysis.

The infrared spectra of all the compounds display the same absorption pattern in the ν_{CO} region, indicating the presence of terminal as well as bridging CO ligands (Table 1). The ^{1}H-NMR spectra of **2**–**5** are complicated by the multiplets of the $[N(PPh_3)_2]^+$ cation; for **2** and **4**, the resonances of the phenyl protons of the alkyne ligands overlap with the signals of the cation. In the case of **4** (containing an unsymmetrical alkyne ligand), only one singlet at δ = 2.82 is observed for the methyl group, indicating the presence of only one isomer. In the case of **3** and **5** (containing a symmetrical alkyne ligand), the two alkyl substituents on the alkyne are nonequivalent, suggesting the alkyne ligand to be coordinated in a nonsymmetrical fashion to the Ru_3Ir framework (Table 1). This is confirmed by the X-ray structure analysis of the bis(triphenylphosphoranylidene)ammonium salts of **2**, **4**, and **5**.

  1434–1948/99/0505–0853 $ 17.50+.50/0

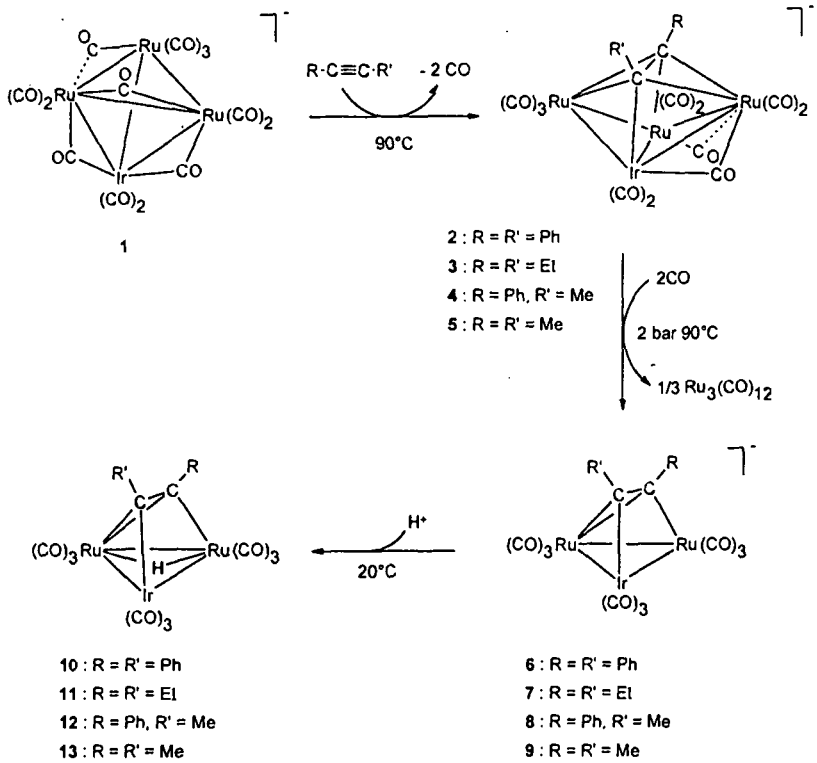

Scheme 1. Synthetic routes to clusters **2**–**13**

Molecular Structures of $[Ru_3Ir(CO)_{11}(RCCR')]^-$ (2, 4, and 5)

Suitable crystals of **2**, **4**, and **5** {$[N(PPh_3)_2]^+$ salts} were grown at room temperature from a mixture of diethyl ether and hexane. The molecular structures of the anions **2**, **4**, and **5** are depicted in Figures 1, 2, and 3, respectively. Selected bond lengths and angles of complexes **2**, **4**, and **5** are summarized in Tables 2, 3, and 4, respectively. The crystal structures consist of discrete $[N(PPh_3)_2]^+$ cations and $[Ru_3Ir(CO)_{11}(RCCR')]^-$ anions showing normal intermolecular contacts between the atoms of the ions. The cluster anions **2**, **4**, and **5** have the same overall structure: The four metal atoms form a butterfly skeleton where the iridium atom occupies a hinge position, whereas in the known cobalt analogue $[Ru_3Co(CO)_{11}(PhCCPh)]^-$,[10] obtained by reaction of $[Ru_3Co(CO)_{13}]^-$ with diphenylacetylene, the cobalt atom occupies a wingtip position. In other mixed-metal clusters anions with the butterfly core structure, such as $[Ru_3M(CO)_{10}Cp(CH_3CCCH_3)]^-$ (M = W, Mo)[11] and $[Co_3Ru(CO)_{10}(PhCCPh)]^-$,[12a] the single metal atom M always occupies a hinge position as found in **2**, **4**, and **5**.

All metal–metal distances in **2**, **4**, and **5** are different (Tables 2, 3, 4), but in the expected range for Ru–Ru and Ru–Ir single bonds.[4,8,9] In the three clusters, the coordination of the eleven carbonyl ligands is the same: While nine carbonyl groups are terminal, one CO ligand [C(6)O(6) in **2**, C(20)O(20) in **4**, C(10)O(10) in **5**] is bridging the Ir–Ru(3) edge, one CO ligand [C(10)O(10) in **2**, C(14)O(14) in **4**, C(15)O(15) in **5**] being coordinated to Ru(2) is semi-

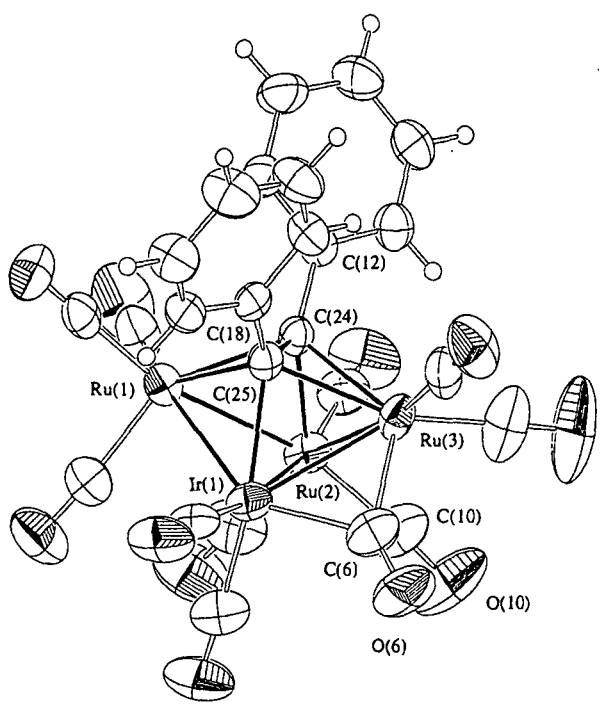

Figure 1. ORTEP plot of $[IrRu_3(CO)_{11}(\mu_4\text{-}\eta^2\text{-}C_2Ph_2)]^-$ (anion **2**); thermal ellipsoids are drawn at 50% of propability

bridging to Ru(3) as indicated by the distances carbon–Ru(2) [**2**: C(10)–Ru(2) = 1.903(7) Å; **4**: C(14)–Ru(2) = 1.896(3) Å; **5**: C(15)–Ru(2) = 1.903(6) Å] and the carbon–Ru(3) [**2**: C(10)–Ru(3) = 2.8893(3) Å; **4**:

Table 1. IR and NMR data of the complexes **2**–**17**

Complexes	ν_{CO} [cm^{-1}][a]	δ (^{1}H) [ppm][b–d]
[N(PPh$_3$)$_2$][Ru$_3$Ir(CO)$_{11}$(PhCCPh)] (**2**)	2055(m), 2009(vs), 1988(s), 1960(sh), 1913(w), 1801(w)	7.70–6.80 (C_6H_5, m)
[N(PPh$_3$)$_2$][Ru$_3$Ir(CO)$_{11}$(EtCCEt)] (**3**)	2052(m), 2002(vs), 1983(s), 1962(sh), 1937(m), 1913(w), 1794(w)	7.70–7.40 (C_6H_5, m); 2.68 ($CH_3CH_2CCCH_2CH_3$, q $^3J_{HH}$ 7.4 Hz); 2.61 ($CH_3CH_2CCCH_2CH_3$, q $^3J_{HH}$ 7.4 Hz); 0.94 ($CH_3CH_2CCCH_2CH_3$, t $^3J_{HH}$ 7.4 Hz); 0.90 ($CH_3CH_2CCCH_2CH_3$, t $^3J_{HH}$ 7.4 Hz)
[N(PPh$_3$)$_2$][Ru$_3$Ir(CO)$_{11}$(PhCCMe)] (**4**)	2055(m), 2007(vs), 1986(s), 1963(sh), 1936(m), 1909(w), 1799(w)	7.70–7.39 (C_6H_5, m); 2.82 (CH_3CCPh, s)
[N(PPh$_3$)$_2$][Ru$_3$Ir(CO)$_{11}$(MeCCMe)] (**5**)	2054(m), 2004(vs), 1984(s), 1959(sh), 1934(m), 1906(w), 1800(w)	7.70–7.42 (C_6H_5, m); 3.14 (CH_3CCCH_3, s); 2.91 (CH_3CCCH_3, s)
[N(PPh$_3$)$_2$][Ru$_2$Ir(CO)$_9$(PhCCPh)] (**6**)	2054(m), 2011(s), 1998(vs), 1980(s), 1940(m)	6.60–7.70 (C_6H_5, m)
[N(PPh$_3$)$_2$][Ru$_2$Ir(CO)$_9$(EtCCEt)] (**7**)	2048(w), 2002(s), 1992(vs), 1971(m), 1932(w)	7.70–7.20 (C_6H_5, m); 3.41 ($CH_{3c}CH_aH_bCCCH_{a'}H_{b'}CH_{3c'}$, dq $^3J_{HaHc}$ 7.2 Hz, $^2J_{HaHb}$ 13.3 Hz); 2.74 ($CH_{3c}CH_aH_bCCCH_{a'}H_{b'}CH_{3c'}$, dq $^3J_{Ha'Hc'}$ 7.3 Hz, $^2J_{Ha'Hb'}$ 13.0 Hz); 2.10 ($CH_{3c}CH_aH_bCCCH_{a'}H_{b'}CH_{3c'}$, dq $^3J_{HbHc}$ 7.2 Hz, $^2J_{HaHb}$ 13.3 Hz); 1.97 ($CH_{3c}CH_aH_bCCCH_{a'}H_{b'}CH_{3c'}$, dq $^3J_{Hb'Hc'}$ 7.3 Hz, $^2J_{Ha'Hb'}$ 13.0 Hz); 1.14 ($CH_{3c}CH_aH_bCCCH_{a'}H_{b'}CH_{3c'}$, t $^3J_{HH}$ 7.3 Hz); 1.07 ($CH_{3c}CH_aH_bCCCH_{a'}H_{b'}CH_{3c'}$, t $^3J_{HH}$ 7.3 Hz)
[N(PPh$_3$)$_2$][Ru$_2$Ir(CO)$_9$(PhCCMe)] (**8**)	2052(w), 2007(s), 1996(vs), 1976(m), 1938(w)	7.70–6.90 (C_6H_5, m); 2.64 (CH_3CCPh, s(isomer 1)); 2.30 (CH_3CCPh, s(isomer 2))
[N(PPh$_3$)$_2$][Ru$_2$Ir(CO)$_9$(MeCCMe)] (**9**)	2049(w), 2002(s), 1993(vs), 1971(m), 1934(w)	7.71–7.35 (C_6H_5, m); 2.70 (CH_3CCCH_3, s); 2.40 (CH_3CCCH_3, s)
[HRu$_2$Ir(CO)$_9$(PhCCPh)] (**10**)	2101(w), 2072(vs), 2061(s), 2034(s), 2022(m), 2016(m), 2005(w)	7.20–6.80 (C_6H_5, m); –15.07 (Ru*H*Ru, s)
[HRu$_2$Ir(CO)$_9$(EtCCEt)] (**11**)	2099(w), 2069(s), 2057(s), 2030(vs), 2018(m), 2008(m), 1990(w)	2.93 ($CH_3CH_2CCCH_2CH_3$, q $^3J_{HH}$ 7.4 Hz); 2.42 ($CH_3CH_2CCCH_2CH_3$, q $^3J_{HH}$ 7.4 Hz); 1.34 ($CH_3CH_2CCCH_2CH_3$, t $^3J_{HH}$ 7.4 Hz); 1.20 ($CH_3CH_2CCCH_2CH_3$, t $^3J_{HH}$ 7.4 Hz); –15.39 (Ru*H*Ru, s)
[HRu$_2$Ir(CO)$_9$(PhCCMe)] (**12**)	2100(w), 2071(vs), 2060(s), 2032(s), 2021(m), 2003(m), 1994(w)	7.20–6.90 (C_6H_5, m); 2.80 (CH_3CCPh, s); –15.27 (Ru*H*Ru, s)
[HRu$_2$Ir(CO)$_9$(MeCCMe)] (**13**)	2099(w), 2069(vs), 2057(s), 2030(vs), 2018(m), 2008(m), 1991(w)	2.83 (CH_3CCCH_3, s); 2.37 (CH_3CCCH_3, s); –15.31 (Ru*H*Ru, s)
[HRu$_3$Ir(CO)$_{11}$(PhCCPh)] (**14**)	2095(w), 2071(s), 2053(s), 2037(vs), 2012(m), 1994(m), 1842(w)	7.30–7.00 (C_6H_5, m); –18.88 (Ru*H*Ru, s)
[HRu$_3$Ir(CO)$_{11}$(EtCCEt)] (**15**)	2095(w), 2070(s), 2051(s), 2034(vs), 2010(m), 1991(m), 1840(w)	2.98 ($CH_3CH_aH_bCCCH_{a'}H_{b'}CH_3$, dq $^3J_{HH}$ 7.3 Hz, $^2J_{HH}$ 15.0 Hz); 2.74 ($CH_3CH_aH_bCCCH_{a'}H_{b'}CH_3$, dq $^3J_{HH}$ 7.3 Hz, $^2J_{HH}$ 15.0 Hz); 1.28 ($CH_3CH_aH_bCCCH_{a'}H_{b'}CH_3$, t $^3J_{HH}$ 7.3 Hz); –19.10 (Ru*H*Ru, s)
[HRu$_3$Ir(CO)$_{11}$(PhCCMe)] (**16**)	2093(w), 2065(s), 2048(s), 2032(vs), 2006(m), 1989(m), 1842(w)	7.50–7.20 (C_6H_5, m); 2.80 (CH_3, s) –18.88 (Ru*H*Ru, s)
[HRu$_3$Ir(CO)$_{11}$(MeCCMe)] (**17**)	2094(w), 2068(s), 2049(s), 2033(vs), 2009(m), 1988(m), 1844(w)	2.72 (CH_3, s); –18.98 (Ru*H*Ru, s)

[a] Recorded in ether (**2**–**5**), CH_2Cl_2 (**6**–**9**, **14**–**17**), hexane (**10**–**12**, **13**). – [b] Measured in $CDCl_3$ solution at 294 K at 200 MHz (**2**, **4**–**6**, **9**, **10**, **12**–**15**, **17**). – [c] Measured in $CDCl_3$ solution at 294 K at 400 MHz (**3**, **7**, **8**, **11**, **16**). – [d] Measured in $CDCl_3$ solution at 215 K at 400 MHz (**7**, **8**).

C(14)–Ru(3) = 2.8115(3) Å; **5**: C(15)–Ru(3) = 2.8613(7) Å]. The angles C(10)–Ru(2)–Ru(3) = 73.7(2)° (**2**), C(14)–Ru(2)–Ru(3) = 71.86(10)° (**4**), C(15)–Ru(2)–Ru(3) = 73.00(19)° (**5**) are found to be similar to the angle observed in the cluster anion [FeRu$_3$(CO)$_{12}$NO]$^-$[13] for a semibridging CO group.[14] These findings are comfirmed by the infrared spectra of **2**–**5** which exhibit a ν_{co} absorption around 1920 cm^{-1}.

The alkyne ligand in **2**, **4**, and **5** is coordinated to the Ru$_3$Ir metal core in a μ_4-η^2 fashion. One of the carbon atoms is σ-bonded to Ir, whereas the second one is σ-bonded to Ru(2), both carbon atoms being π-bonded to Ru(1) and Ru(3). This observation is confirmed by the ^{1}H-NMR spectra of **3** and **5** which display two different chemical shifts for the two ethyl or methyl substituents, respectively. The carbon–carbon bond is closer to Ru(1) than to Ru(3) in the three clusters, the torsion angle between the carbon–carbon backbone and the Ir(1)–Ru(2) edge is close to 0° [**2**: 0.0°(18); **4**: –0.04(11); **5**: 0.3°(2)] indicating that these two bonds are almost parallel.

With an electron count of 60e, **2**, **4**, and **5** are electron-deficient, since an M$_4$ butterfly cluster consistent with the noble-gas rule would require 62 electrons. However, considering **2**, **4**, and **5** as octahedral Ru$_3$IrC$_2$ clusters, an electron count of 60e is consistent with Wade's rules which predict a *closo* structure.[15]

Synthesis of [Ru$_2$Ir(CO)$_9$(RCCR′)]$^-$ (6–9)

The cluster anions [Ru$_3$Ir(CO)$_{11}$(RCCR′)]$^-$ (**2**: R = R′ = Ph; **3**: R = R′ = Et; **4**: R = Ph; R′ = Me; **5**: R = R′ = Me) undergo fragmentation of the metal core under CO pressure (2 bar) at 90 °C to give the trinuclear alkyne cluster anions [Ru$_2$Ir(CO)$_{11}$(RCCR′)]$^-$ (Scheme 1). They can be isolated as the bis(triphenylphosphoranylidene)ammonium salts from a mixture of CH_2Cl_2 and diethyl ether (**6**) or from ethanol and pentane (**7**–**9**). The loss of metal fragments from a cluster has already been observed;[16][17] for example the cluster anion [RuCo$_3$(CO)$_{10}$(μ_4-η^2-C$_2$Ph$_2$)]$^-$ can release a "Co(CO)" fragment to give the trinuclear complex [RuCo$_2$(CO)$_9$(μ_3-η^2-C$_2$Ph$_2$)] in which the alkyne adopts a parallel coordination.[12][18]

The infrared spectra of **6**–**9** exhibit in the carbonyl region absorptions of only terminal CO ligands (Table 1). The room-temperature ^{1}H-NMR spectrum of **8** reveals, in addition to the signals of the [N(PPh$_3$)$_2$]$^+$ cation, two singlets for the methyl group of the MeCCPh ligand in a ratio of

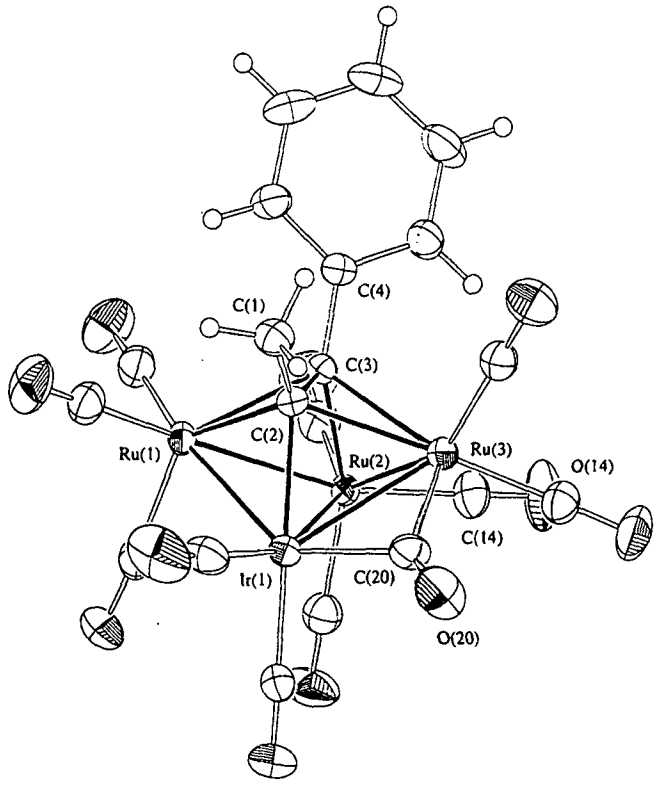

Figure 2. ORTEP plot of $[IrRu_3(CO)_{11}(\mu_4\text{-}\eta^2\text{-}PhCCMe)]^-$ (anion **4**); thermal ellipsoids are drawn at 50% of propability

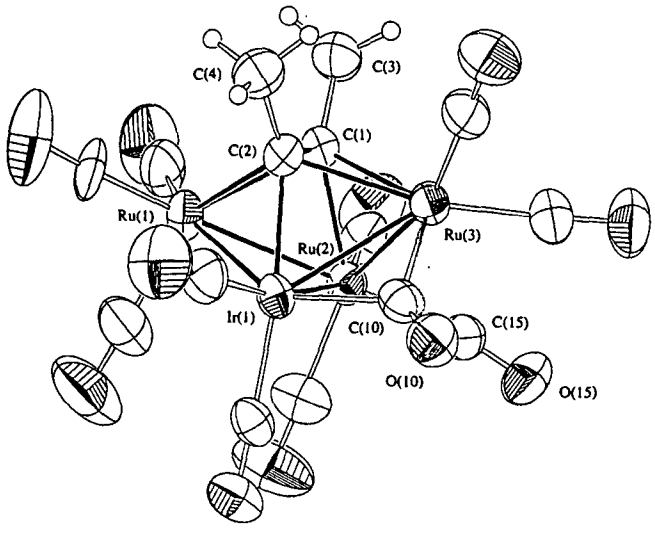

Figure 3. ORTEP plot of $[IrRu_3(CO)_{11}(\mu_4\text{-}\eta^2\text{-}C_2Me_2)]^-$ (anion **5**); thermal ellipsoids are drawn at 50% of propability

45:55. This ratio does not change down to −58 °C ($CDCl_3$), suggesting the presence of two isomers.[19–22] In the case of $[Ru_2Ir(CO)_9(MeCCMe)]^-$ (**9**), two singlets for the methyl substituents are observed in a ratio of 1:1, because the chemical environment of each CCH_3 moiety is different. The spectrum of $[Ru_2Ir(CO)_9(EtCCEt)]^-$ (**7**) is more complicated, presenting a temperature dependence of the signals of the ethyl substituents: At room temperature, four broad signals for the hydrogen atoms of the methylene groups are observed, resulting in four well-resolved multiplets at −58 °C, in a ratio of 1:1:1:1. In a selective decoupling experiment by irradiating at the resonances of the methyl proton, the four methylene multiplets resolve into four doublets with a coupling constant of 13 Hz, showing the protons of each methylene group to be diastereotopic (Table 1).[20,22a,22c,23a]

Table 2. Selected bond lengths [Å], bond angles [°], and torsion angles [°] for the anion **2**; estimated standard deviations in parentheses

Ir(1)–Ru(1)	2.7223(5)	Ru(3)–C(25)	2.298(4)
Ir(1)–Ru(3)	2.7235(6)	Ru(3)–C(24)	2.335(4)
Ir(1)–Ru(2)	2.7756(5)	Ru(3)–C(6)	1.993(6)
Ir(1)–C(6)	2.133(7)	C(24)–C(25)–C(18)	126.1(4)
Ir(1)–C(25)	2.188(4)	C(25)–C(24)–C(12)	127.1(4)
Ru(1)–Ru(2)	2.7357(6)	O(6)–C(6)–Ir(1)	134.9(6)
Ru(1)–C(25)	2.242(4)	O(6)–C(6)–Ru(3)	142.5(6)
Ru(1)–C(24)	2.258(5)	C(10)–Ru(2)–Ru(3)	73.7(2)
C(24)–C(25)	1.443(6)	O(10)–C(10)–Ru(2)	173.6(7)
		C(25)–Ir(1)–Ru(2)–C(24)	0.00(18)

Table 3. Selected bond lengths [Å], bond angles [°], and torsion angles [°] for the anion **4**; estimated standard deviations in parentheses

Ir(1)–Ru(1)	2.7025(4)	Ru(3)–C(2)	2.338(3)
Ir(1)–Ru(3)	2.7018(4)	Ru(3)–C(3)	2.375(3)
Ir(1)–Ru(2)	2.8690(4)	Ru(3)–C(20)	1.977(3)
Ir(1)–C(20)	2.105(3)	C(1)–C(2)–C(3)	124.8(2)
Ir(1)–C(2)	2.132(3)	C(2)–C(3)–C(4)	123.5(2)
Ru(1)–Ru(2)	2.7158(5)	O(20)–C(20)–Ir(1)	135.5(3)
Ru(1)–C(2)	2.282(3)	O(20)–C(20)–Ru(3)	141.6(3)
Ru(1)–C(3)	2.297(3)	C(14)–Ru(2)–Ru(3)	71.86(10)
Ru(2)–Ru(3)	2.7483(5)	O(14)–C(14)–Ru(2)	167.4(3)
Ru(2)–C(14)	1.896(3)	C(3)–Ru(2)–Ir(1)–C(2)	0.04(11)
Ru(2)–C(3)	2.151(3)	C(2)–C(3)	1.429(4)

Table 4. Selected bond lengths [Å], bond angles [°], and torsion angles [°] for the anion **5**; estimated standard deviations in parentheses

Ir(1)–Ru(1)	2.7044(7)	Ru(3)–C(1)	2.356(6)
Ir(1)–Ru(3)	2.7182(7)	Ru(3)–C(2)	2.321(5)
Ir(1)–Ru(2)	2.8000(8)	Ru(3)–C(10)	2.012(6)
Ir(1)–C(10)	2.125(6)	C(3)–C(1)–C(2)	123.7(5)
Ir(1)–C(2)	2.150(6)	C(1)–C(2)–C(4)	124.3(5)
Ru(1)–Ru(2)	2.7114(9)	O(10)–C(10)–Ir(1)	136.1(5)
Ru(1)–C(1)	2.272(5)	O(10)–C(10)–Ru(3)	141.8(5)
Ru(1)–C(2)	2.242(6)	C(15)–Ru(2)–Ru(3)	73.00(19)
Ru(2)–Ru(3)	2.7647(8)	O(15)–C(15)–Ru(2)	170.5(6)
Ru(2)–C(1)	2.154(6)	C(2)–Ir(1)–Ru(2)–C(1)	0.3(2)
Ru(2)–C(15)	1.903(6)	C(1)–C(2)	1.406(8)

Molecular Structure of $[Ru_2Ir(CO)_9(PhCCPh)]^-$(6)

The molecular structure of **6** was confirmed by a single-crystal X-ray structure analysis of the bis(triphenylphosphoranylidene)ammonium salt. Suitable crystals were obtained by slow diffusion of diethyl ether into a concentrated dichloromethane solution at room temperature. The molecular structure of the anion is depicted in Figure 4. Selected bond lengths and angles are presented in Table 5. The crystal structure consists of discrete $[N(PPh_3)_2]^+$ cations and

$[Ru_2Ir(CO)_9(PhCCPh)]^-$ anions showing normal intermolecular contacts between the atoms of the ions. The ruthenium and iridium atoms of the cluster anion form a closed triangle in which all the metal–metal distances are different but within the range of Ru–Ru and Ir–Ru single bonds (Table 5). Each metal atom is bonded to three terminal CO groups.

Table 5. Selected bond lengths [Å], bond angles [°], and torsion angles [°] for the anion **6**; estimated standard deviations in parentheses

Ir(1)–Ru(1)	2.7120(8)	Ru(2)–C(1)	2.096(8)
Ir(1)–Ru(2)	2.7952(10)	Ru(2)–C(1)	2.096(8)
Ir(1)–C(2)	2.117(8)	C(1)–C(2)	1.363(11)
Ru(1)–Ru(2)	2.7084(11)	C(1)–C(2)–C(3)	125.4(7)
Ru(1)–C(1)	2.260(8)	C(2)–C(1)–C(9)	123.5(7)
Ru(1)–C(2)	2.246(8)	C(9)–C(1)–C(2)–C(3)	−9.8(13)

The alkyne ligand is coordinated in a classical μ_3-η^2 fashion over the metal triangle[18] as observed in $[Co_2Ru(CO)_9(C_2Ph_2)]$[12] The C(1)–C(2) backbone is almost parallel to the Ir(1)–Ru(2) edge [C(2)–Ir(1)–Ru(2)–C(1) 1.2(3)°]. The carbon atoms C(1) and C(2) are σ-coordinated to Ir(1) and Ru(2), respectively, and are both π-bonded to Ru(1).

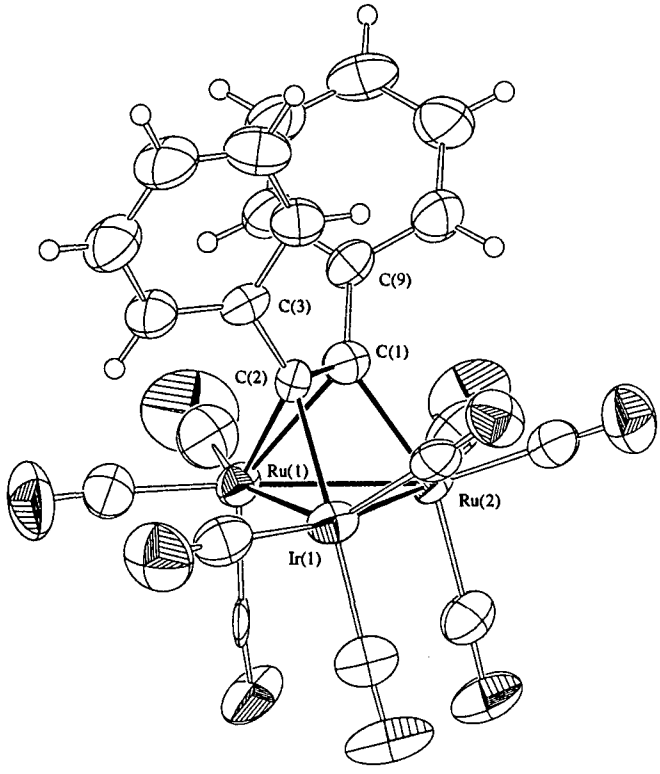

Figure 4. ORTEP plot of $[IrRu_2(CO)_9(\mu_3\text{-}\eta^2\text{-}C_2Ph_2)]^-$ (anion **6**); thermal ellipsoids are drawn at 50% of propability

The carbon–carbon bond is shorter in **6** [C(1)–C(2) 1.363(11) Å] than in **2** [C(24)–C(25) 1.443(6) Å]. This is due to the coordination of the alkyne to only three metal atoms in **6** with respect to **2** where it is coordinated to four metal atoms. The carbon–carbon bond length in **6** [C(1)–C(2) 1.363(11) Å] compares well with that in $[Co_2Ru(CO)_9(C_2Ph_2)]$ (C–C 1.370(3) Å)[12] and related complexes in which the C–C bond length varies from 1.33 to 1.47 Å.[18] Clusters **6**–**9** have the expected electron count of 48e for trinuclear clusters which obey the noble gas rule.

Synthesis of $[HRu_2Ir(CO)_9(RCCR')]$ (10–13)

The reaction of the anions $[Ru_2Ir(CO)_9(RCCR')]^-$ (**6**–**9**) with an excess of $HBF_4 \cdot OEt_2$ at room temperature leads to the formation of the neutral hydrido clusters $[HRu_2Ir(CO)_9(RCCR')]$ (**10**: R = R′ = Ph; **11**: R = R′ = Et; **12**: R = Ph; R′ = Me; **13**: R = R′ = Me), which can be isolated by chromatographic methods and recrystallized from hexane at −18 °C (Scheme 1).

The infrared spectra of **10**–**13** display an almost identical ν_{CO} absorption pattern in the region of terminal carbonyl ligands (Table 1). The ^{1}H-NMR spectra of **10**–**13** indicate, in addition to the signals of the alkyne substituents, the resonance of a bridging hydrido ligand at around δ = −15 (Table 1). In all cases, only one isomer is observed. For $[HRu_2Ir(CO)_9(EtCCEt)]$ (**11**) and $[HRu_2Ir(CO)_9(MeCCMe)]$ (**13**), the two ethyl or methyl groups are found to be nonequivalent.

Molecular Structure of $[HRu_2Ir(CO)_9(RCCR')]$ (10, 12)

Suitable crystals of $[HRu_2Ir(CO)_9(PhCCPh)]$ (**10**) and $[HRu_2Ir(CO)_9(PhCCMe)]$ (**12**) have been obtained from a concentrated hexane solution at −18 °C. The molecular structure of **10** is depicted in Figure 5 and that of **12** in Figure 6. Selected bond lengths and angles are presented in Tables 6 and 7. The crystal-structure analysis of **10** reveals two independent molecules per asymmetric unit of the unit cell, which have the same constitution, but differ slightly in bond lengths and angles.

The two clusters **10** and **12** have the same overall structure, showing the same carbonyl and alkyne coordination. The three metal atoms form a closed triangle. Each metal atom is bonded to three terminal CO groups. In both complexes the longer Ru(1)–Ru(2) distance [**10**: 2.7965(10); **12**: 2.7943(7) Å] suggests the presence of the hydrido bridge across this edge.

The alkyne ligand is coordinated in a μ_3-η^2 fashion over the Ru_2Ir framework as also found in cluster **6**. All carbon–carbon and carbon–metal distances compare well with those in other $M_3(\mu_3\text{-}\eta^2\text{-}RCCR')$ complexes.[18] The neutral complexes $[HRu_2Ir(CO)_9(RCCR')]$ (**10**–**13**) have, as the anions **6**–**9**, the expected electron count of 48e.

Reaction of $[Ru_3Ir(CO)_{11}(RCCR')]^-$ with $HBF_4 \cdot OEt_2$

Protonation of the anions $[Ru_3Ir(CO)_{11}(RCCR')]^-$ gives different results depending on the nature of the coordinated alkyne ligand. For R = R′ = Ph (**14**) or R = R′ = Et (**15**), the neutral hydrido complexes $[HRu_3Ir(CO)_{11}(PhCCPh)]$

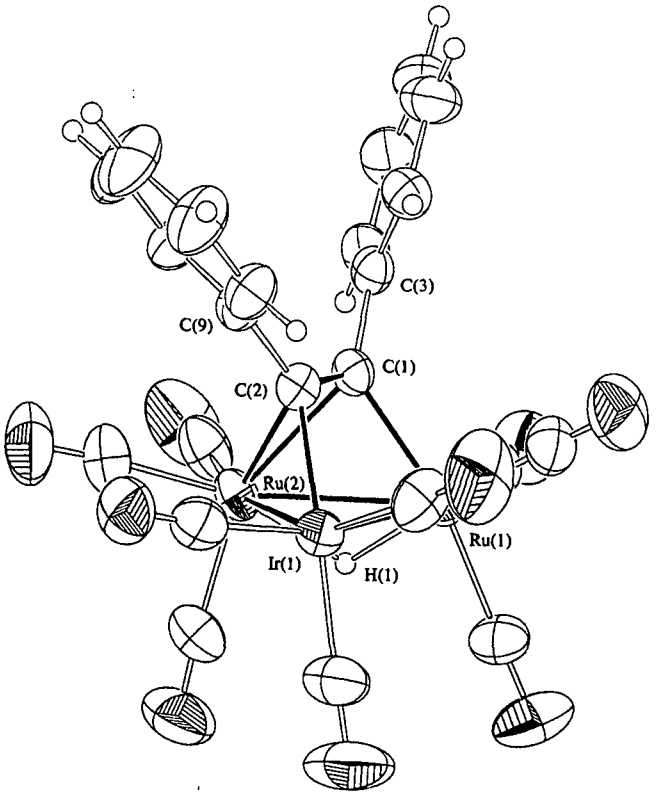

Figure 5. ORTEP plot of $[HIrRu_2(CO)_9(\mu_3\text{-}\eta^2\text{-}C_2Ph_2)]$ **10**; thermal ellipsoids are drawn at 50% of propability

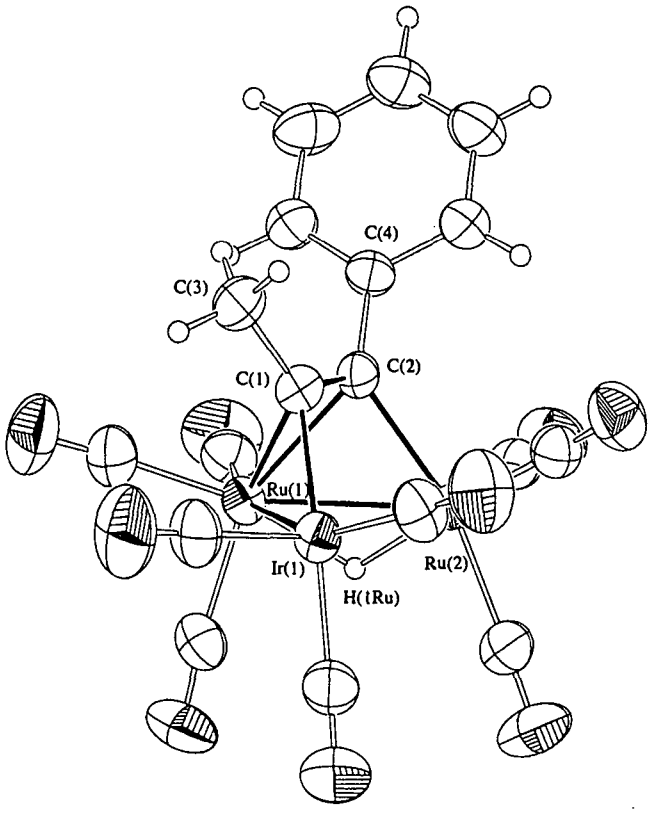

Figure 6. ORTEP plot of $[HIrRu_2(CO)_9(\mu_3\text{-}\eta^2\text{-}PhCCMe)]$ **12**; thermal ellipsoids are drawn at 50% of propability

Table 6. Selected bond lengths [Å], bond angles [°], and torsion angles [°] for **10**; estimated standard deviations in parentheses

Molecule A		Molecule B	
Ir(1)–Ru(2)	2.6901(7)	Ir(2)–Ru(4)	2.6936(9)
Ir(1)–Ru(1)	2.7523(8)	Ir(2)–Ru(3)	2.7517(8)
Ir(1)–C(2)	2.076(6)	Ir(2)–C(25)	2.080(6)
Ru(1)–Ru(2)	2.7965(10)	Ru(3)–C(24)	2.119(7)
Ru(1)–C(1)	2.113(7)	Ru(3)–Ru(4)	2.7938(9)
Ru(1)–H(1)	1.77(11)	Ru(3)–H(2)	1.63(11)
Ru(2)–C(1)	2.295(6)	Ru(4)–C(25)	2.310(6)
Ru(2)–C(2)	2.307(6)	Ru(4)–C(24)	2.325(7)
Ru(2)–H(1)	1.85(11)	Ru(4)–H(2)	1.91(11)
C(1)–C(2)	1.374(9)	C(24)–C(25)	1.375(9)
C(2)–C(1)–C(3)	123.9(6)	C(25)–C(24)–C(26)	124.4(6)
C(1)–C(2)–C(9)	125.0(6)	C(24)–C(25)–C(32)	124.9(6)
C(3)–C(1)–C(2)–C(9)	8.7(10)	C(26)–C(24)–C(25)–C(32)	−6.5(10)

Table 7. Selected bond lengths [Å], bond angles [°], and torsion angles [°] for **12**; estimated standard deviations in parentheses

Ir(1)–Ru(1)	2.6924(6)	Ru(2)–C(2)	2.111(6)
Ir(1)–Ru(2)	2.7578(5)	Ru(2)–H(1Ru)	1.78(7)
Ir(1)–C(1)	2.074(6)	C(1)–C(2)	1.372(9)
Ru(1)–Ru(2)	2.7943(7)	C(2)–C(1)–C(3)	123.9(6)
Ru(1)–C(2)	2.285(6)	C(1)–C(2)–C(4)	124.4(5)
Ru(1)–C(1)	2.318(6)	C(3)–C(1)–C(2)–C(4)	−0.3(10)
Ru(1)–H(1Ru)	1.81(7)		

(**14**) and $[HRu_3Ir(CO)_{11}(EtCCEt)]$ (**15**) are formed (Scheme 2). When R or R′ is a methyl group, the reaction does not afford the neutral hydrido complex, but leads to an unidentified green decomposition product. The expected clusters $[HRu_3Ir(CO)_{11}(PhCCMe)]$ (**16**) and $[HRu_3Ir(CO)_{11}(MeCCMe)]$ (**17**) are, however, accessible from the reaction of the neutral hydrido cluster $[HRu_3Ir(CO)_{13}]$ with the corresponding alkyne (Scheme 2). Clusters **14** and **17** have already been reported[8] and they are included here for the sake of completeness.

The infrared spectra of **14**–**17** display in the ν_{CO} region the same absorption pattern: Five bands are assigned to terminal CO ligands and one absorption around 1840 cm^{-1} corresponds to a bridging CO group (Table 1). In the ^1H-NMR spectra of **14**–**17**, the hydrido ligand resonates as a singlet around $\delta = -19$. In **15** the ethyl substituents of the alkyne ligand are found to be equivalent, but the two hydrogen atoms of the methylene groups are diastereotopic (Table 1). The molecular structure of **15** is confirmed by a single-crystal X-ray structure analysis.

Molecular Structure of $[HRu_3Ir(CO)_{11}(EtCCEt)]$ (15)

Suitable crystals of **15** were grown at −18 °C in hexane. The molecular structure of **15** is depicted in Figure 7. Selected bond lengths and angles of **15** are listed in Table 8. The complex **15** has the same overall structure as found in **14** and **17**,[8] showing the same carbonyl, alkyne and hydride coordination pattern.

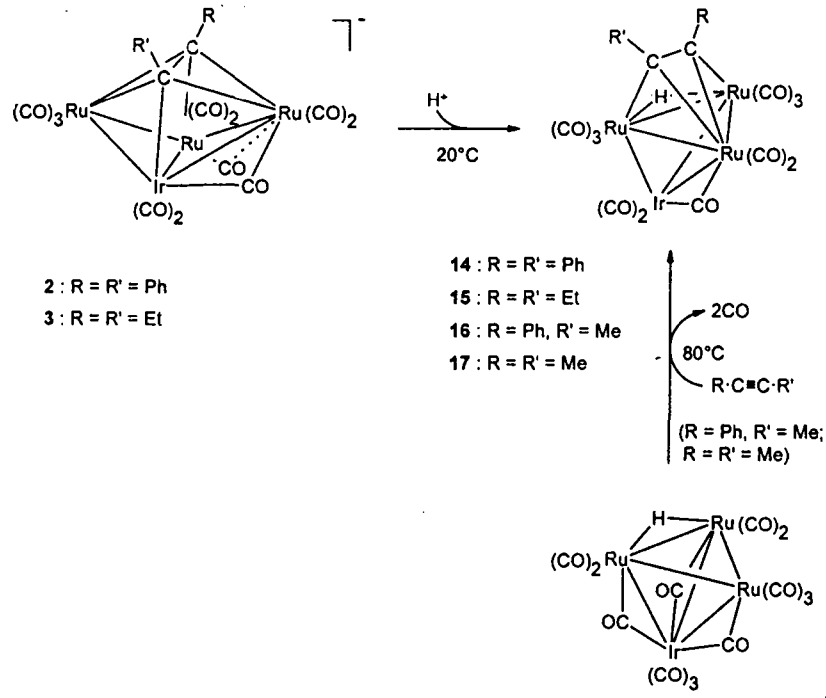

Scheme 2. Synthetic routes to clusters **14**–**17**

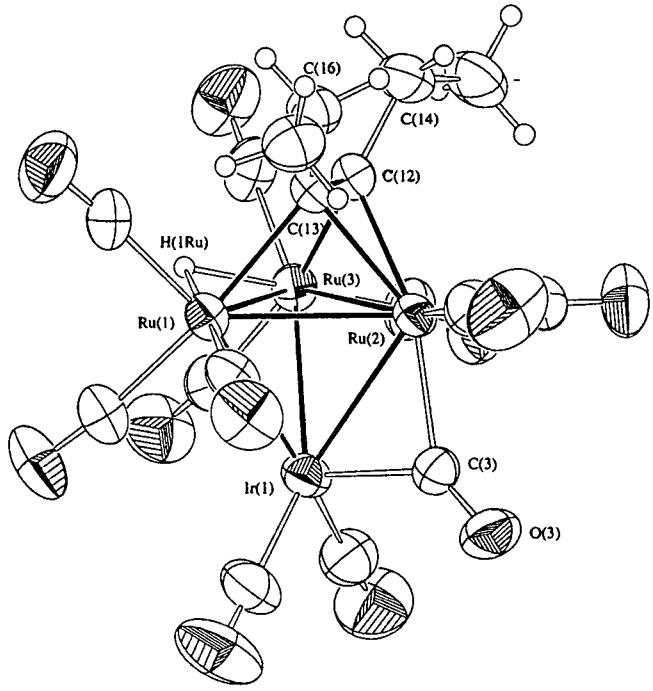

Figure 7. ORTEP plot of $[HIrRu_3(CO)_{11}(\mu_3\text{-}\eta^2\text{-}C_2Et_2)]$ **15**; thermal ellipsoids are drawn at 50% of propability

The four metal atoms form a tetrahedron in which the Ru–Ir distances vary from 2.7228(11) to 2.7833(8) Å and the Ru–Ru distances from 2.7981(10) to 2.8514(9) Å, in accordance with metal–metal single bonds.[8] The cluster **15** presents, as expected for a tetrahedral arrangement, an electron count of 60 e. The short distance Ru(2)–Ir [2.7228(11) Å] is due to the bridging carbonyl ligand over this edge. The base of the tetrahedron is composed of three ruthenium atoms. The longer Ru(1)–Ru(3) distance [2.8514(9) Å] suggests the presence of the hydrido bridge across this edge. Two of the three ruthenium atoms are bonded to three terminal CO groups, whereas Ru(2) and Ir are bonded to two terminal CO groups and share the bridging CO ligand. The alkyne is coordinated in a μ_3-η^2-bonding mode over the Ru_3 face of the tetrahedron. Due to the coordination of the alkyne group to the metal core, the carbon–carbon bond is lengthened [C(12)–C(13) 1.395(11) Å], but is in the range observed in **14**, **17**,[8] and other clusters such as $HCpWOs_3[\mu_3\text{-}\eta^2\text{-}C_2(Tol)_2]$.[24][25]

Table 8. Selected bond lengths [Å], bond angles [°], and torsion angles [°] for **15**; estimated standard deviations in parentheses

Ir(1)–Ru(1)	2.7727(9)	Ru(2)–C(12)	2.183(7)
Ir(1)–Ru(2)	2.7228(11)	Ru(2)–C(13)	2.168(7)
Ir(1)–Ru(3)	2.7833(8)	Ru(3)–C(12)	2.149(8)
Ru(1)–Ru(2)	2.7981(10)	Ru(3)–H(1Ru)	1.75(6)
Ru(1)–Ru(3)	2.8514(9)	C(12)–C(13)	1.395(11)
Ru(1)–C(13)	2.154(7)	C(13)–C(12)–C(14)	121.7(7)
Ru(1)–H(1Ru)	1.81(6)	C(12)–C(13)–C(16)	122.7(7)
Ru(2)–Ru(3)	2.8110(9)	C(14)–C(12)–C(13)–C(16)	0.4(11)

Conclusions

The Ru_3Ir framework shows a great fexibility with respect to the coordination of alkyne ligands: The tetrahedral metal skeleton in $[Ru_3Ir(CO)_{13}]^-$ (**1**) opens up upon coordination of an alkyne ligand to give a butterfly framework in $[Ru_3Ir(CO)_{11}(RCCR)]^-$ (**2**–**5**). Protonation of the butterfly clusters **2** and **3** leads, with closure of the Ru–Ru bond, back to a tetrahedral metal skeleton in the neutral clusters $[HRu_3Ir(CO)_{11}(RCCR')]$ (**14**–**15**). The second important

feature is the fragmentation of the tetranuclear anions in $[Ru_3Ir(CO)_{11}(RCCR)]^-$ (**2**–**5**) under CO pressure to give the trinuclear anions $[Ru_2Ir(CO)_9(RCCR)]^-$ (**6**–**9**). In a comparison of the 3-hexyne complexes, it is interesting to note that in the case of **3** and **11**, the two protons of the two different CH_2 groups of the 3-hexyne ligand are equivalent, whereas in **7** and **15** they are nonequivalent (diastereotopic). In the case of the tetranuclear cluster $[Ru_3Ir(CO)_{11}(EtCCEt)]^-$ (**3**) the averaging of the methylene protons may be explained by a carbonyl fluxionality involving the bridging and semi-bridging carbonyl ligands which could brigde equally well to both wingtip ruthenium atoms. In the case of the trinuclear cluster $[HRu_2Ir(CO)_9(EtCCEt)]$ (**11**), the μ_3-alkyne ligand itself might be fluxional on the trinuclear metal core, as observed in $[H_2Ru_3(CO)_9(EtCCEt)]$,[122a] $[Co_2Ru(CO)_9(EtCCEt)]$,[119] $[FeCo_2(CO)_9(EtCCEt)]$,[121] $[CpNiCoM(CO)_6(EtCCEt)]$ (M = Fe, Ru, Os),[123a] $[H_2Os_3(CO)_9(C_9H_6)]$.[23b]

Experimental Section

General: All reactions were carried out under pure nitrogen with standard Schlenk techniques. Solvents were destilled with appropriate drying agents, deoxygenated, and nitrogen-saturated prior to use.[26] – Preparative thin-layer chromatography was performed using 20 cm × 20 cm plates coated with Fluka silica gel G. The starting complexes $[Ru_3Ir(CO)_{13}]^-$ and $[HRu_3Ir(CO)_{13}]$ were prepared according to a published method.[9] – Diphenylacetylene was purchased from Fluka; 3-hexyne, 1-phenyl-1-propyne, and 2-butyne were purchased from Aldrich and used as recieved. – NMR spectra were recorded with a Varian Gemini 200 BB or a Bruker AMX 400 spectrometer, using the resonance of the residual protons of the deuterated solvents as reference. – Infrared spectra were recorded with a Perkin–Elmer 1720X FT IR spectrometer. – Micro-analyses were carried out by the Mikroelementaranalytisches Laboratorium of the ETH Zürich, Switzerland.

Preparations

$[N(PPh_3)_2][Ru_3Ir(CO)_{11}(RCCR')]$ (Anions 2–5): A solution of $[N(PPh_3)_2][Ru_3Ir(CO)_{13}]$ (anion **1**) (100 mg, $7.15 \cdot 10^{-2}$ mmol) in CH_2Cl_2 (30 mL) was stirred with an excess of RC≡CR' (**2**: 38 mg, $21.46 \cdot 10^{-2}$ mmol; **3**: 24 μL, $21.46 \cdot 10^{-2}$ mmol; **4**: 27 μL, $21.46 \cdot 10^{-2}$ mmol; **5**: 17 μL, $21.46 \cdot 10^{-2}$ mmol) at 90 °C in a pressure Schlenk tube. During the reaction the pressure was released once. The reaction was followed by infrared spectroscopy; after 2.5 h, the IR spectrum in the ν_{CO} region indicated the complete desappearance of the starting complex **1**. Then the solvent was evaporated and the red-orange oil was washed three times with 10 mL of hexane to remove the excess of the unreacted alkyne. The residue was dissolved in 20 mL of Et_2O, and the solution was filtered. Dark-red air-stable crystals of the $[N(PPh_3)_2]^+$ salts of **2**, **4**, **5** were obtained by slow evaporation (room temperature) of a diethyl ether/hexane solution. The crystals were dried in vacuo. – **2**: Yield 92 mg (85%). – $C_{61}H_{40}IrNO_{11}P_2Ru_3$ (1520.36): calcd. C 48.19, H 2.65, N 0.92; found C 48.32, H 2.58, N 0.93. – **4**: Yield 83 mg (80%). – $C_{56}H_{38}O_{11}NP_2Ru_3Ir$ (1458.28): calcd. C 46.12, H 2.63, N 0.96, found C 45.94, H 2.37, N 1.00. – **5**: Yield 75 mg (75%). – $C_{51}H_{36}O_{11}NP_2Ru_3Ir$ (1396.22): calcd. C 43.87, H 2.60, N 1.00; found C 43.77, H 2.45, N 1.01. – For **3**, a different method of crystallisation was used. The filtered diethyl ether solution containing **3** was concentrated to dryness, the residue was dissolved in 10 mL of ethanol, followed by the dropwise addition of pentane until the solution became cloudy. Then the solution was cooled to −18 °C for a few days giving the $[N(PPh_3)_2]^+$ salt of **3** as dark-violet needles. The crystals were dried in vacuo. – **3**: Yield 76 mg (75%). – $C_{53}H_{40}IrNO_{11}P_2Ru_3 \cdot H_2O$ (1424.28): calcd. C 44.13, H 2.93, N 0.97; found C 43.96, H 2.76, N 1.02.

$[N(PPh_3)_2][Ru_2Ir(CO)_9(PhCCPh)]$ (Anion 6): A solution containing $[N(PPh_3)_2][Ru_3Ir(CO)_{11}(PhCCPh)]$ (anion **2**), prepared from 0.0715 mmol of **1** as described above, in Et_2O (20 mL) was placed in a pressure Schlenk tube and stirred at room temperature for 20 h under a pressure of 2 bar of CO. The colour changed from red-orange to wine-red, then to orange with precipitation of the $[N(PPh_3)_2]^+$ salt of **6** as a yellow powder. The precipitate was filtered off, washed with Et_2O (3 × 10 mL) and crystallised at room temperature by slow diffusion of Et_2O into a CH_2Cl_2 solution. The yellow crystals were dried in vacuo. **6**: Yield (with respect to **1**): 73 mg (75%). – $C_{59}H_{40}IrNO_9P_2Ru_2$ (1363.27): calcd. C 51.98, H 2.99, N 1.03; found C 51.68, H 2.99, N 1.04.

$[N(PPh_3)_2][Ru_2Ir(CO)_9(RCCR')]$ (Anions 7, 8, 9): A solution containing $[N(PPh_3)_2][Ru_3Ir(CO)_{11}(RCCR')]$ (**3**: R = R' = Et; **4**: R = Ph; R' = Me; **5**: R = R' = Me), prepared from 0.0715 mmol of **1** as described above, in CH_2Cl_2 (25ml) was placed in a pressure Schlenk tube and stirred at 90 °C for 45 min under a pressure of 2 bar of CO. The colour changed, from red-orange to wine-red, then to orange. After removal of the solvent, the orange residue was washed with hexane (3 × 10 ml) to remove $Ru_3(CO)_{12}$ formed during the reaction. The remaining orange oil was dried and dissolved in 5–10 mL of ethanol, followed by the addition of pentane until the solution became cloudy. In the case of **8** no pentane was added. Then the solution was cooled to −18 °C for a few days which gave the $[N(PPh_3)_2]^+$ salt of **7** as yellow-orange crystals and the $[N(PPh_3)_2]^+$ salts of **8** and **9** precipitated as a yellow-brown powder. The solids were dried in vacuo. – **7**: Yield (with respect to **1**): 51 mg (56%). – $C_{51}H_{40}IrNO_9P_2Ru_2 \cdot 2.5\,H_2O$ (1267.19): calcd. C 46.65, H 3.42, N 1.06; found C 46.42, H 3.02, N 1.11. – **8**: Yield (with respect to **1**): 56 mg (60%). – $C_{54}H_{38}IrNO_9P_2Ru_2$ (1301.20): calcd. C 49.85, H 2.94, N 1.08; found C 49.66, H 3.16, N 1.16. – **9**: Yield (with respect to **1**): 49 mg (55%). – $C_{49}H_{36}IrNO_9P_2Ru_2$ (1239.13): calcd. C 47.50, H 2.93, N 1.13; found C 47.24, H 3.13, N 1.19.

$[HRu_2Ir(CO)_9(RCCR')]$ (10–13): To a solution of $[N(PPh_3)_2][Ru_2Ir(CO)_9(RCCR')]$ (anions **6**: R = R' = Ph; **7**: R = R' = Et; **8**: R = Ph; R' = Me; **9**: R = R' = Me) (0.0370 mmol) in CH_2Cl_2 (30 mL) a slight excess of $HBF_4 \cdot OEt_2$ (54%, 60 μL) was added under stirring. After 30 min, the solvent was evaporated, and the residue was dissolved in the minimum quantity of CH_2Cl_2. The solution was separated by thin-layer chromatography with a mixture of CH_2Cl_2 and hexane (1:6) as eluent. The yellow band containing the product was extracted with CH_2Cl_2, followed by concentration to dryness. The resulting yellow oil was dissolved in hexane and cooled to −18 °C to give yellow crystals of **10**–**13**. The crystals were dried in vacuo. – **10**: Yield 21 mg (68%). – $C_{23}H_{11}IrO_9Ru_2$ (825.69): calcd. C 33.46, H 1.34; found C 33.48, H 1.32. – **11**: Yield 18 mg (66%). – $C_{15}H_{11}IrO_9Ru_2$ (729.61): calcd. C 24.69, H 1.52; found C 24.51, H 1.54. – **12**: Yield 17 mg (60%). – $C_{18}H_9IrO_9Ru_2$ (763.62): calcd. C 28.31, H 1.19; found C 28.40, H 1.24. – **13**: Yield 16 mg (62%). – $C_{13}H_7IrO_9Ru_2$ (701.55): calcd. C 22.26, H 1.01; found C 22.12, H 1.04.

$[HRu_3Ir(CO)_{11}(RCCR')]$ (14–15): To a solution of $[N(PPh_3)_2][Ru_3Ir(CO)_{11}(RCCR')]$ (**2**: R = R' = Ph; **3**: R = R' = Et), prepared from 0.0715 mmol of $[N(PPh_3)_2]$**1** as described above, in 20 mL of Et_2O was added a slight excess of $HBF_4 \cdot OEt_2$ (54%,

Table 9. Crystallographic data and refinement details for compounds **2**, **4**, **5**, and **6**

	2	**4**	**5**	**6**
Formula	$C_{61}H_{40}O_{11}NP_2IrRu_3$ 0.25 C_6H_{14}	$C_{56}H_{38}O_{11}NP_2IrRu_3$	$C_{51}H_{36}O_{11}NP_2IrRu_3$	$C_{59}H_{40}O_9NP_2IrRu_3$
M	1520.42	1458.22	1396.16	1363.20
Crystal system	Triclinic	Triclinic	Triclinic	Triclinic
Space group	$P\bar{1}$	$P\bar{1}$	$P\bar{1}$	$P\bar{1}$
a [Å]	10.1350(8)	9.2769(10)	10.678(2)	10.5124(11)
b [Å]	15.5218(13)	16.7823(16)	15.741(4)	15.545(3)
c [Å]	19.8838(17)	17.2250(17)	15.705(3)	17.830(3)
α [°]	98.652(10)	88.034(12)	102.672(19)	100.04(2)
β [°]	99.163(10)	84.463(12)	91.363(12)	101.543(14)
γ [°]	94.583(10)	80.982(12)	103.730(13)	101.551(19)
V [Å^3]	3035.6(4)	2635.7(5)	2493.7(9)	2726.3(8)
Z	2	2	2	2
Crystal size [mm]	0.38 × 0.15 × 0.11	0.50 × 0.50 × 0.30	0.65 × 0.58 × 0.53	0.57 × 0.27 × 0.27
Colour	Dark-red	Black	Black	Yellow
D_c [g cm^{-3}]	1.687	1.837	1.859	1.661
μ [mm^{-1}]	3.028	3.482	3.675	3.097
Transmission factors: min/max	–	0.479/0.832	0.3979/0.6612	0.3427/0.3917
F(000)	1505	1416	1352	1336
θ limits [°]	2.13–25.88	2.38–25.88	2.10–25.48	2.01–25.49
hkl ranges	−12 to 11, −19 to 18, −24 to 24	−11 to 11, −20 to 20, −20 to 21	−12 to 12, −19 to 18, 0 to 19	−12 to 12, −18 to 18, 0 to 21
Reflections measured	23865	20460	9251	10126
Independent reflections	10950	9406	9251	10126
Observed reflections	7930	8994	8542	8153
$R1$ [$I > 2\sigma(I)$]/$R1$ (all data)[a]	0.0316/0.0483	0.0226/0.0240	0.0371/0.0433	0.0551/0.0778
$wR2$ [$I > 2\sigma(I)$]/$wR2$ (all data)[b]	0.0739/0.0783	0.0567/0.0576	0.1004/0.1107	0.1184/0.1334
Goodness of fit on F^2[c]	0.882	1.065	1.379	1.169
Maximum δ/σ	0.002	0.002	0.061	0.019
Largest diff. peak and hole [e Å^3]	1.070/−1.829	1.342/−1.125	1.580/−1.373	1.749/−1.457

[a] $R1 = \Sigma||F_o| - |F_c||/\Sigma|F_o|$. – [b] $wR2 = [\Sigma w(F_o^2 - F_c^2)^2/\Sigma w(F_o)^4]^{1/2}$. – [c] $S = [\Sigma w(F_o^2 - F_c^2)^2/(n - p)]^{1/2}$ (n: number of reflections; p: number of parameters).

Table 10. Crystallographic data and refinement details for compounds **10**, **12**, and **15**

	10	**12**	**15**
Formula	$C_{23}H_{11}O_9IrRu_2$	$C_{18}H_9O_9IrRu_2$	$C_{17}H_{11}O_{11}IrRu_3$
M	825.66	763.59	886.67
Crystal system	Triclinic	Triclinic	Triclinic
Space group	$P\bar{1}$	$P\bar{1}$	$P\bar{1}$
a [Å]	10.927(2)	9.1281(5)	8.0650(14)
b [Å]	14.480(3)	9.9456(6)	9.4766(13)
c [Å]	16.793(2)	12.6212(14)	16.423(4)
α [°]	70.080(13)	96.966(9)	96.392(19)
β [°]	85.071(17)	108.833(9)	101.47(2)
γ [°]	86.106(19)	96.349(7)	109.063(14)
V [Å^3]	2486.8(8)	1062.70(15)	1141.4(4)
Z	4	2	2
Crystal size [mm]	0.57 × 0.57 × 0.42	0.68 × 0.34 × 0.34	0.95 × 0.65 × 0.36
Colour	Yellow	Yellow	Red-orange
D_c [g cm^{-3}]	2.205	2.386	2.580
μ [mm^{-1}]	6.586	7.695	7.811
Transmission factors: min/max	0.0474/0.0845	0.0671/0.1236	0.0137/0.0460
F(000)	1544	708	820
θ limits [°]	2.20–25.47	2.09–25.48	2.32–25.46
hkl ranges	−13 to 13, −16 to 17, 0 to 20	−11 to 10, −12 to 11, 0 to 15	−9 to 9, −11 to 11, 0 to 19
Reflections measured	9223	3941	4324
Independent reflections	9223	3941	4234
Observed reflections	8141	3774	4134
$R1$ [$I > 2\sigma(I)$]/$R1$ (all data)[a]	0.0360/0.0441	0.0290/0.0309	0.0365/0.0387
$wR2$ [$I > 2\sigma(I)$]/$wR2$ (all data)[b]	0.0870/0.0920	0.0833/0.0849	0.1071/0.1127
Goodness of fit on F^2[c]	1.258	1.292	1.280
Maximum δ/σ	0.004	0.001	0.001
Largest diff. peak and hole [e Å^3]	0.916/−0.876	1.237/−0.987	1.831/−1.445

[a] $R1 = \Sigma||F_o| - |F_c||/\Sigma|F_o|$. – [b] $wR2 = [\Sigma w(F_o^2 - F_c^2)^2/\Sigma w(F_o)^4]^{1/2}$. – [c] $S = [\Sigma w(F_o^2 - F_c^2)^2/(n - p)]^{1/2}$ (n: number of reflections; p: number of parameters).

60 μL). After 30 min at room temperature, the white precipitate was filtered off, washed twice with 10 mL of Et_2O and then discarded. The solution was concentrated, the residue dissolved in CH_2Cl_2 (2 mL) and submitted to thin-layer chromatography (silica gel, CH_2Cl_2/hexane, 1:3). The product was extracted from the orange main band with CH_2Cl_2 and crystallised from hexane at

−18 °C. The orange air-stable crystals were dried in vacuo. − **14**: Yield (starting from **1**) 36 mg (51%). − **15**: Yield (starting from **1**) 29 mg (45%) − $C_{17}H_{11}IrO_{11}Ru_3$ (886.69): calcd. C 23.02, H 1.25; found C 23.21, H 1.30.

[$HRu_3Ir(CO)_{11}$(PhCCMe)] (16): A solution of $[HRu_3Ir(CO)_{13}]$[9] (83 mg, 0.096 mmol) and PhC≡CMe (18 μL, 0.145 mmol) in hexane (30 mL) was stirred at 80−85 °C in a pressure Schlenk tube. During the reaction, the pressure was released once. After 1 h, the solution changed colour from red to orange. After removal of the solvent, the dark orange residue was dissolved in 5 ml of CH_2Cl_2 and submitted to thin-layer chromatography (silica gel. CH_2Cl_2/hexane, 1:3). From the orange main band, **16** was extracted with CH_2Cl_2 and crystallised from hexane at −18 °C. The orange air-stable crystals were dried in vacuo. − **16**: Yield 27 mg (31%) − $C_{20}H_9IrO_{11}Ru_3$ (920.71): calcd. C 26.09, H 0.99; found, C 26.02, H 0.99.

X-ray Structure Analyses: Single crystals of **2**, **4**, **5**, **6**, **10**, **12**, and **15** were obtained as described under Preparations. Selected crystallographic data for the complexes are summarised in Tables 9 and 10, and selected bond lengths and bond angles are listed in Tables 2−8. Single-crystal X-ray diffraction data of the $[N(PPh_3)_2]^+$ salts of **2** and **4** were collected at room temperature and −50 °C, respectively with a Stoe Imaging Plate Diffractometer System (Stoe & Cie, 1995) equipped with a one-circle goniometer and a graphite monochromator. 200 exposures (3 min per exposure) were obtained at an image-plate distance of 70 mm with $0° < \phi < 200°$ and with the crystal oscillating through 1° in ϕ. The $[N(PPh_3)_2]^+$ salts of **5** and **6** and complexes **10**, **12**, and **15** were measured at room temperature with a Stoe-Siemens AED2 four-circle diffractometer using Mo-K_α graphite-monochromated radiation (λ = 0.71073 Å; ω-2θ scans). The structures of the $[N(PPh_3)_2]^+$ salts of **2**, **4**, **5**, **6**, and that of complex **15** were solved by direct methods, whereas those of **10** and **12** were solved by Patterson methods using the program SHELXS-97.[27] All the structures were refined by full-matrix least squares on F^2 with SHELXL-97.[28] The salt $[N(PPh_3)_2]$**2** crystallises with a quarter of a disordered molecule of hexane. The five carbon atoms C62A, C62B, C63A, C63B, and C64 were refined isotropically using the SHELXL-97 default parameters. In compounds $[N(PPh_3)_2]$**5** and $[N(PPh_3)_2]$**6** one of the carbonyl ligands is found to be disordered and has been split into C6A-O6A and C6B-O6B (anion **5**), C21A-O21A and C21B-O21B (anion **6**), respectively, with an occupancy of a half for each atom. The position of the hydride ligands in **10**, **12**, and **15** were located from Fourier difference maps and refined isotropically, while the remaining hydrogen atoms of the methyl, ethyl or phenyl substituents were included in calculated positions and treated as riding atoms with SHELXL-97 default parameters. For $[N(PPh_3)_2]$**4**, an empirical absorption correction was applied using DIFABS[29] and for $[N(PPh_3)_2]$**5**, $[N(PPh_3)_2]$**6**, **10** **12**, **15** it was based on ψ scans.[30] The Figures were drawn with ORTEP[31] (thermal ellipsoids, 50% probability level). Complete tables of bond lengths and angles and lists of thermal parameters have been deposited with the Cambridge Crystallographic Data Centre, 12 Union Road, Cambridge CB2 1EZ, UK. Copies of the data can be obtained free of charge on application to CCDC, 12 Union Road, Cambridge CB2 1EZ, UK [Fax: int. code + 44-1223/336-033; E-mail: deposit@ccdc.cam.ac.uk], on quoting the deposition numbers CCDC-111752−111758.

Acknowledgments

We thank the Fonds National Suisse de la Recherche Scientifique for financial support of this work. A generous loan of ruthenium(III) chloride hydrate from the Johnson Matthey Research Centre is gratefully acknowledged.

[1] R. D. Adams, in *Comprehensive Organometallic Chemistry 2* (Eds.: E. W. Abel, F. G. A. Stone, G. Wilkinson), Elsevier, Oxford, **1995**, vol. 10, p. 1.
[2] Y. Chi, D. K. Hwang, in *Comprehensive Organometallic Chemistry 2* (Eds.: E. W. Abel, F. G. A. Stone, G. Wilkinson), Elsevier, Oxford, **1995**, vol. 10, p. 85.
[3] [3a] P. Braunstein, J. Rosé, in *Comprehensive Organometallic Chemistry 2* (Eds.: E. W. Abel, F. G. A. Stone, G. Wilkinson), Elsevier, Oxford, **1995**, vol. 10, p. 351. − [3b] For a general review see: *Catalysis by Di- and Polynuclear Metal Cluster Complexes* (Eds.: R. D. Adams, F. A. Cotton), Wiley-VCH, Chichester, **1998**. − [3c] R. D. Adams, T. S. Barnard, Z. Li, W. Wu, J. H. Yamamoto, *J. Am. Chem. Soc.* **1994**, *116*, 9103. − [3d] R. D. Adams, T. S. Barnard, *Organometallics* **1998**, *17*, 2567. − [3e] R. D. Adams, T. S. Barnard, *Organometallics* **1998**, *17*, 2885.
[4] E. Sappa, A. Tiripicchio, A. J. Carty, G. E. Toogood, *Prog. Inorg. Chem.* **1987**, *35*, 437 and references therein.
[5] P. R. Raithby, M. J. Rosales, *Adv. Inorg. Chem. Radiochem.* **1985**, *29*, 169.
[6] E. L. Muetterties, T. N. Rhodin, E. Band, C. F. Brucker, W. R. Pretzer, *Chem. Rev.* **1979**, *79*, 91.
[7] A. Fusi, R. Ugo, R. Psaro, P. Braunstein, J. Dehand, *J. Mol. Catal.* **1982**, *16*, 217.
[8] V. Ferrand, G. Süss-Fink, A. Neels, H. Stoeckli-Evans, *J. Chem. Soc., Dalton Trans.* **1998**, 3825.
[9] G. Süss-Fink, S. Haak, V. Ferrand, A. Neels, H. Stoeckli-Evans, *J. Chem. Soc., Dalton Trans.* **1997**, 3861.
[10] O. Benali-Baitich, J. C. Daran, Y. Jeannin, *J. Organomet. Chem.* **1988**, *344*, 393.
[11] M. Cazanoue, N. Lugan, J. J. Bonnet, R. Mathieu, *Organometallics* **1988**, *7*, 2480.
[12] [12a] P. Braunstein, J. Rosé, *J. Organomet. Chem.* **1983**, *252*, C101. − [12b] E. Roland, H. Vahrenkamp, *Organometallics* **1983**, *2*, 1048.
[13] D. E. Fjare, W. L. Gladfelter, *J. Am. Chem. Soc.* **1984**, *106*, 4799.
[14] R. H. Crabtree, M. Lavin, *Inorg. Chem.* **1986**, *25*, 805.
[15] K. Wade, *Adv. Inorg. Chem. Radiochem.* **1976**, *18*, 1.
[16] J. C. Wang, Y. Chi, S.-M. Peng, G.-H. Lee, S.-G. Shyu, F.-H. Tu, *J. Organomet. Chem.* **1994**, *481*, 143.
[17] M. Bergamo, T. Beringhelli, G. Dalfonso, P. Mercandelli, M. Moret, A. Sironi, *Organometallics* **1997**, *19*, 4129.
[18] S. Deabate, R. Gordiano, E. Sappa, *J. Cluster Sci.* **1997**, *8*, 407.
[19] E. Roland, W. Bernhardt, H. Vahrenkamp, *Chem. Ber.* **1985**, *118*, 2858.
[20] S. Aime, R. Gobetto, L. Milone, D. Osella, L. Violano, A. J. Arce, Y. De Sanctis, *Organometallics* **1991**, *10*, 2854.
[21] D. Boccardo, M. Botta, R. Gobetto, D. Osella, A. Tiripicchio, M. Tiripicchio-Camellini, *J. Chem. Soc., Dalton Trans.* **1988**, 1249.
[22] [22a] J. Evans, G. Mc Nulty, *J. Chem. Soc., Dalton Trans.* **1981**, 2017. − [22b] D. Boccardo, M. Botta, R. Gobetto, D. Osella, A. Tiripicchio, M. Tiripicchio-Camellini, *J. Chem. Soc., Dalton Trans.* **1988**, 1249. − [22c] M. A. Gallop, B. F. G. Johnson, R. Khattar, J. Lewis, P. Raithby, *J. Organomet. Chem.* **1990**, *386*, 121.
[23] [23a] F. W. B. Einstein, K. G Tyers, A. S. Tracey, D. Sutton, *Inorg. Chem.* **1986**, *25*, 1631. − [23b] A. J. Deemings, *J. Organomet. Chem.* **1978**, *150*, 123.
[24] J. T. Park, J. R. Shapley, M. Rowen Churchill, C. Bueno, *J. Am. Chem. Soc.* **1983**, *105*, 6182.
[25] J. T. Park, J. R. Shapley, C. Bueno, J. W. Ziller, M. Rowen Churchill, *Organometallics* **1988**, *7*, 2307.
[26] D. D. Perrin, W. L. F. Armarego, *Purification of Laboratory Chemicals*, 3rd ed., Pergamon Press, Oxford, **1988**.
[27] G. M. Sheldrick, *Acta Crystallogr., Sect. A* **1990**, 46, 467.
[28] G. M. Sheldrick, *SHELXL-97, Program for crystal structure refinement*, University of Göttingen, Germany, **1997**.
[29] N. Walker, D. Stuart, *Acta Crystallogr., Sect. A* **1990**, *46*, 158.
[30] A. C. T. North, D. C. Phillips, F. C. Mathews, *Acta Crystallogr., Sect. A* **1968**, *24*, 351.
[31] C. K. Johnson, *ORTEP*, Oak Ridge National Laboratory, Oak Ridge, TN, modified for PC by L. Zsolnai, H. Pritzkow, University of Heidelberg, Germany, **1994**.

Received November 30, 1998
[198407]